Atlantic seaboard offshore stability risk evaluation & service

NOWRDC Award 192899-132

Final Report

Prepared for:

National Offshore Wind Research and Development Consortium

Mel Schultz and Kori Groenveld, Project Managers

Prepared by:

Clarkson University

Potsdam, New York

Research Team

Clarkson University: Tuyen Vu, Thomas Ortmeyer, Jianhua Zhang, Manh Bui, Minh Vu

GE Vernova's Consulting Services: Jason MacDowell, Neethu Abraham, Baozhuang Shi

NYPA AGILe Lab: Hossein Hooshyar, Thanh Nguyen

Abstract

The project addresses the **Challenge area R2c2** - Electrical and Grid Challenges Unique to Offshore Wind Transmission by developing advanced modeling methods and risk assessment strategies for the transient and dynamic performance of offshore wind farm (OSW) in applications where multiple large wind farms connect in close proximity to the electric power grid. In Task 1 of this project, electromagnetic transient (EMT) models for each of the proposed 30GW of proposed NYISO, ISO-NE and PJM offshore wind farms were developed and validated. Reduced order system equivalent models were developed for the associated onshore power grid. Separate small signal and electromagnetic transient (EMT) models were developed. The EMT models developed accommodate unbalanced and nonfundamental frequency studies of the performance of multiple offshore wind farms transient performance. The small signal models as well as controls stability of inverter-based resources.

In Task 2, the Task 1 models were used to evaluate the potential operational risks that would arise from the installation of multiple gigawatt level offshore wind farms on the U.S. North Atlantic coast. This effort includes development of risk metrics evaluating the level of load rejections, unit tripping, and the number of outages with the applicable standards including NERC PRC-006, PRC-024, IEEE 2800-2022, and regional operator and utility requirements. The team investigated the following risk factors:

- Weak grid
- Low inertia grid
- Resonance and control interactions associated with series compensated transmission lines
- IBR Converter interaction
- Load Rejection
- Critical Clearing time reductions
- Stuck Breaker Contingencies
- High and low load cases
- High and low wind cases

The factors with highest risk were found to be

- Weak grid
- IBR converter interactions
- Low critical clearing times for stuck breaker contingencies

This research study has shown that small signal analysis is an efficient and effective screening method to determine lightly damped subsynchronous frequencies that can lead to sustained oscillations as well as extend the recovery period following the clearing of system faults. However, key results should be verified with EMT studies. It was found that EMT studies of faults, line trips and generator trips are the most effective method to determine the stability and overvoltage risks from transient events.

Full details of the methods developed in this project are presented in the Task 1 section of this report. Study results for the NYSIO, ISO_NE and PJM systems are presented in the Task 2 section of the report.

Keywords

Offshore Wind Farm (OSW) Modeling

Electromagnetic transient (EMT) studies

Onshore Grid System (OGS) reduction methods

Sustained Oscillations from IBR Control Interactions

High Penetration Offshore Wind transient and dynamic risk factors

Transient and dynamic risk mitigation

Table of Contents

Abstract 2

Keywords 3

List of Figures 6

List of Tables 9

Acronyms and Abbreviations 10

1 Introduction 11

2 Task 1.1: EMT model development for 30GW of Atlantic OSW 13

2.1. Wind Turbine-Generator Modeling 13

2.2. Offshore Windfarm Modeling- HVAC Transmission 20

2.3. Offshore Windfarm Modeling- HVDC Transmission 22

2.4. Applying IEEE Standard 2800-2022 for OSW 25

2.5. OSW Farms in NYISO, ISO-NE and PJM systems 26

3 Task 1.2. Electromagnetic (EMT) System Equivalent Models for the Onshore Bulk Power Grid 27

3.1. Convert FERC 715 model to reduced PSCAD models 27

Onshore Power System Data 27

3.2. Small Signal Model for Eastern Power System 28

3.3. Compile onshore system designs for PJM and ISO-NE 32

3.4. Parallel process to simulate the onshore and offshore system 37

3.5. Validate full regional onshore + offshore system model with NY RTDS model 39

3.6. Task 1 Summary 42

4. Task 2.1. Controls Instability Risk Identification and Metrics 44

4.1. Develop risk metrics 44

4.2. Identify high-risk conditions 45

4.3.ISO-NE Contingencies and Faults Analysis 71

4.4. PJM Fault Analysis 78

4.5. Task 2.1 Summary 83

5. Task 2.2. Risk Analysis and Mitigation 85

5.1. Identify the potential original sources of risk 85

5.2. ISO-NE Small-Signal Stability Analysis 90
5.3. PJM Small-Signal Stability Analysis 91
5.4. Deploying Damping Equipment 92
5.5. Tuning Controllers 101
5.6. Impact of Series Compensation Project 107
5.7. Evaluate the effectiveness of wind speed forecasting in the mitigation 108
5.8. Summary 109

6. Task 3. Dissemination and Technology Transfer 110
6.1. Dissemination 110
6.2. Technology Transfer 112
6.3. Commercialization 113

7. Conclusions 117

References 119

List of Figures

Figure 1. General diagram of the direct-drive permanent magnet synchronous generator (PMSG) wind turbine generator (WTG) of this project. 13
Figure 2. WTG response to a 3% step increase in voltage at the Point of Interconnection (POI) at 9 sec. 16
Figure 3. Low Voltage Ride Through (LVRT) test results. 17
Figure 4. Real and reactive power response to an 0.3 Hz step increase in frequency at 7.0 seconds. 18
Figure 5. Wind turbine peak power output versus windspeed. 19
Figure 6. Aggregated model response to step increases in wind speed in the constant power region above rated wind speed. 19
Figure 7. Aggregated model response to step decreases in wind speed in the maximum power point operating region below rated wind speed. 20
Figure 8. Generic Offshore Wind Farm Layout with AC transmission. 21
Figure 9. Wind Plant Level Control Diagram 22
Figure 10. OSW with HVDC transmission. 23
Figure 11. Three phase fault performance at offshore bus T2. 24
Figure 12. Unbalanced fault response at the offshore bus T2. 25
Figure 13. Minimum reactive power capability at point of applicability (RPA), with V2=1.00, V3=1.04, and V4=1.05. 26
Figure 14. DYNRED Reduction process. 29
Figure 15. The flow of data during an E-TRAN conversion 31
Figure 16. Generator ST1 initialization process. 32
Figure 17. Three-phase fault response at Bus A (345 kV). Vrms_A = RMS line-to-line voltage; V_A = instantaneous line-to-neutral voltage; I_A→B = line current from Bus A to Bus B. 35
Figure 18. Three-phase fault response at Bus B (345 kV). Vrms_B, V_B, I_B→A (line current Bus B→Bus A) 35
Figure 19. Three-phase fault response at Bus C (345 kV). Vrms_C, V_C, I_C→D (line current from Bus C to an adjacent corridor). 36
Figure 20. Onshore + offshore model with (a) parallel network interface (b) direct interface 38
Figure 21. Fault current signal of PSS/E model 42
Figure 22. Fault current signal of the EMT model 42
Figure 23. Underfrequency Thresholds of Generators for Eastern Interconnection [3] 44
Figure 24. Frequency No Trip Boundaries for Eastern Interconnection [7] 45
Figure 25. POI Voltage No-Trip Boundaries for Eastern Interconnection [7] 45
Figure 26. Strategic NYS OSW Deployment: Substations, Wind Farms, Atlantic-Ocean Interconnection. 46
Figure 27. Voltage and frequency response at 5 OSW farms terminal 47
Figure 28. The output power of 5 farms. 48
Figure 29. Machine speed (per unit) profiles (a) and rotor-angle (rad) profiles (b) of the onshore generator fleet with the 5 farms 49
Figure 30. Onshore generator speed (per unit) (a) and rotor-angle (rad) (b) responses during the sequential trip of the five offshore wind farms. 50

Figure 31. Frequency and voltage responses at the Gowanus and Holbrook POIs during the sequential trip of the five offshore wind farms. 51
Figure 32. Comparison of machine speed (a, b) and rotor-angle (c, d) profiles for the 4-wind case at Gowanus under stable (15-cycle clearing) and unstable (16-cycle clearing) conditions. 57
Figure 33. Comparison of machine speed (a, b) and rotor-angle (c, d) profiles for the 5-wind farm case for a fault at Gowanus under stable (13-cycle clearing) and unstable (14-cycle clearing) conditions. 59
Figure 34. EGC Voltage and Frequency Dynamics—Offshore HVDC Terminal vs. POI Bus for 13- and 14-Cycle Fault Clearing of a fault at Gowanus.....59
Figure 35. Ruland Road Single-Phase Fault (A-G) with 5 OSWs for 12- and 13-Cycle Fault Clearing ...61
Figure 36. Comparison of machine speed (a) and rotor-angle (b) profiles for the 5-wind case at Ruland Rd under unstable (21-cycle clearing) conditions. (Note: each plot of speed and angle show half of the synchronous generators in the study). 64
Figure 37. FFT of turbine generator speed following the fault event.....64
Figure 38. Damping ratio of unstable turbine generator speed following the fault event.....65
Figure 39. Frequency & voltage of Gowanus POI following the synchronous generator trip event. 67
Figure 40. Generator speed profiles on-line units after generator trip.....68
Figure 41. Voltage and frequency of East Garden City POI after generator trip 68
Figure 42. Voltage (kV) profile at Ruland RD substation.....70
Figure 43. Current (kA) on the faulted transmission line.....70
Figure 44. Voltage and frequency responses at Ruland RD Substation and OSW terminal 71
Figure 45. Comparison of machine speed (a, b) and rotor-angle (c, d) profiles for the 4-wind case at West Barnstable under stable (19-cycle clearing) and unstable (20-cycle clearing) conditions. Spring Light Load Case 74
Figure 46. Bus 1 RMS voltage and frequency responses following the transmission line trip event 76
Figure 47. Overvoltage Event leading to shutdown of West Barnstable OSW 77
Figure 48. Generator speed profiles following transmission line tripping 77
Figure 49. Generator speed profiles following the contingency 82
Figure 50. Voltage and frequency response at faulted substation and Atlantic Shores South Wind 1 terminal (Frequency measured by the GFM HVDC controller). 83
Figure 51. Model synchronous condenser in PSCAD 93
Figure 52. ESAC8B - Basler DECS-type exciter/AVR [9] 94
Figure 53. 6 Pulse STATCOM 94
Figure 54. EGC onshore HVDC terminal voltage and frequency dynamics for 15-cycle fault clearing (five-OSW case, with and without 250 MVAr SC) 95
Figure 55. Generator speed and rotor-angle profiles for the five-OSW case at Gowanus under 96
Figure 56. EGC onshore HVDC terminal voltage and frequency dynamics for 5- and 6- cycle fault clearing (five-OSW case, without adding damping equipment) 96
Figure 57. EGC onshore HVDC terminal voltage and frequency dynamics for 17- and 18- cycle fault clearing (five-OSW case, with 250 MVAr SC) 97
Figure 58. EGC onshore HVDC terminal voltage and frequency dynamics for 18- cycle fault clearing (five-OSW case, with 250 MVAr STATCOM) 98
Figure 59. Generator speed and rotor-angle profiles for the five-OSW case at Ruland under 98
Figure 60. Ruland Rd Single-Phase Fault (A-G) with 5 OSWs for 30-Cycle Fault Clearing (stable) 98

Figure 61. Rotor-angle profiles for the five-OSW configuration at Gowanus during summer-peak load with 9-cycle clearing 99
Figure 62. Rotor-angle profiles for the five-OSW configuration at Gowanus during summer-peak load with 12-cycle clearing (with one 250 MVAr SC) 99
Figure 63. Rotor-angle profiles for the five-OSW configuration at Gowanus during summer-peak load with 14-cycle clearing (with two 250 MVAr SC) 100
Figure 64. West Barnstable fault: critical generator speed and rotor angle for 12-cycle (stable) vs 13-cycle (unstable) clearing (4-OSW case, no mitigation)....101
Figure 65. West Barnstable fault: critical generator speed and rotor angle for 13-cycle (stable) vs 14-cycle (unstable) clearing (4-OSW case, with 250 MVAr SC)....101
Figure 66. PLL control diagram....102
Figure 67. RMS POI terminal voltage of Vineyard Mid Atlantic Wind (Left) and Sunrise Wind (Right) 103
Figure 68. PLL Controller Tuning 103
Figure 69. RMS voltage of Vineyard Mid Atlantic Wind (Left) and Sunrise Wind (Right) after tuning 104
Figure 70. RMS terminal voltage of Vineyard Mid Atlantic Wind 105
Figure 71. HVDC grid-side inverter control topology....105
Figure 72. HVDC grid-side inverter controller tuning 106
Figure 73. DC voltage before tuning the controller 106
Figure 74. RMS terminal voltage and DC-link voltage of Vineyard Mid Atlantic Wind after tuning 107
Figure 75. Onshore HVDC terminal voltages at (a) Beacon Wind and (b) Sunrise Wind for a 12-cycle clearing time (five-OSW case), with and without the series compensation in service. 107
Figure 76. Onshore HVDC terminal voltages at (a) Beacon Wind and (b) Juno Express Wind for a 17-cycle clearing time (five-OSW case), with and without the series compensation in service.....108
Figure 77. RMS terminal voltage and frequency of Juno Express Wind with 100% and 50% rated power 108
Figure 78. Diagram illustrating the model components that make up the service to be commercialized based on this project. 114

List of Tables

Table 1. Parameters of the Base Case Wind Turbine System 14
Table 2. Wind Turbine Operation Regions 15
Table 3. Small signal analysis performed on different versions of reduction model 30
Table 4. Area-Specific EMT Models for NYISO, ISO-NE, and PJM 37
Table 5. Steady State Load Flow Comparison between PSS/E and PSCAD Models during flat start scenario 40
Table 6. Configuration of NYISO Proposed Offshore Wind Farms 46
Table 7. Dominant states of OSWs in NYISO 53
Table 8. Dominant states of OSWs in ISO-NE 54
Table 9. Dominant states of OSWs in PJM 54
Table 10. Critical clearing time for a three-phase fault at the Gowanus substation using the spring light load model 58
Table 11. Critical Clearing Time for a balanced/ unbalanced fault at the Ruland Rd substation using the Spring Light Load model 60
Table 12. Critical Clearing Time for a three-phase fault at the Gowanus substation using the summer peak load model 62
Table 13. Critical Clearing Time for a three-phase fault at the Ruland Road substation using the summer peak load model 63
Table 14. Studied contingencies for NYISO 66
Table 15. Configuration of ISO-NE Proposed Offshore Wind Farms 71
Table 16. Critical Clearing Time for a three-phase fault at the West Barnstable substation using the spring light load model 73
Table 17. Critical Clearing Time for a three-phase fault at the West Barnstable substation using the summer peak load model 74
Table 18. Studied contingencies for ISO-NE 75
Table 19. Critical buses to study for ISO-NE 75
Table 20. Configuration of PJM Proposed Offshore Wind Farms 78
Table 21. Summary of three-phase fault at PJM POIs using the SLL model. 79
Table 22. Summary of three-phase fault at PJM POIs using the summer peak load model for 25 cycles 80
Table 23. Studied contingencies for PJM 81
Table 24. Small-Signal Analysis Description 86
Table 25. Contingencies of the NYISO area 86
Table 26. Specific contingencies of the ISONE area 86
Table 27. Specific contingencies of the PJM area 87
Table 28. SSAT results of 5 OSWs in NYISO for the TLINE NY contingency. 88
Table 29. SSAT results of 5 OSWs in NYISO for GEN NYC 89
Table 30. SSAT results of 4 OSWs in ISO-NE for contingency GEN NE1. 90
Table 31. Key SSAT results of 7 OSWs in PJM under generator tripping 91
Table 32: Potential market opportunity & revenue estimate. Note that cost units are in thousands..... 116

Acronyms and Abbreviations

AVR: automatic voltage regulator
BPS: Bulk power system
CCT: Critical Clearing Time
CEII: critical energy/electricity infrastructure information
DYNRED: dynamic reduction software product
EGC: East Garden City
EMT: electromagnetic transient
ERCOT: Electric Reliability Council of Texas
E-TRAN: Translator for Power System Simulation
FERC: Federal Energy Regulatory Commission
FFT: Fast Fourier Transform
GSC: The grid-side converter
HVAC: high voltage alternating current
HVRT: high voltage ride through
IAB: Industry Advisory Board
ISO: Independent System Operator
ISO-NE: New England the independent system operator for the New England region
LI: Long Island
LVRT: low voltage ride through
MMWG: Multiregional Modeling Working Group
MSC: The machine-side converter
MSSCP: Marcy South Series Compensation Project
NERC: North American Electric Reliability Corporation
NOWRDC: National Offshore Wind Research and Development Consortium
NYC: New York City
NYCA: New York Clearing Area
NYISO: New York Independent System Operator
OSW: Offshore Wind
PJM: PJM Interconnection LLC, a regional transmission operator for the Mid-Atlantic region
PLL: phase-locked loop POI: point of interconnection
PSCAD: power systems computer aided design (software package)
PSSE: power system simulator software product
ROCOF: Rate of Change of Frequency
RTO: Regional Transmission Operator
SC: synchronous condenser
SCR: short circuit ratio
SLG: single line to ground (fault)
SLL: Spring Light Load
SSAT: small signal analysis software tool
STATCOM: static synchronous compensator
TPL: NERC's Transmission Planning (TPL) body of standards deal with how transmission systems must be planned and analyzed by the Transmission Planner (TP).
UFLS: Underfrequency load shedding

1 Introduction

The United States is in the process of moving toward carbon-free electricity generation, in order to address global warming. In the northeastern states, this has led to ambitious plans to develop significant levels of offshore wind generation. There have been plans announced for as much as 30 GW of offshore wind generation in the coming few decades, through initiatives and policy mandates such as New York's Climate Leadership & Community Protection Act (NY CLCPA). As of 2025, however, only 3 offshore wind farms are in service, Block Island Wind was put in service in 2016 with 30 MW capacity, the Coastal Virginia Offshore Wind Pilot Project was completed in 2020 with 12 MW capacity, and The South Fork Wind Farm went into service in 2024 with 132 MW capacity.

The current US offshore wind (OSW) pipeline of existing and proposed projects will create high concentrations and penetrations of inverter-based resources (IBRs). Additionally, many of the new farms will connect to the power grid using HVDC transmission, with voltage source converters at both terminals. The installation of these wind farms will contribute to unprecedented challenges for the electric power grid. The top OSW reliability and resilience challenge will include controls instability, weak system instability, and issues due to the reduced system inertia when there are reduced numbers of synchronous generators on line. These issues can lead to transient instabilities, transient overvoltages, sustained sub-synchronous oscillations (below 60 hertz), and high rates of frequency change. In extreme cases, the transient and dynamic issues can result in unit tripping and even area blackouts. In the current interconnection process, the focus is on the project being developed and the required transmission upgrades. This process involves greatly simplified models of the power grid. There is an opportunity to improve the process to emphasize how plant controls, performance and modeling could mitigate critical risks associated with rapid deployment of offshore wind technology. There is a need for more comprehensive studies that analyze the performance of multiple large wind farms installed in concentrated areas.

These studies require accurate and efficient models of both the OSW installations and the bulk power grid. In order to achieve this goal, this project has

- Developed a set of flexible models of both OSW and HVDC installation models that can readily adapt to represent the range of these installations and their controllers.
- Developed an efficient network reduction methodology using existing reduction tools.

These two goals were addressed in Task 1 of this project, and the methods were validated in this Task. As a result of the methods developed in this task, it is now possible to efficiently develop models for EMT and

small signal studies that are suitable for usage in a service providing interconnection studies and operational studies of multiple large scale OSW installations located in close proximity. This advanced modeling capability allows for a more comprehensive capability to identify and mitigate grid stability risks associated with rapidly increasing renewable IBR penetration.

The project has also developed a controls and performance stability risk evaluation methodology and risk mitigation strategies. These methods and strategies can be readily adapted for use in OSW interconnection studies involving multiple large farms connecting in close proximity.

Together, these tools and processes can be used as the foundation for advanced interconnection services as well as for the ongoing assessment of OSW wind farm performance in the operating phases of these projects. This capability will help offshore wind projects demonstrate their value of providing reliable,

stable and clean power, and to meet their targeted Commercial Operation Date (COD), as well as to address operating challenges and controller updates that occur after the project is commissioned.

This project was led by Clarkson University, with subcontracts with GE Vernova and NYPA. Key personnel on the project included:

- Clarkson University: Tuyen Vu, Thomas Ortmeyer, Jianhua Zhang, Manh Bui, Minh Vu
- GE Vernova's Consulting Services: Jason MacDowell, Neethu Abraham, Baozhuang Shi
- NYPA AGILe Lab: Hossein Hooshyar, Thanh Nguyen

Members of the Industrial Advisory Committee for the project were:

- Saad Syed, Ocean Winds
- Robert Eisenhuth, PSEG
- Matthew Koenig, Consolidated Edison
- Rachel MacDonald, California Energy Commission
- Jian Fu, DOE
- Scott Egbert, NYSERDA

The IAC was active in this project, particularly in providing advice and insights into the critical contingencies that face the bulk power grid of this study.

This report is divided into chapters based on the technical subtasks of the project.

2 Task 1.1: EMT model development for 30GW of Atlantic OSW

2.1. Wind Turbine-Generator Modeling

The general diagram for the offshore wind turbines modeled in this study is shown in Figure 1. The system model for this task was an infinite bus behind an impedance.

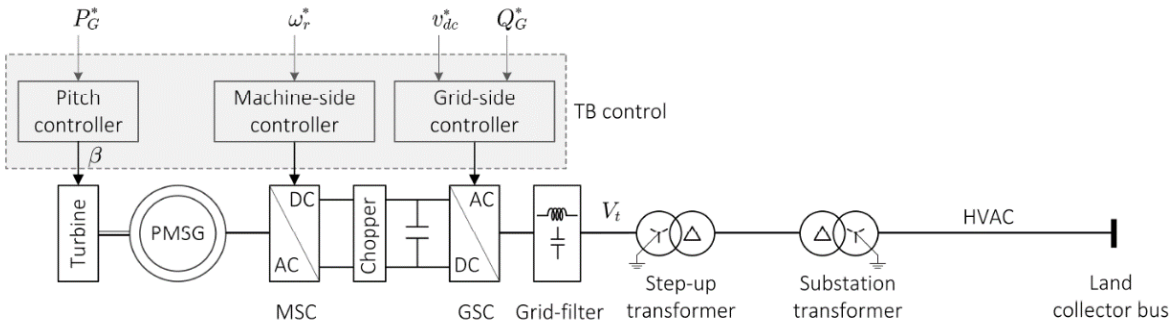

Figure 1. General diagram of the direct-drive permanent magnet synchronous generator (PMSG) wind turbine generator (WTG) of this project.

The parameters of the base case wind turbine are given in Table 1. The turbine model included pitch angle and variable speed control, and cut-in and cut-out wind speed limits to provide the 4 regions of operation described in Table 2.

The specific WTG model used in the study was taken from the previous project "Real-Time Interconnection Studies and Control of New York Offshore Wind (NYSERDA Project 148516)" (Clarkson University 2023) The project 148516 involved Matlab/Simulink modeling, and these models were converted to PSCAD models in this project. The machine side converter (MSC) controlled PMSG performance and the turbine power output in the MPPC mode. The grid side converter (GSC) controlled the DC link voltage and the vars injected into the power grid. The GSC controller included negative sequence current injection which was not active during balanced voltage conditions, using the WECC based current injection scheme. The current limit logic employed in this study was based on the WECC defined current limit logic.

Table 1. Parameters of the Base Case Wind Turbine System

Components	Parameters	Values
PMSG	Rated power, P_{rated} Stator winding resistance, R_s Stator leakage reactance, X_s Unsaturated d-axis reactance, X_d Unsaturated q-axis reactance, X_q Damper winding d-axis resistance, R_{kd} Damper winding d-axis reactance, X_{kd} Damper winding q-axis resistance, R_{kq} Damper winding q-axis reactance, X_{kq} Magnetic strength, T Angular moment of inertia, J Mechanical damping, D	12 MVA 0.0017 pu 0.0364 pu 0.55 pu 1.11 pu 0.055 pu 0.62 pu 0.183 pu 1.175 pu 1.0 pu 4 s 0.01 pu
BTB converter	Rated power DC link capacitance DC link voltage	12 MVA 15000 μF 1.45 kV
Step-up transformer	Rated power Rated voltage (RMS line) Positive sequence leakage reactance	15 MVA 4 kV | 66 kV 0.025 pu
Wind turbine	Rated wind speed Turbine radius	10 m/s 50 m

The specific WTG model used in the study was taken from the previous project "Real-Time Interconnection Studies and Control of New York Offshore Wind (NYSERDA Project 148516)" (Clarkson University 2023) The project 148516 involved Matlab/Simulink modeling, and these models were converted to PSCAD models in this project. The machine side converter (MSC) controlled PMSG performance and the turbine power output in the MPPC mode. The grid side converter (GSC) controlled the DC link voltage and the vars injected into the power grid. The GSC controller included negative sequence current injection which was not active during balanced voltage conditions, using the WECC based current injection scheme. The current limit logic employed in this study was based on the WECC defined current limit logic.

The GSC model also includes a Low-voltage ride-through (LVRT) function. This function is also based on the WECC LVRT logic, and includes both positive and negative sequence current limits. The positive sequence active and reactive currents are limited accordingly based on the voltage condition. For example, these would be forced to zero during very low voltage scenario. In order to detect the normal and abnormal

conditions, the positive sequence component of voltage is used and then the injected reactive power is proportional to the voltage drop while the active power is determined according to the machine-side power.

Table 2. Wind Turbine Operation Regions

	Operating Region	Operating Mode	Power Output
1	Parking Region	<Cut-in wind speed	0
2	MPPT (Maximum Power Point Tracking) Region	Cut in speed to the rated wind speed	Constant blade pitch to achieve maximum power output
3	Constant Power Region	Rated speed to cut-out wind speed	Constant rated power output
4	Parking Region	> Cut-Out speed limit	0

A DC link chopper is used to avoid overvoltage on the DC-link capacitor during fault conditions. The chopper uses hysteresis control to limit the voltage, and dissipates energy to reduce the overvoltage during abnormal conditions. At that time, the DC voltage control loop is frozen, and the current loop controls the active and reactive currents injected into the grid.

Due to the nature of the MSC and GSC, these power electronic converters generate a significant amount of harmonics impacting the system. Therefore, passive RLC low pass filters are utilized on the AC side of the converters.

Validation of Wind Turbine-Generator PSCAD Models

The WT model validation was performed to verify compliance with the industry standards. The testing benchmark is designed based on the Procedure Manual of the Dynamic Working Group of the ERCOT (Electric Reliability Council of Texas) with the purpose of evaluating the dynamic performance of the model.

For these tests, a 200 MW wind farm was represented by an aggregated wind turbine model representing the entire farm. The farm's POI is 230kV.

The start-up sequence for the wind turbine simulation is:

- Close the circuit breaker linking the WT to the power grid
- De-block the grid side converter after an 0.1 second delay
- Release the rotor with turbine in the torque control mode after an 0.1 second delay
- Release the rotor side converter after an 0.5 second delay

The turbine successfully operated in the steady state with 1MW output power at unity power factor for a wind speed of 10 m/s.

Small Voltage Disturbance Test In this test case, two scenarios are designed to test the plant automatic voltage regulator (AVR) ability to regulate the original voltage set point. The voltage at the Point of Interconnection (POI) is applied a 3% step increase and a 3% step decrease in two separate simulations. The real and reactive power flow plots for the step increase in voltage is shown in Figure 2.

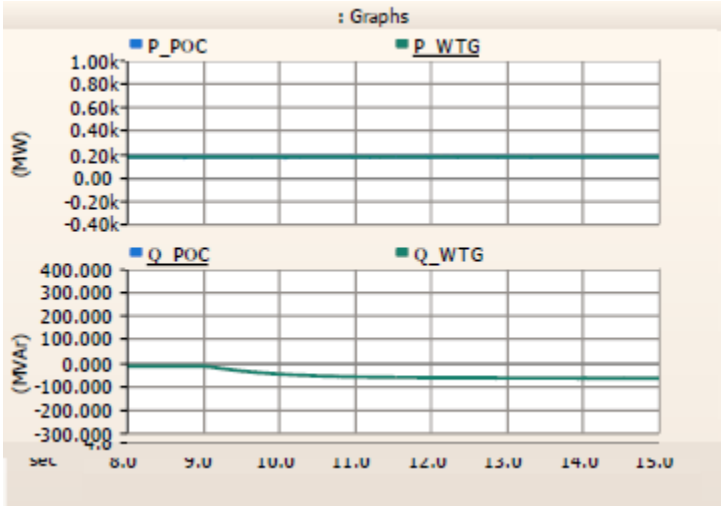

Figure 2. WTG response to a 3% step increase in voltage at the Point of Interconnection (POI) at 9 sec.

Large Voltage Disturbance Test The large voltage disturbance test is also divided into two situations: Low Voltage Ride-Through (LVRT) and High Voltage Ride-Through (HVRT). Both scenarios apply the voltage profile boundary illustrated in the North American Electric Reliability Corporation (NERC) Gaps Whitepaper (PRC-024-2).

The results of the LVRT test are shown in Figure 3. The voltage profile shown in Figure 3 starts at 1.0 per-unit voltage (the base voltage is 230kV), then drops to zero, and from that the voltage rises up to 0.45, 0.65, 0.75 per-unit and ends at 0.9 per-unit.

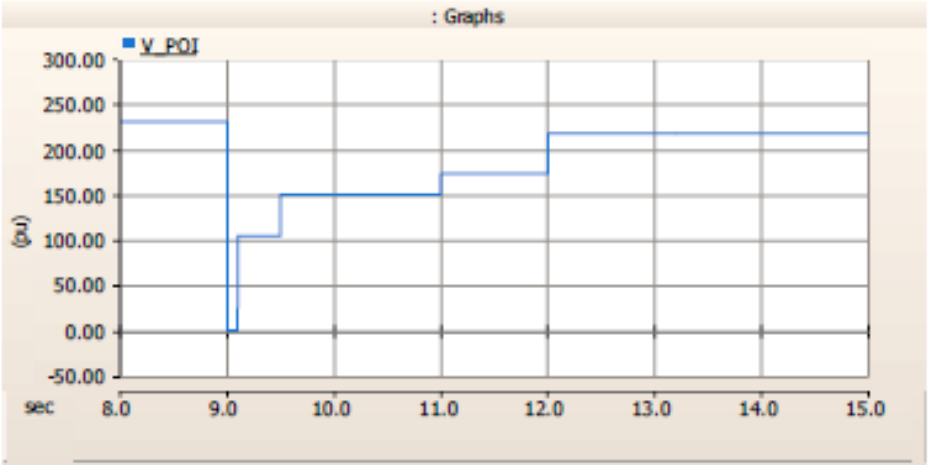

(A) Applied Voltage at POI

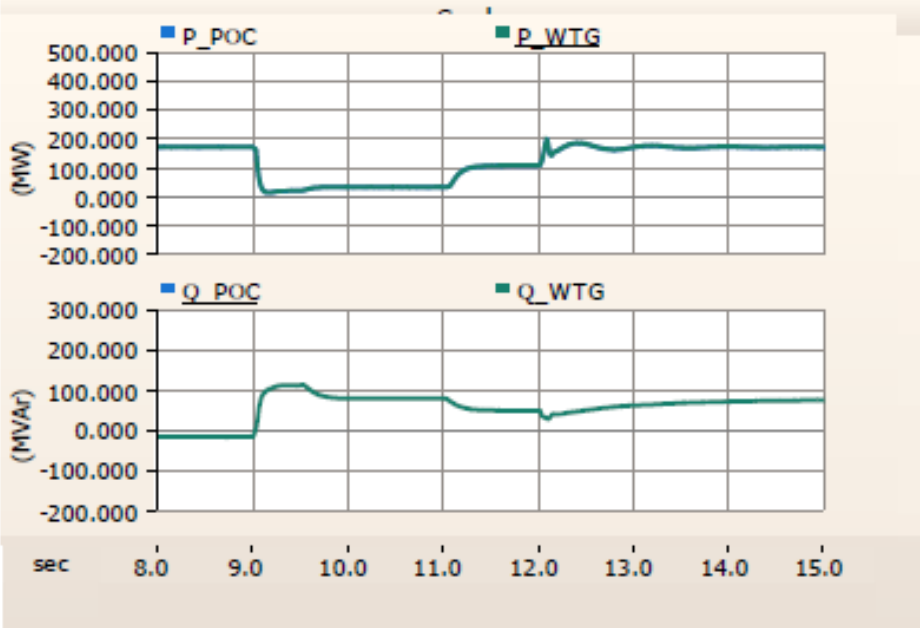

(B) Wind Turbine Real and Reactive Power Response

Figure 3. Low Voltage Ride Through (LVRT) test results.

For the low voltage transient, the model injected reactive current to compensate the sudden fall of the voltage. As shown in Figure 3, the active power felt to close to zero while the reactive injection at the POI was observable immediately when the voltage dropped to zero. As the voltage gradually increases, the reactive power still is injected into the system corresponding to each voltage condition throughout the active

power recovery period. When the voltage profile recovers to 0.9 p.u, the AVR continually increases the reactive output power and remains consistently as the final POI voltage is still below the initial 1.0 p.u value and the active output power recovered to full output capability with a modest reduction at the initial recover interval which is acceptable to accommodate greater reactive power injection. Figure 3 shows that the WT model successfully remains on line through the test and has appropriate responses from the real and reactive power controllers. The WT model also passed the HVRT test successfully.

Small Frequency Disturbance Test: The inertia characteristic of the system is verified through two situations comprising a 0.3 Hz step increase and a 0.3 Hz step decrease of system frequency from nominal frequency (60 Hz). As shown in Figure 4, the frequency controller lowered the real power output according to its droop characteristic following the frequency change. For the frequency reduction case, a similar transient in real power occurred, while the power settled back to the original value as the turbine was operating at its maximum power point.

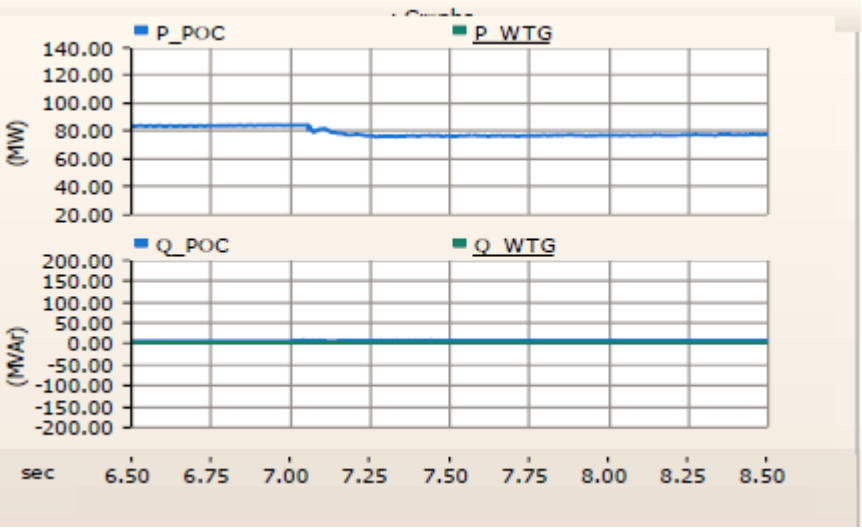

Figure 4. Real and reactive power response to an 0.3 Hz step increase in frequency at 7.0 seconds.

Wind Speed Variation Test: As the wind energy availability varies significantly depending on many factors such as weather, location, and time, this test investigates the performance of the system under a wide range of wind speed. The output power of a WT is a non-linear function of wind speed and WT availability, as depicted in Figure 5 where V_{ci} is cut-in speed, V_{co} is cut-out speed, V_r is rated speed. If the wind speed is smaller than the rated value and greater than the cut-in speed, the turbine operates in the variable speed fixed pitch mode of operation, and the output power increases with the wind speed. Above rated wind speed, the turbine operates in the constant speed variable pitch mode,

and the real power is maintained at the rated power value. In this turbine, the cut-in speed is 3 (m/s), the cut-out speed is 25 (m/s), and the rated speed is 10 (m/s). Figure 6 shows the turbine response for a step change in wind in the variable pitch mode, and Figure 7 shows the response to a step change in wind speed in the variable speed mode.

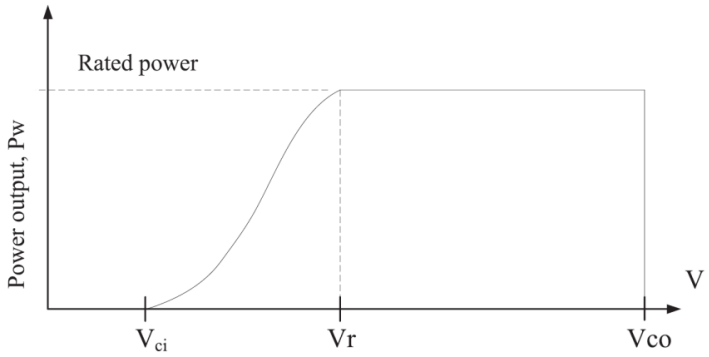

Figure 5. Wind turbine peak power output versus windspeed.

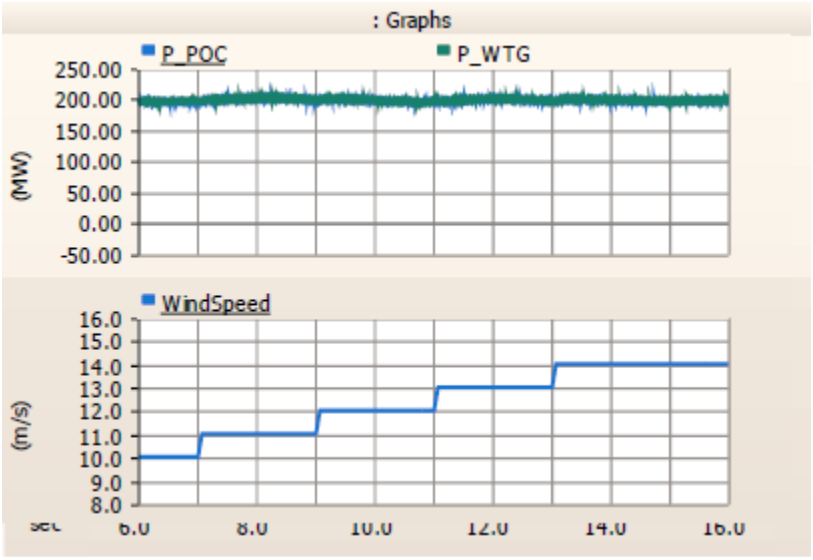

Figure 6. Aggregated model response to step increases in wind speed in the constant power region above rated wind speed.

System strength and phase jumps tests were also conducted. In sum, these tests validate the performance of the PSCAD wind turbine model and demonstrate that the PSCAD wind turbine models accurately represent the published generic models of offshore wind turbines and farms when they are connected to a grid model that is an infinite bus behind and impedance.

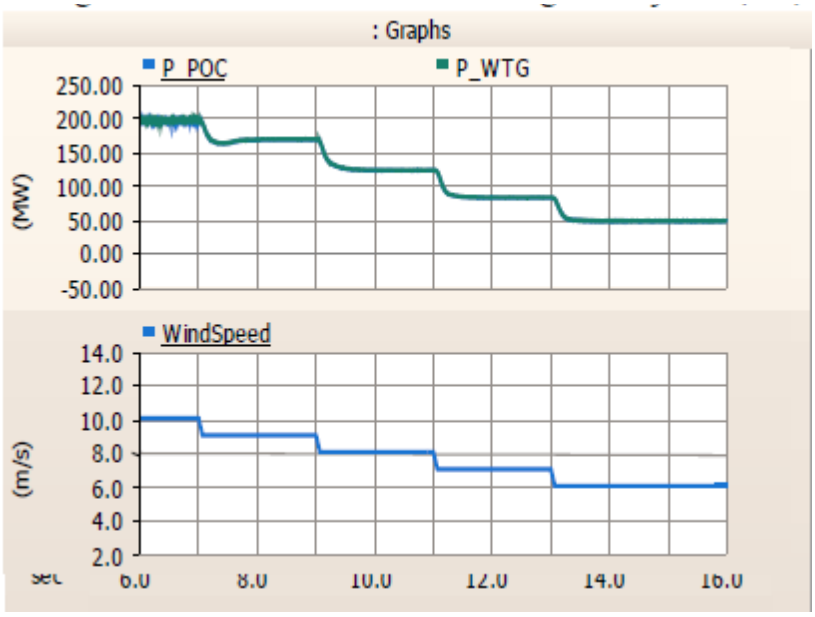

Figure 7. Aggregated model response to step decreases in wind speed in the maximum power point operating region below rated wind speed.

These tests demonstrate that the PSCAD wind turbine models accurately represent the published generic models of offshore wind turbines and farms when they are connected to a grid model that is an infinite bus behind and impedance.

2.2. Offshore Windfarm Modeling- HVAC Transmission

The general configuration of offshore wind farms consists of multiple wind turbines connected by a set of 69kv collector lines, an offshore substation, a transmission system, and the onshore substation. The medium-voltage submarine collector cables are used to transmit wind power to the offshore substation. The step-up substation transformer has the purpose to boost up the voltage to the transmission level. An example for the wind farm configuration is depicted in Figure 8. In this case, high voltage alternative current (HVAC) submarine export cables are utilized to carry the wind power to the onshore substations. The onshore transformer at the onshore substation would transform the transmission voltage to the utility grid level. The offshore wind farm system is connected to the utility grid at the point of interconnection (POI). Shunt reactors are applied at both ends of the HVAC cables to compensate the reactive power generated by the capacitance of the transmission cables.

The Figure 8 inset shows the individual wind turbine model including the step-up transformer to collector voltage.

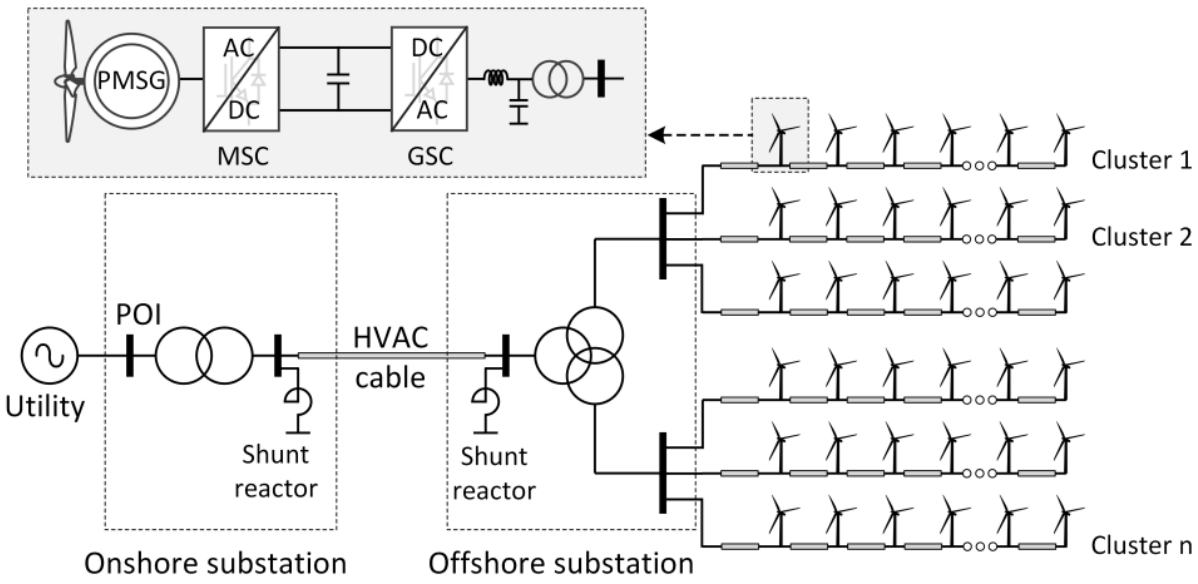

Figure 8. Generic Offshore Wind Farm Layout with AC transmission.

Large OSW farms have the potential to create disturbances and abnormal conditions that can severely impact the connected utility system. Therefore, the offshore wind farm systems need to have the capability of voltage and frequency support for the utility grid. The wind farm control system is designed to regulate the total injected active power into the POI, and control of terminal voltage.

The wind farm control system developed for this project is shown in Figure 9. There would be two modes regarding active power control, which are active power curtailment mode and droop active power-frequency control mode. The active power curtailment mode is used to regulate the wind farm power based on the requirement from the transmission system operator (TSO), meanwhile the droop active power-frequency control mode is developed to provide power sharing and damping support the high during contingency induced transient conditions. The active power reference to each WT is limited by the maximum available power of each WT. The reactive power control has the capability to provide voltage control, droop reactive power-voltage control, and constant reactive power control. The reactive power limiter calculates the reactive power reference to each WT based on the output active power and their reactive power capability.

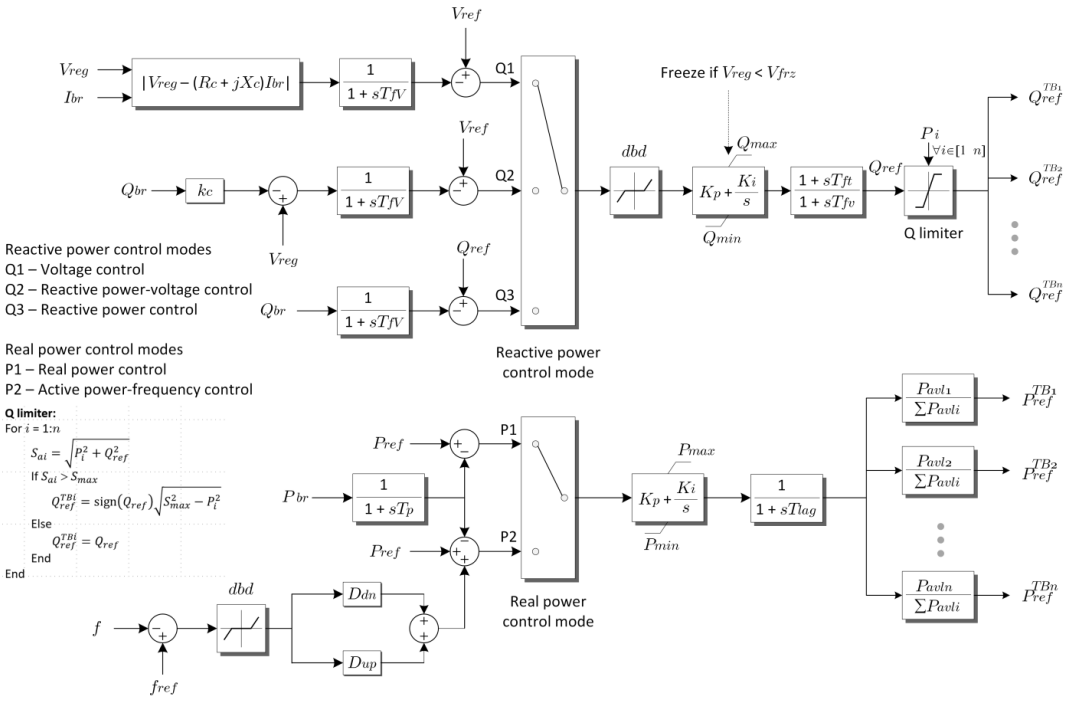

Figure 9. Wind Plant Level Control Diagram

2.3. Offshore Windfarm Modeling- HVDC Transmission

The proposed offshore wind farms that are a part of this study use either HVAC or HVDC transmission lines to connect the OSW power to the bulk power grid. The basic diagram for an OSW with HVDC transmission is shown in Figure 10. In modern farms, PWM Voltage Source Converters (VSC) converters are used for both the offshore rectifier and onshore inverter. A typical VSC HVDC transmission system is comprised of converters, transformers, phase reactors, AC filters, DC cables and breakers, DC capacitors and filters, a control system, and third harmonic filters. The converter is the most important module since

it performs the conversion from AC to DC (rectification) at the sending end and from DC to AC (inversion) at the receiving end of the DC link. The three-phase AC voltage is converted to a DC voltage.

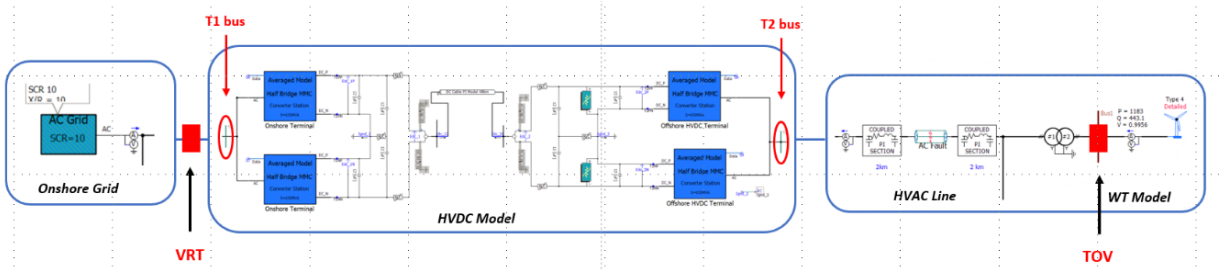

Figure 10. OSW with HVDC transmission.

In this study, a model of this HVDC transmission line was created in PSCAD. This model was coupled with the OSW model using the aggregated model of the wind turbines. was used to investigate the steady state and fault performance of this wind farm. The HVDC line has a grid following converter at the onshore substation and a grid forming converter at the offshore substation. The aggregated wind farm model uses a grid following converter that controls the active and reactive power flow from the farm. The grid supplying the onshore substation is a strong grid, with SCR=10, X/R=5.

The topology for the single wind turbine model is type 4, which consists of 2 back-to-back converters that decouple the turbine from the grid. The generator type is used as PMSG. The model consists of 2 converters, a machine side converter (MSC) and grid side converter (GSC). Additional equipment for the model is DC chopper, LC filter, and a step-up transformer. The GSC generates output in 4kV. A step-up transformer converts that into 66kV and transfers power into the offshore substation through submarine array cables. The aggregated farms would be scaled using the current scaling block to scale up from one wind turbine to

80 wind turbines. This HVDC connected OSW model was used to conduct studies including fault performance, transient over-voltage assessment, and fault ride-through capability.

Figure 11 shows the response to a three-phase fault at offshore bus T2. The results show a temporary

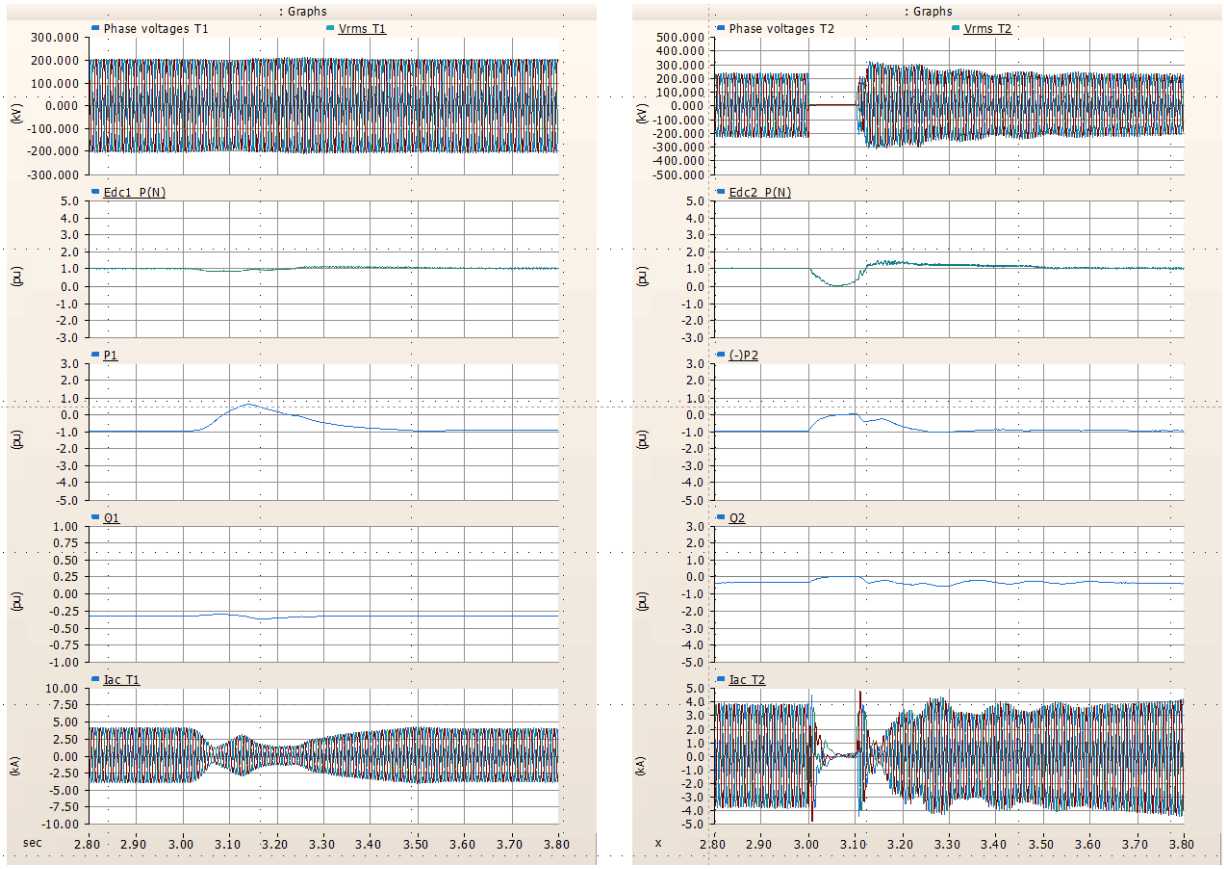

Figure 11. Three phase fault performance at offshore bus T2.

overvoltage (TOV) at bus T2 of approximately 50% following the fault. While not a direct concern of this project, this TOV at the offshore substation would need to be mitigated. Simultaneously, the reactive power is injected into the system to support the system stability. Although the onshore side does not observe the voltage fall, the active and reactive power also respond based on the response of the offshore side. The

HVDC line does not experience overvoltage during the fault. Note that negative real and reactive power flows in this figure indicates power flowing from OSW to the grid.

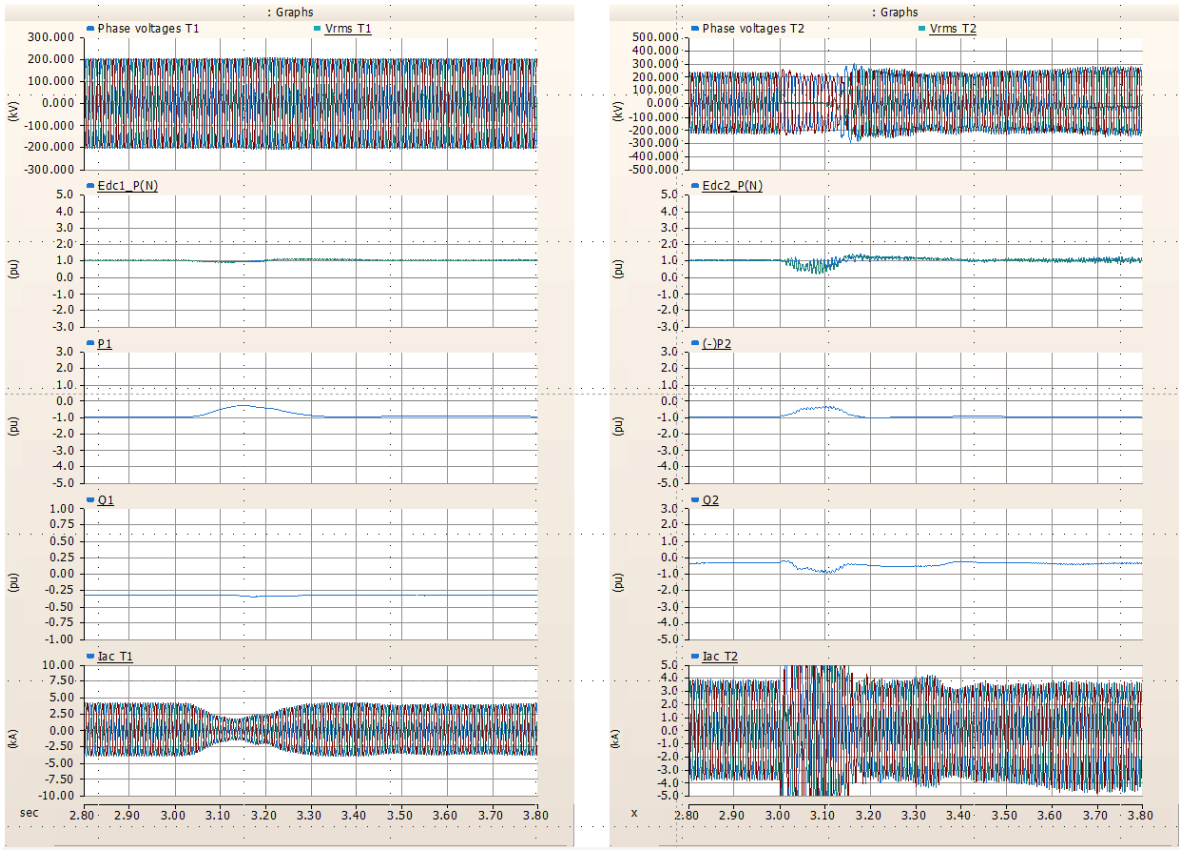

Figure 12. Unbalanced fault response at the offshore bus T2.

Next, an unbalanced fault test was simulated at the same location at the offshore substation. For a bolted A phase to ground fault, the response of our model is shown in Figure 12. Since this fault is unbalanced, the fault current includes a negative sequence current component. The output active power does not decrease to zero value during the fault period as the remaining two phases still provide the energy to the onshore grid.

Fault studies were also conducted on bus T1 at the onshore substation. In general, these faults were not as severe as the fault at T2. For all cases, inverter controllers also responded correctly to the fault-ride through requirements, keeping the inverters on line during this fault.

2.4. Applying IEEE Standard 2800-2022 for OSW

The IEEE Standard 2800-2022 establishes the required interconnection capability and performance criterion for inverter-based resources interconnected with transmission system including voltage and

frequency ride-through, active and reactive power control, power quality, and system protection. The reactive power – voltage control, active power – frequency response requirements are tested with our model. In our model, the IBR continuous rating (ICR) is 22 MVA for the 15MW turbines under study. Studies were conducted that demonstrated the ability of the study model to meet this requirement. Studies were also conducted that showed the model meets the IEEE 2800 requirement for overfrequency operation, and demonstrates the real power droop which will enhance grid recovery from events.

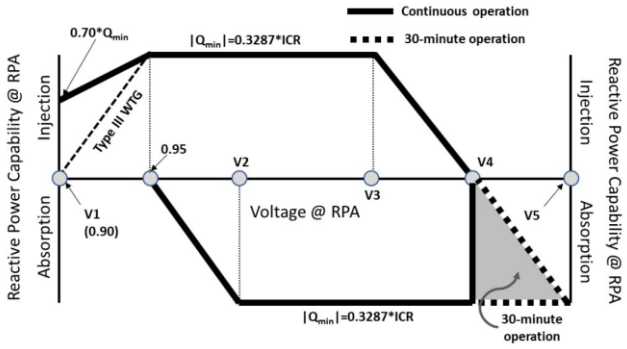

Figure 13. Minimum reactive power capability at point of applicability (RPA), with V2=1.00, V3=1.04, and V4=1.05.

2.5. OSW Farms in NYISO, ISO-NE and PJM systems

The status of the proposed OSW in this study changed considerably over the course of this project. The initial list of awarded projects that was compiled in 2023 quickly became outdated. This list was updated at the start of Task 2. The wind farms considered in the Task 2 studies are given in Tables 6, 15, and 20.

3 Task 1.2. Electromagnetic (EMT) System Equivalent Models for the Onshore Bulk Power Grid

In Task 1.2, a set of dynamic equivalent models of the onshore bulk power grid were developed. These equivalent models were for the East Coast regional transmission systems, including NYISO, ISO-NE and PJM. The reduced EMT model is developed based on NYISO data from FERC 715 (MMWG2022Series and MMWG2023Series) provided by NYISO. The system-wide East Coast regional transmission grid model is used in conjunction with up to 30 GW of wind farms.

This task included 5 distinct steps. This milestone report documents each of these steps, in sections **A** through **E**.

3.1. Convert FERC 715 model to reduced PSCAD models

This section describes the process of converting power grid models from NYISO data FERC 715 (MMWG2022Series) in PSS/E [1] to develop an EMT reduced model in PSCAD. The EMT reduced model has been developed based on NYISO data (MMWG2022Series) using the PSS/E model. This process will demonstrate the accuracy and fidelity of the expanded models integrating other RTO transmission systems.

Onshore Power System Data

After developing the Offshore Wind Farm (OSW) model from Task 1.1, the team aims to develop the Onshore Grid System (OGS) model including the Eastern Interconnection area. As a result, the team requested and received the FERC 715 (Annual Transmission Planning) data from NYISO. This information is critical energy infrastructure information (CEII), and is covered by non-disclosure agreements. This confidential information is therefore not included in this report.

Not only does the data cover the Eastern Interconnection domain, but FERC 715 also comprises some Western Interconnection data, demonstrating the diversity of the grid model. To be specific, the Multiregional Modeling Working Group (MMWG) develops comprehensive power system models that represent the interconnected electric transmission networks across North America [2]. These models included in FERC 715 data are crucial for conducting power flow and dynamic stability studies, which help ensure the reliability and security of the bulk electric system. The team used the MMWG data, which is

developed for the year 2022, to develop the OGS model. These models include detailed data on transmission lines, generation units, loads, and system configurations for various scenarios and timeframes.

The MMWG consists of both the steady state power flow data and dynamic data including generator characteristics and control systems. There are several power flow cases included in the MMWG2022Series data comprising Summer Peak Load, Winter Peak Load, and Spring Peak Load. The MMWG2022Series power flow encompasses approximately 94000 buses and 11000 generators, there are over 9000 dynamic machine models representing the dynamic behavior of the Eastern power system. From this data, the team developed Onshore Grid Electromagnetic Transient (EMT) model providing a detailed and accurate picture of high-frequency events and Small Signal Models (SSM) for use in frequency domain studies of system stability and oscillatory performance. These reduced models will then be coupled with the OSW and IBR models of Task 1.1 for the system studies of Task 2.

3.2. Small Signal Model for Eastern Power System

Dynamic Reduction Process

The project's goal is to dynamically reduce the full Eastern Interconnection data case, which is received from NYISO, to an acceptably small size model that can be practically simulated in PSCAD. To this end, the EPRI's DYNRED application [3] is utilized to implement the reduction process and create the dynamically reduced system. The reduction algorithm of DYNRED is based on identifying coherent generators and aggregating them together into one equivalent machine. Figure 14 shows the process steps for this reduction.

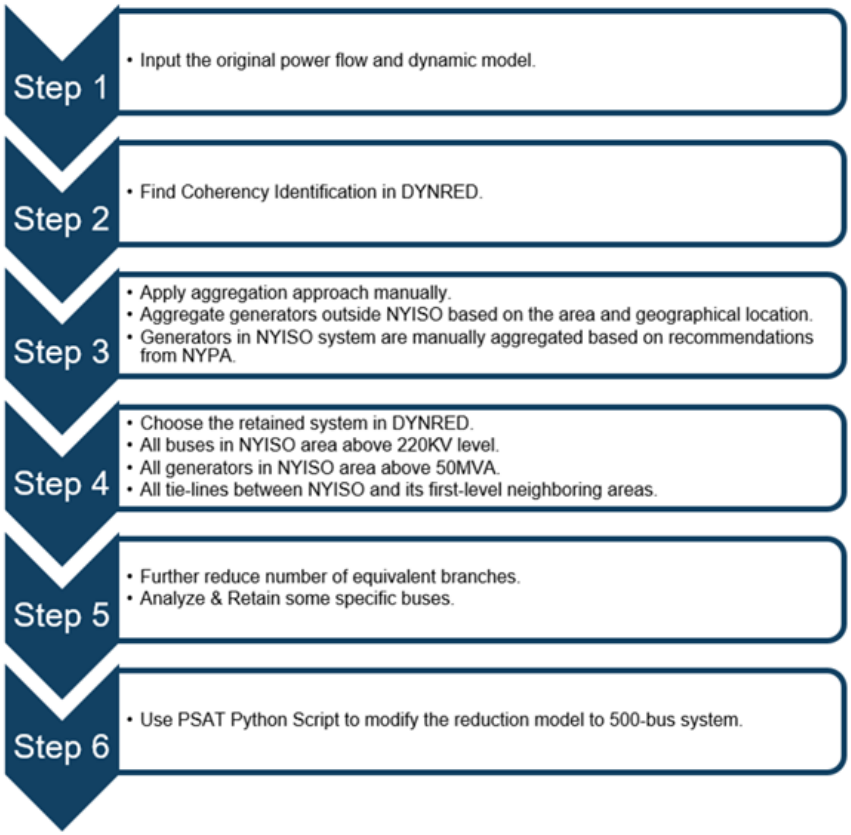

Figure 14. DYNRED Reduction process

After each implemented step, there are different versions of the reduced system produced by DYNRED. Step 1 and 2 deals with the original CEII full case, approximately 94000-bus data. With the retained center (NYISO), the scale of the (Electranix n.d.) system steadily decreased after each step: from 94000 buses to 5000 buses at step 3, 3000-bus model at step 4, remaining 2000 buses at step 5, and finally the reduced model contains 1400 buses after finishing step 6.

Small Signal Analysis Validation

To cross-validate the power flow and dynamic behavior of the reduced models against the original case, the SSAT from Powertech Labs is applied to determine the inter-area modes where NYISO generators have large mode shape. Table 3 shows the 4 inter-area modes identified by SSAT and compares these mode shapes between varied versions of the reduction model. This data validates the 3000 and 1400 bus reduced models.

Table 3. Small signal analysis performed on different versions of reduction model

Mode #	5000-Bus Model		3000-Bus Model		1400-Bus Model	
	Frequency (Hz)	Damping (%)	Frequency (Hz)	Damping (%)	Frequency (Hz)	Damping (%)
1	0.9848	6.16	0.9845	7.79	0.9886	7.65
2	0.968	8.17	0.9658	8.51	0.9656	8.56
3	0.8642	9.22	0.8128	6.81	0.8514	7.21
4	0.7546	6.98	0.7333	6.62	0.7345	6.64

Electromagnetic Transient Model for Eastern Power System

This section describes the procedure to convert the MMWG2022Series models from PSS/E software to PSCAD software using PSSE-PSCAD conversion tools, Electranix E-TRAN (Translator for Power System Simulation) [4], and significant custom development.

Procedure to Convert the MMWG2022Series from PSS/E to PSCAD Using E-TRAN:

1. Load PSS/E Data Files in E-TRAN:
   - Import the .raw file (steady-state power flow data) and .dyr file (dynamic device parameters) from the PSS/E model into E-TRAN as shown in Figure 15.
2. Define Conversion Scope:
   - Identify which parts of the NYISO model will be retained in detailed EMT format.
   - Determine the boundaries for network equivalencing.
3. Select Line Model:
   - Use the Bergeron traveling wave line model for transmission lines.
4. Set PSCAD Properties:
   - Configure key PSCAD settings such as time step, finish time, plot step, and fundamental frequency (60 Hz).
   - Specify initialization times for sources, machines, and loads:
     - Source Initialization Time: Set for initializing sources and generators.
     - Machine Initialization Time: Release exciter and governor after initialization.
     - Load Initialization Time: Gradually transition loads from constant RLC to the specified load type in the .raw file to ensure stability during startup.
5. Add Detailed Component Data:
   - Use the E-TRAN PSCAD data substitution library to input detailed information for specific components, such as wind and solar plants.
   - Save this detailed data in a PSCAD library file (.psl).
   - Replace unsupported models to ensure compatibility between PSS/E, E-TRAN, and PSCAD.
6. Generate PSCAD Files:
   - E-TRAN automatically generates .psc and .pscx files in PSCAD format. These files include detailed, interconnected data for buses, loads, DC links, switched shunt devices, branches, generators, transformers, and phase shifters. Bus voltages, angles, and PQ loadflow data from the

solved loadflow input file are used to directly initialize sources, generators, and non-linear loads in PSCAD.

- A network equivalent for the remaining system is created using fundamental frequency impedance and power flow data. This equivalent is a multi-port representation, accurate for steady-state, open-circuit, and short-circuit conditions. It incorporates Thevenin voltage sources to match PQ flow and accurately represent generation within the equivalent network.

Figure 15 illustrates this process.

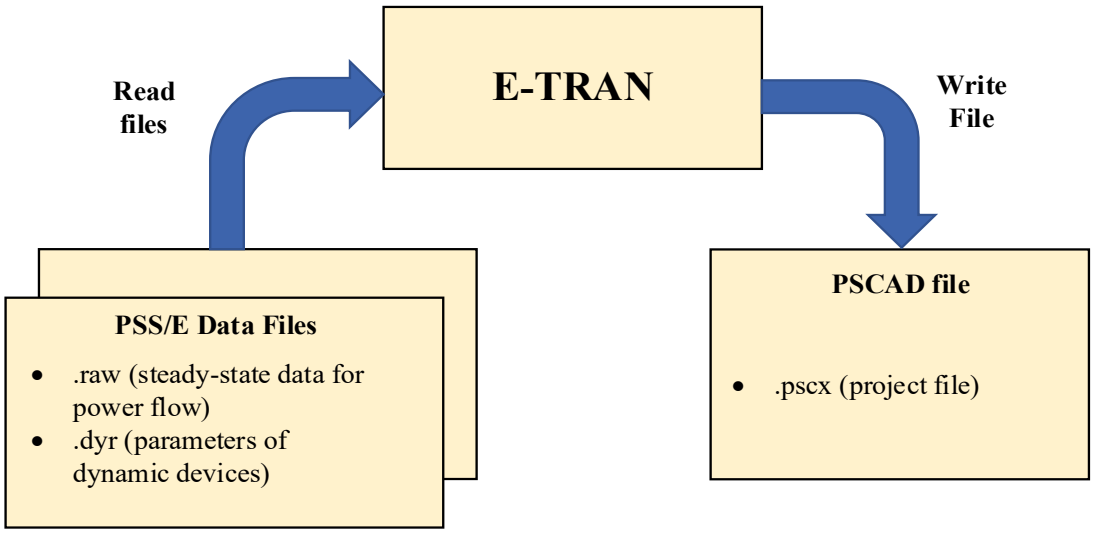

Figure 15. The flow of data during an E-TRAN conversion

EMT models for Zone JK:

- Case: 2028 NY Spring Light Load, MMWG 2022 Series, FINAL, CEII Data (94k buses).
- Tools Used: E-TRAN, PSS/E, and PSCAD.
- EMT-Reduced Model:
  - Retains buses in New York City (Zone J) above 345 kV and Long Island (Zone K) above 138 kV, including all buses connected to generators in these areas.
  - The remainder of the network is represented as Thevenin-equivalent sources.
  - Unsupported models for EMT (e.g., governors and compensators) are replaced to ensure compatibility between PSS/E, E-TRAN, and PSCAD.
- Final EMT Model for Zone J-K Reduced System:
  - Total buses: 187 (NYC: 77 buses, Long Island: 105 buses, Buffer zones: 5 buses.)
- EMT Model Initialization time:
  - Source initialization time: 0.1s
  - Machine release time (kick-in exciter, governor): 2s
  - Load release time: 5.5s

Measurements for generator ST1 (Steam Turbine) on Long Island.

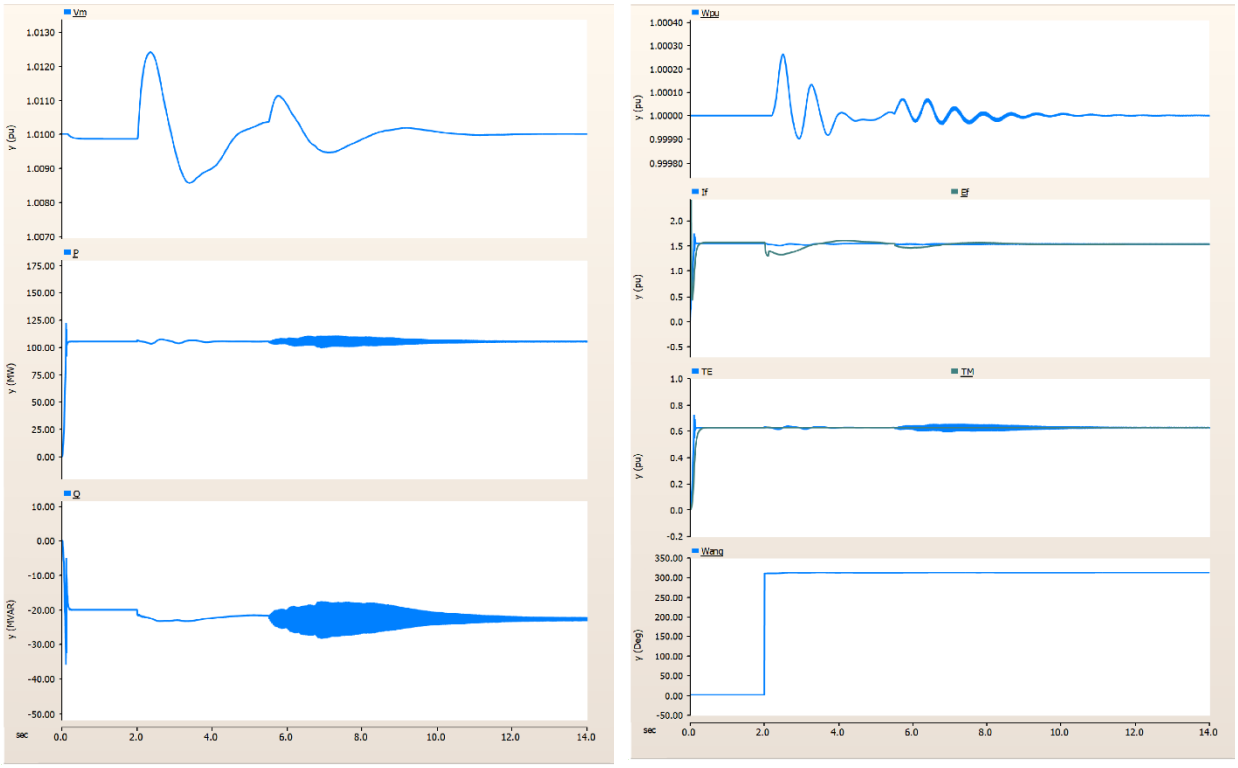

Figure 16. Generator ST1 initialization process.

Figure 16 show the initialization process for the generator ST1 on Long Island with RMS terminal voltage (p.u), Reactive Power (MVAr), Active Power (MW), Speed (p.u), Field Voltage – Field Current (p.u), Electrical and Mechanical Torque (p.u), and Internal phase angle (degrees). At 2 seconds, machine release time (exciter and governor activation), and load release time is at 5.5 seconds occurs for the entire reduced EMT model.

3.3. Compile onshore system designs for PJM and ISO-NE

Upgraded Public Policy Transmission Need data for the year 2029

As mentioned from part A, the team initially received the MMWG data case for the year 2022. However, the team decided to upgrade the initial data case to study the power system in the future by adding Public Policy Transmission Need (PPTN) data. PPTN data refers to a dataset developed to address specific public policy requirements in the context of power system planning and development. These needs typically arise from government-mandated policies, such as renewable energy targets, emissions reductions, grid reliability standards, or energy market reforms, such as what is demonstrated in New York's CLCPA. The data is used to evaluate and plan transmission system upgrades or new infrastructure to meet these policy-driven goals. After upgrading, our data comprising around 97000-bus and 1200-generator models, is

developed for the year 2029. Before implementing further developments and analyses, the team conducted the flat start study of the updated 2029 data case. The system model converged in the steady state and was determined to be reliable.

Retired generation planning

The planned retirements of natural gas and dual fuel generation in Zones J and K were also investigated. Again, this list changed significantly during the course of this project, due to the changes in OSW and the delays in the scheduled deliverable dates for those continuing. Additionally, concerns were raised about NYCA reliability if these retirements had occurred as originally scheduled. In Task 2, the 2028 NY Spring Light Load case was selected to investigate the impacts of the loss of inertia of these plants, as these Zone J and K plants are off-line in this case.

Reduced PSCAD onshore model for NYISO, PJM and ISO-NE

This section describes the procedure for developing the model reduction technique for the entire study area. In addition, the EMT reduced models must retain critical points of interconnection (POIs) and other local devices (e.g., series capacitors, thermal generators) that pose sub-synchronous oscillation risks for evaluation in Task 2.1 and future studies. To ensure the models meet the requirements of local transmission system operators, the EMT reduced models will be tested under three-phase faults.

Procedure to convert the updated MMWG2022 Model from PSS/E to PSCAD to achieve a combined EMT model that includes NYISO, ISONE, and PJM.

(Tools Used: E-TRAN, PSS/E, and PSCAD.)

1. Load PSS/E Data Files in E-TRAN:
   - Using case: 2028 NY Spring Light Load, MMWG 2022 Series, FINAL, CEII Data (94k buses) with power flow and dynamic data.
   - PSSE Summary:
     - PSSE Busses: 94178, PSSE Generators: 11744, PSSE Loads: 50528
     - PSSE Branches: 113703, PSSE Transmission Lines: 86258
     - PSSE Transformers: 27367
2. Define areas will be retained in detailed EMT format:
   - Identify which parts of the NYISO model will be retained in detailed EMT format.
   - Retain buses in New York City (Zone J) above 345 kV and Long Island (Zone K) above 138 kV, including all buses connected to generators in these areas. Total: 182 buses.
   - Retain buses in ISO-NE specifically, Massachusetts and Maine above 345 kV including all buses connected to generators in these areas. Total: 200 buses.
   - Retain buses in PJM and part of NC: New Jersey (Atlantic City Electric) above 230 kV, Delaware (DP&L) above 230 kV, and Dominion (Virginia Beach–North Carolina), including all buses connected to generators in these areas. Also, retain New Jersey (PSE&G, which is connected to New York City). Total: 239 buses.

- Keep these buses for wind farm interconnection. The rest of the network will be modeled as Thevenin-equivalent sources.
- Total buses in EMT model for NYISO, ISONE, and PJM: 621 buses
- Total generators (with full dynamic models) in EMT model for NYISO, ISONE, PJM, and NC: 154 generators with full dynamic models

3. Select Line Model:
   - Use the Bergeron traveling wave line model for transmission lines.
4. Set PSCAD Properties:
   - Time step: 50 us, plot step: 250 us, and fundamental frequency (60 Hz).
   - Source initialization time: 0.1s
   - Machine release time (kick-in exciter, governor): 0.5s
   - Load release time: 5s
5. Add Detailed Component Data:
   - Use the E-TRAN PSCAD data substitution library (for wind plants) to replace unsupported models by E-TRAN, PSSE and PSCAD.
6. Generate PSCAD Files:
   - E-TRAN automatically generates .psc and .pscx files in PSCAD format. These files include detailed, interconnected data for buses, loads, DC links, switched shunt devices, branches, generators, transformers, and phase shifters. Bus voltages, angles, and PQ loadflow data from the solved loadflow input file are used to directly initialize sources, generators, and non-linear loads in PSCAD.
   - After that, unsupported models for EMT (e.g., governors and compensators) are replaced to ensure compatibility between PSS/E, E-TRAN, and PSCAD.

-

A three-phase fault study was performed on the 621-bus model. A bolted fault was applied at an urban 345-kV POI (Bus A), one of the substations proposed for offshore-wind interconnection at t = 71 s and cleared after 6 cycles. Responses at two adjacent 345-kV substations, Bus B and Bus C, were analyzed. (Actual names are masked for CEII.)

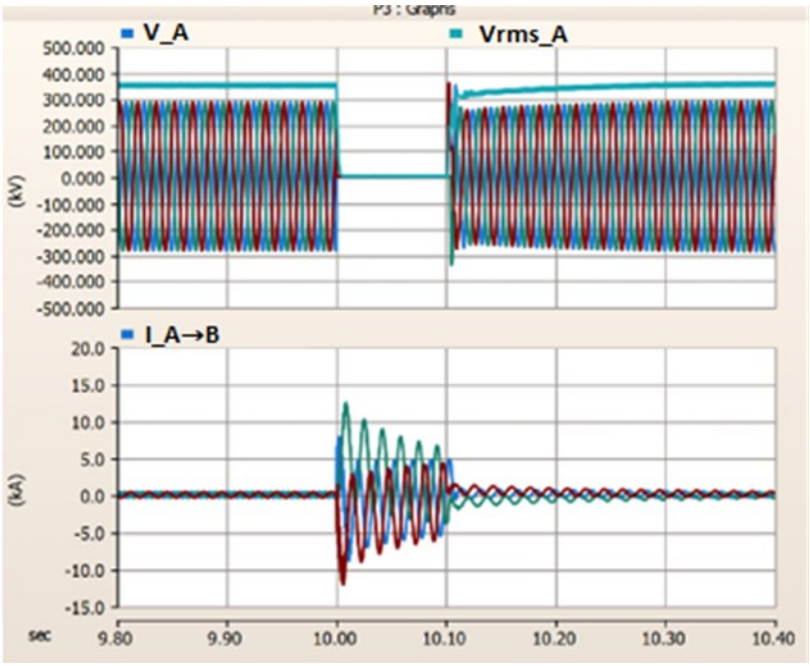

Figure 17. Three-phase fault response at Bus A (345 kV). Vrms_A = RMS line-to-line voltage; V_A = instantaneous line-to-neutral voltage; I_A→B = line current from Bus A to Bus B.

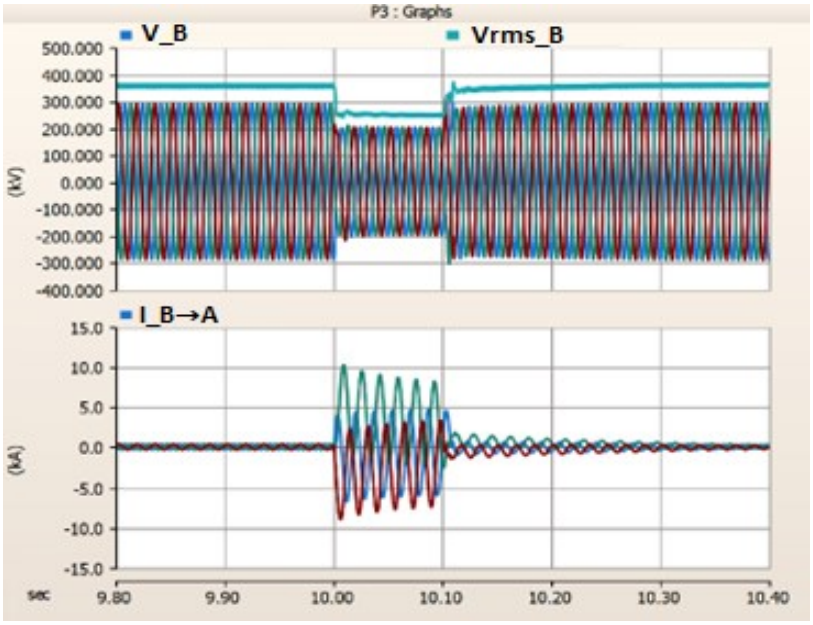

Figure 18. Three-phase fault response at Bus B (345 kV). Vrms_B, V_B, I_B→A (line current Bus B→Bus A)

Figures 17–19 show voltage and current responses at Bus A an urban 345-kV POI proposed for OSW interconnection and adjacent Buses B and C during a three-phase fault.

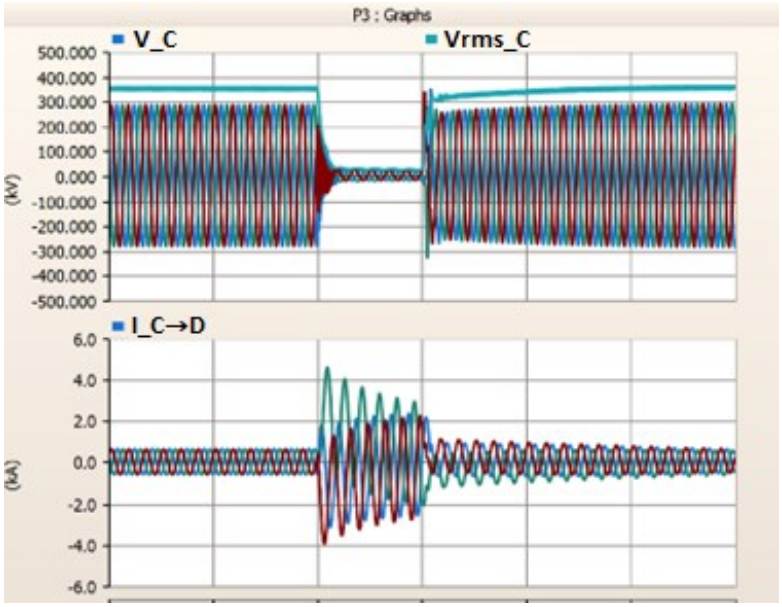

Figure 19. Three-phase fault response at Bus C (345 kV). Vrms_C, V_C, I_C→D (line current from Bus C to an adjacent corridor).

Pre-fault voltages and line currents are flat and consistent across Bus A, Bus B, and Bus C, indicating a well-initialized base case. During the 6-cycle three-phase fault at Bus A, Vrms_A shows the deepest sag and the Bus A→Bus B line current peaks as expected; the nearby buses exhibit smaller but time-aligned depressions and current surges. After clearing, both RMS and instantaneous voltages recover promptly with only bounded ringdown, and currents settle back to steady values. Taken together, these responses validate the base model as a sound starting point for subsequent studies that connect offshore wind and assess its impact on local voltages, line currents, and stability margins. This result shows that the 621-bus system operated in the steady state prior to the fault, and the fault study is performed successfully.

Alongside a combined EMT model covering NYISO, ISO-NE, and PJM (621 buses) for the Spring Light-Load condition, we built separate area-specific models for NYISO, ISO-NE, and PJM for both Summer Peak and Spring Light-Load, as shown in Table 4. These modular models reduce simulation runtime and focus the studies on the landing zones where OSW projects primarily affect local generators and network performance.

Table 4. Area-Specific EMT Models for NYISO, ISO-NE, and PJM

Model	Retained Areas	Total buses
Zone JK - Spring Light Load	• Zone J (NYC) buses ≥ 345 kV, and Zone K (Long Island) buses ≥ 138 kV • All internal generators in service in the spring	187 buses
Zone JK - extend- Spring Light Load	• Zone J (NYC) buses ≥ 345 kV, Zone K (Long Island) buses ≥ 138 kV, Zones G (Hudson Valley) ≥ 345 kV, H (Milwood) ≥ 345 kV, I (Dunwoodie) ≥ 345 kV, E (Mohawk Valley), and F (Capital) ≥ 345 kV. • All internal generators are in service in the spring. • Including series-compensated lines (Marcy South Series Compensation Project, Knickerbocker Series Compensation Project, Leeds-Hurley Smart Wire Smart Valve Project).	288 buses
Zone JK - Summer Load	• Zone J (NYC) buses ≥ 345 kV, and Zone K (Long Island) buses ≥ 138 kV, • All internal generators are in service in the summer. • Including series-compensated lines (Marcy South Series Compensation Project, Knickerbocker Series Compensation Project, Leeds-Hurley Smart Wire Smart Valve Project).	303 buses
ISO-NE - Spring Light Load	• Massachusetts (MA) buses ≥ 220kV, and Rhode Island (RI) buses ≥ 220kV. • All internal generators are in service in the spring.	169 buses
ISO-NE- Summer Load	• Massachusetts (MA) buses ≥ 220kV, and Rhode Island (RI) buses ≥ 220kV. • All internal generators are in service in the summer.	218 buses
PJM- Spring Light Load	• PJM backbone (all buses ≥ 500 kV), Dominion (DVP) buses ≥ 500 kV, Atlantic City Electric (AE) buses ≥ 230 kV, Delmarva Power & Light (DP&L) buses ≥ 230 kV, and Virginia Beach (VABEACH) buses ≥ 230 kV. • All generating units within the AE, DP&L, and VABEACH areas are in service in the spring.	351 buses
PJM - Summer Load	• PJM backbone (all buses ≥ 500 kV), Dominion (DVP) buses ≥ 500 kV, Atlantic City Electric (AE) buses ≥ 230 kV, Delmarva Power & Light (DP&L) buses ≥ 230 kV, and Virginia Beach (VABEACH) buses ≥ 230 kV. • All generating units within the AE, DP&L, and VABEACH areas are in service in the summer.	351 buses

3.4. Parallel process to simulate the onshore and offshore system

Our reduced EMT model in PSCAD includes the onshore system, comprising a total of 621 buses and 154 generators for the NYISO, ISO-NE, PJM, and parts of North Carolina. Due to the model's large size, integrating offshore wind farms significantly increases computation time, for example, simulating 1 second with one wind farm takes 2.5 hours. Moreover, because of the onshore model's size, the workspace for a single PSCAD project is insufficient when connecting more than two wind farms.

To address these issues, we separated the onshore model into one project and distributed the 15 wind farms across seven other projects to enhance parallel computing capabilities. This approach is based on the

Parallel Network Interface (PNI) introduced by (Clarkson University 2023) (Clarkson University 2023) (IEEE 2022) (Clarkson University 2023, ERCOT 2024). With PNI process a single electric network in PSCAD may be split so that each electric subsystem is represented by a separate case project, and thereby run using a separate EMTDC process. Each EMTDC process is linked together via Parallel Network Interface (PNI) to form a cohesive simulation that is run from within a single workspace.

- Project 1: an onshore system for the NYISO, ISO-NE, PJM, and parts of North Carolina
- Project 2: Windfarm 1, Windfarm 2 (NYISO)
- Project 3: Windfarm 3, Windfarm 4 (NYISO)
- Project 4: Windfarm 5, Windfarm 6 (NYISO)
- Project 5: Windfarm 7, Windfarm 8 (ISO-NE)
- Project 6: Windfarm 9, Windfarm 10 (ISO-NE)
- Project 7: Windfarm 11, Windfarm 12 (PJM)
- Project 8: Windfarm 13, Windfarm 14, Windfarm 15 (PJM)

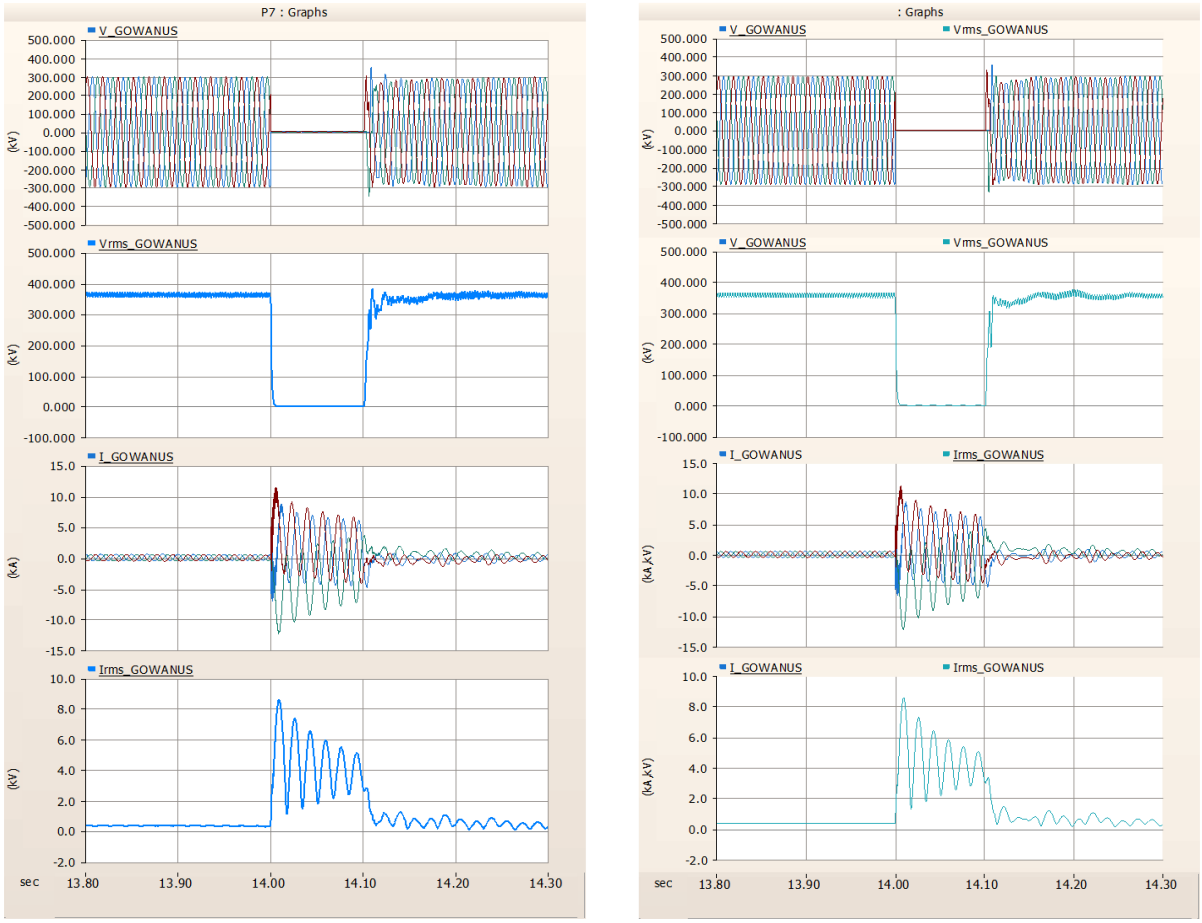

(a) (b)

Figure 20. Onshore + offshore model with (a) parallel network interface (b) direct interface

To validate the onshore and offshore model with the Parallel Network Interface (PNI), we compared its behavior with that of a model using a direct interface during a three-phase fault. From Figure 20, after applying a three-phase fault at the Gowanus bus at 14 seconds for 6 cycles, the model with the PNI exhibits the same behavior as the model where the wind farm is connected directly to the onshore system. Additionally, the simulation time for the case with only one wind farm integrated with the onshore system using the direct interface is 45 hours, whereas with the PNI, it is 15 hours. Therefore, the simulation time has been reduced by two-thirds.

3.5. Validate full regional onshore + offshore system model with NY RTDS model

The validation of the full regional onshore and offshore system model against the NY RTDS model faces two key challenges. Firstly, the current NY RTDS model utilizes data from 2018, while our model is designed for the year 2029, creating a temporal discrepancy that may impact the accuracy of the comparison. Secondly, if we aim to compare our model with the 2029 version of the NY RTDS model, we will need to wait until next year, as the 2029 version of the RTDS model is still under development and has not yet been completed. These challenges need to be considered when assessing the model's performance and future validation timelines. In order to meet the deadline and overcome these challenges, the team decided to validate the full regional onshore and offshore system model in another way. While the OSW model was already validated through multiple criteria and standards from Task 1.1, the onshore grid EMT model would be benchmarked with the original PSS/E grid model to ensure that both models provide consistent and reliable results under identical operating conditions.

Benchmarking of Onshore Grid EMT model

Since the team verified the initialization for the data case by running flat start from Section B, the onshore grid model in PSS/E would be the accurate benchmark to validate the EMT model of onshore system. As the EMT onshore system is developed from PSS/E model, EMT and PSS/E models represent the same system configuration. Initial validation involves comparing steady-state results, such as bus voltages, line flows, and system losses, obtained from power flow solutions in PSS/E and EMT simulations. Once steady-state alignment is achieved, dynamic validations are conducted by applying identical disturbances, such as faults, generator trips, or load changes, to compare the system's transient responses, including voltage, frequency, and power oscillations. Discrepancies in results are analyzed to identify potential model differences, such as control system settings, network impedance mismatches, or time-step resolution in EMT simulations. The validation process also considers inherent differences in modeling

fidelity, with the EMT model capturing high-frequency phenomena and detailed device-level interactions, while the PSS/E model focuses on system-level behavior. Addressing these differences ensures the EMT model provides a refined representation while maintaining consistency with the broader PSS/E model, ultimately enabling accurate and scalable system analysis.

Steady-state validation

While EMT models focus on time-domain simulations with high temporal resolution, PSS/E models are widely used for load flow and stability studies, emphasizing steady-state power system analysis. The objective of this validation is to confirm that the EMT model accurately replicates the steady-state operating conditions, such as active and reactive power flows, voltage magnitudes, and system losses, as computed by the PSS/E model. Steady-state load flow results from the PSS/E model serve as the reference, and the EMT model's initial conditions are configured to match these results. Comparisons are made for critical metrics, such as active and reactive power flows of generator units, and loads.

To implement the validation, PSCAD simulations are started from a de-energized state, which demands a far more involved start-up procedure, meanwhile PSS/E model would run a flat-start case as in Part B. The startup of the EMT model is accomplished by initializing the synchronous generators in the model as ideal voltage sources, subsequently turning on all of the synchronous generator dynamics, and then releasing the loads. The verification of steady-state power flow is summarized in Table 5, with the achieved aggregates from the PSCAD generation and load presented against the PSSE quantities. By comparing a variety of numbers of generating units and loads in active power and reactive power flows, the respective total deviations were demonstrated to be minimal. The individual generator/load quantities were well within accepted bounds ($\pm$2% from the PSS/E case). Once the EMT model matches the PSS/E results within acceptable tolerances, confidence is established that it correctly represents the system's steady- state operating point. This validation provides a robust foundation for further dynamic and transient analyses using the EMT model, ensuring that its steady-state assumptions align with those of the well-established PSS/E framework

Table 5. Steady State Load Flow Comparison between PSS/E and PSCAD Models during flat start scenario

Aspect	Simulation	Real Power (MW)	Reactive Power (MW)
Generation	Gen A (ISONE) – PSSE Model	181.9	53.3
	Gen A (ISONE) – PSCAD Model	181.87	53.338
	Gen B (NYC) -PSSE Model	217.8	-127.6
	Gen B (NYC) -PSCAD Model	217.81	-127.62
	Gen C (Long Island) -PSSE Model	105.1	-9.5

	Gen C (Long Island) -PSCAD	105.117	-9.505
Load	Load X (Long Island) – PSSE Model	29.942	1.442
	Load X (Long Island) – PSCAD Model	29.95	1.442
	Load Y (ISONE) – PSSE Model	8.749	5.249
	Load Y (ISONE) – PSCAD Model	8.75	5.25

To verify that the PSCAD conversion preserves the operating point, we compared the flat-start power-flow solution from PSS/E and PSCAD at identical bus numbers for representative generators and loads across ISO-NE, NYC, and Long Island. Table 5 reports active power (MW) and reactive power (MVAr) for generations and loads in these study areas. The values agree to within rounding precision in all cases, confirming that the reduced PSCAD model reproduces the PSS/E steady-state operating point prior to dynamic studies.

Dynamic behavior validation

The dynamic validation process involves comparing key responses (such as voltage, current, and frequency) under identical system disturbances. The EMT model typically captures transient oscillations with higher fidelity due to its detailed time-domain simulations, whereas the PSS/E model provides insights into steady-state and slower dynamics. Consistency checks are performed by matching dynamic parameters such as generator inertia, governor, exciter, and protection settings. Key metrics, such as fault current and recovery time, are then compared.

The first step of the dynamic validation involved three-phase fault tests for both PSS/E and PSCAD models. Three-phase fault were applied at the POI interconnection of an OSW to the power grid. A fault at the Long Island Holbrook bus was of particular interest, due to the relatively low SCR at that location. In these results, a 6-cycle balanced fault was initiated at 14 (s), after the startup transients had decayed. The study was done for the spring light load, as the majority of natural gas and dual fuel generation in Zones J and K was offline for this case. The rms fault current response of the PSS/E and EMT models are illustrated in Figure 21 and 22, respectively. It can be seen that the maximum magnitude of fault current of both models would be approximately equal to 2.7 per unit. The onshore grid models in PSS/E and PSCAD. The RMS fault currents both show a low frequency oscillation of 1.5 hz. In both simulations, these oscillations are similarly well damped. The EMT model does show a well damped oscillation immediately following fault inception, due to the transient and sub-transient effects of the synchronous generators. The EMT model also shows a lightly damped subsynchronous oscillation following fault clearing. The PSS/E model is not expected to capture either of these responses.

The validated EMT model not only provides confidence in its ability to represent system behavior but also acts as a benchmark for studying phenomena that cannot be captured by the PSS/E model alone, such as high-frequency switching transients or interactions between inverter-based resources. Ultimately, this validation ensures that the EMT model can be reliably used for detailed analyses, such as transient stability studies, protection scheme evaluations, and grid-forming inverter interactions, complementing the broader insights offered by the PSS/E model.

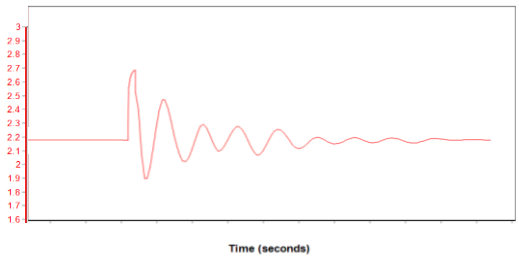

Figure 21. Fault current signal of PSS/E model

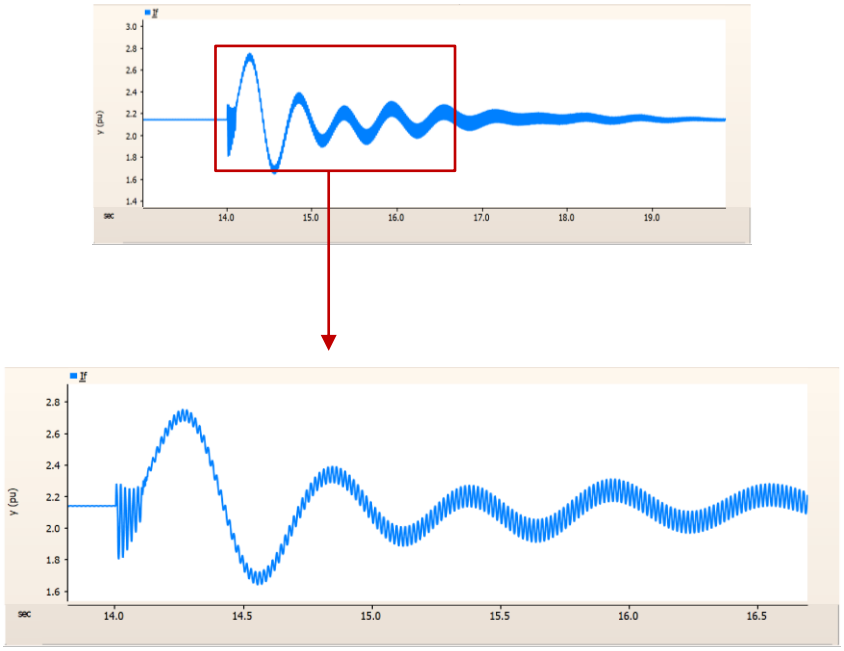

Figure 22. Fault current signal of the EMT model

3.6. Task 1 Summary

In Task 1 of this project involved the development of models for the project NOWRDC Award 192899-132 “Atlantic seaboard offshore stability risk evaluation & service”. The focus of Task 1.1 was on the offshore wind turbines, offshore substation, and transmission system up to the point of interconnection (POI). Individual models were created for each of the proposed wind farm. The work done on Task 1.2

involved the modeling of the bulk power system that the OSW farms that the NYISO, ISO-NE and PJM areas. This modeling was achieved in 5 discrete steps. These steps are presented individually in Sections A-E of the Task 1.2 chapter of this report. The PSCAD model includes the East Coast regional transmission grids (including NYISO, ISO-NE, and PJM), and wind farms for these areas have been developed and validated in this task. The development of these power system models presented many challenges. Significant model reductions in the model size were required, and these reduced order models were validated. Still, these models required significant computational time and space, and parallel computing methods were developed to reduce this time. In Task 2, the Task 1 models will be used to conduct small-signal and transient stability analyses, and subsequently risk analysis and mitigation methods will be developed.

4. Task 2.1. Controls Instability Risk Identification and Metrics

The Task 2.1 goals were to complete the risk identification method, including risk metrics, simulation cases and results, applied to the onshore equivalent PSCAD models of the East Coast regional transmission grids (NYISO, ISO-NE and PJM) and their associated wind farms. This task comprised three distinct steps, which are documented in Sections **A** through **C** of this section.

4.1. Develop risk metrics

Develop risk metrics evaluating the level of load rejections, unit tripping, and the number of outages with the applicable standards, including NERC PRC-006, PRC-024, IEEE 2800, regional operator, and utility requirements. For IEEE 2800 standard [5], the team already designed risk metrics for interconnection and interoperability of Inverter-Based Resources (IBRs) with the Bulk Power System (BPS) in Section 2.5 of this project.

NERC PRC-006 Standard

PRC-006 is a NERC Reliability Standard designed "To establish design and documentation requirements for automatic underfrequency load shedding (UFLS) programs to arrest declining frequency, assist recovery of frequency following underfrequency events and provide last resort system preservation measures." [6].

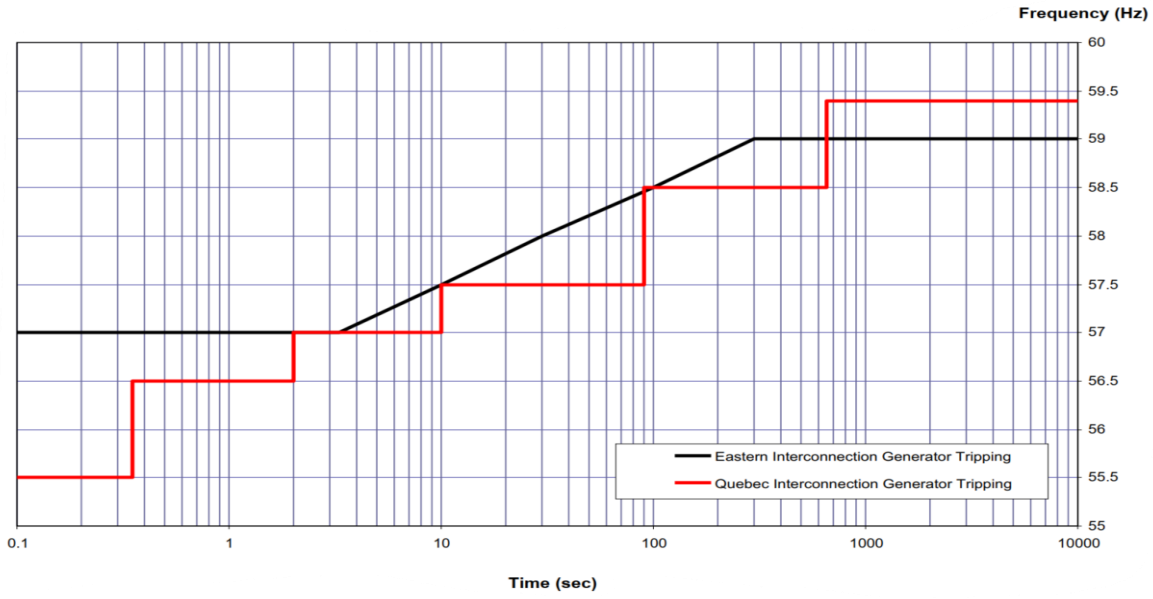

Figure 23. Underfrequency Thresholds of Generators for Eastern Interconnection [3]

In the NOWRDC project, the team designed risk metrics for generators underfrequency based on limited requirements for simulation and system performance in this standard. The underfrequency metric, shown in Figure 23, is specified for the Eastern Interconnection model.

NERC PRC-024 Standard

NERC PRC-024 Standard is developed "To assure that protection of synchronous generators and synchronous condensers do not cause tripping during defined frequency and voltage excursions in support of the BPS." [7]. This standard also applies to IBR technology, and the offshore wind plants would need to have adequately coordinated protection and control settings to comply. In this standard, risk metrics are designed for the frequency and voltage of generating resources. The Eastern Interconnection boundaries are presented in Figure 24 and Figure 25 for frequency and voltage metrics, respectively.

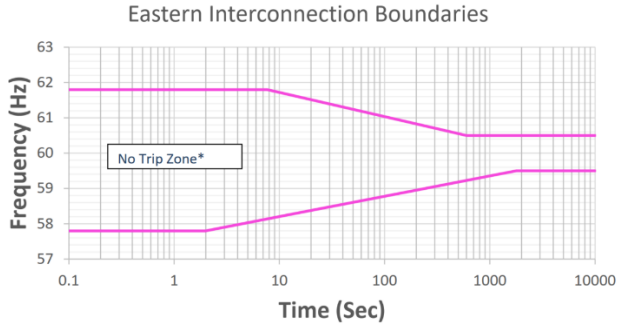

Figure 24. Frequency No Trip Boundaries for Eastern Interconnection [7]

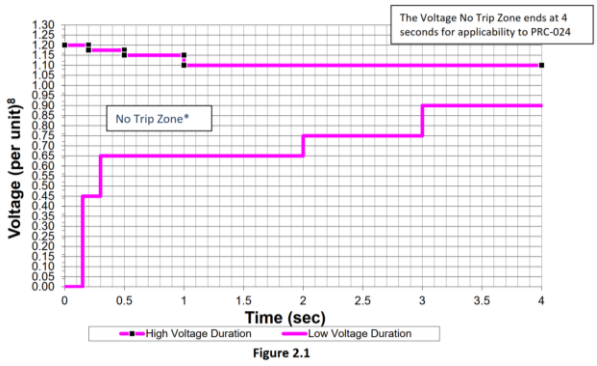

Figure 25. POI Voltage No-Trip Boundaries for Eastern Interconnection [7]

4.2. Identify high-risk conditions

Table 6 summarizes the NYISO OSW projects studied in this project. It includes their capacities, proposed POIs, voltage levels, designated onshore substations, and transmission type.

Table 6. Configuration of NYISO Proposed Offshore Wind Farms

Name	Capacity	Transmission	POI Substation	Voltage
Empire Wind 1	810 MW	HVAC	Gowanus (NYC)	345 kV
Beacon Wind	1230 MW	HVDC	Mott Haven (NYC)	345 kV
Sunrise Wind	924 MW	HVDC	Holbrook (LI)	138 kV
Vineyard Mid-Atlantic Wind	1300 MW	HVDC	East Garden City (LI)	345 kV
Juno Power Express	1200 MW	HVDC	Ruland Road (LI)	138 kV

These 5 OSWs with a total of 5.5GW are proposed to connect to two points of interconnection (POIs) in New York City (NYC) and three POIs in Long Island (LI), as illustrated in Figure 26.

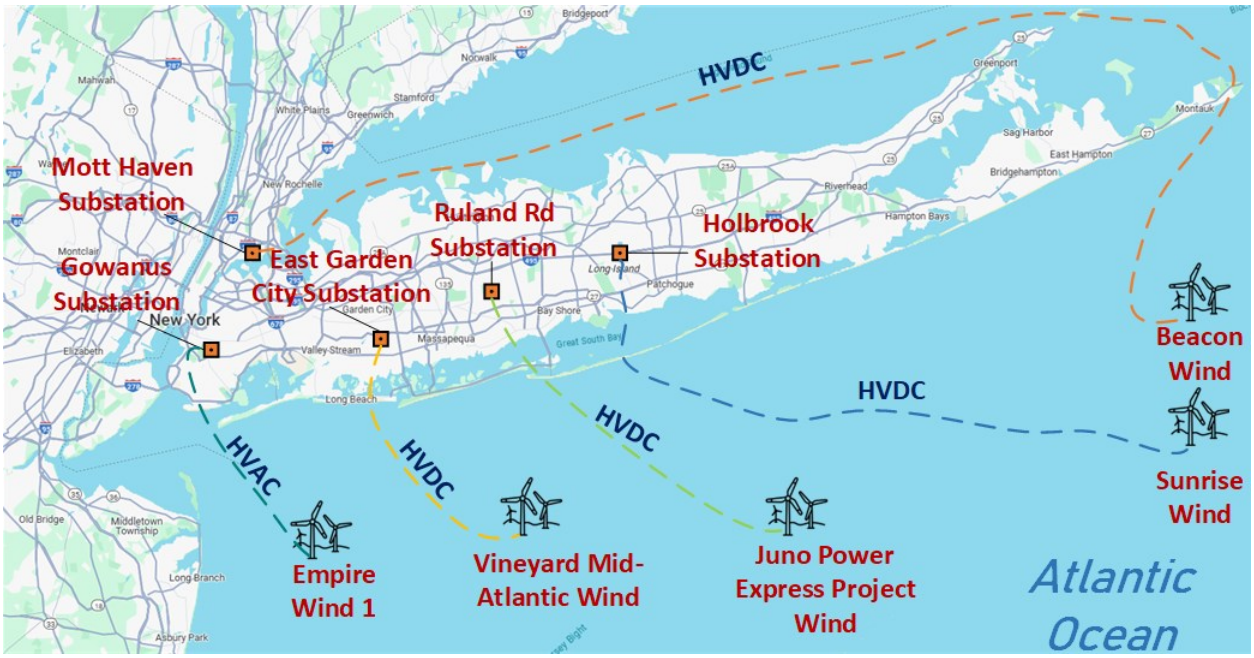

Figure 26. Strategic NYS OSW Deployment: Substations, Wind Farms, Atlantic-Ocean Interconnection.

High-Wind 100 % Output Evaluation

In this scenario, 5 OSW projects (combined rating of 5.5 GW) are connected to the NYISO spring light-load case, which contains 187 buses with a total generation capacity of 2.5 GW in retained areas. Wind speeds are assumed high enough that each turbine operates at its rated output, so the offshore complex exports its full nameplate power to shore throughout the study window.

Figure 27 shows the simulation results as the 5 wind farms are brought on line in sequence. The results show that the RMS voltage at all five offshore wind terminals remains between 0.95 pu and 1.03 pu throughout the simulation within the continuous-operation ("no-trip") band of 0.95–1.05 pu specified by IEEE Std. 2800-2022 (IEEE Std. for Interconnection and Interoperability of Inverter-Based Resources

(IBRs) Interconnection with Associated Transmission Electric Power Systems). System frequency is maintained between 59.85 Hz and 60.30 Hz, comfortably inside IEEE 2800 indefinite ride-through band of 59.4–60.6 Hz. No undamped oscillations or post-disturbance frequency dips are observed. Fast primary-frequency control at every offshore converter damp RoCoF (Rate of Change of Frequency) excursions, keeping the spring light-load grid stable under these conditions.

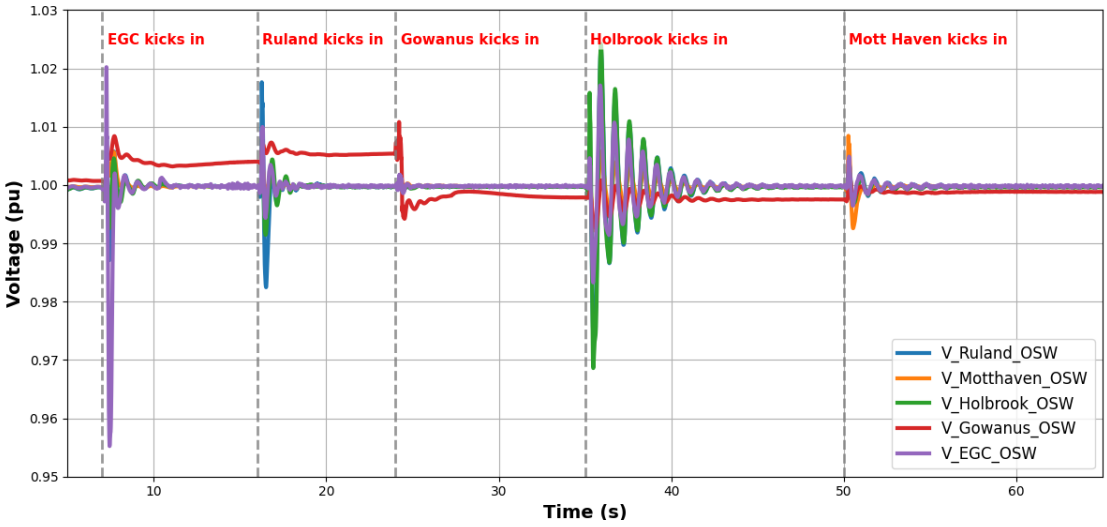

(a) Voltage (pu) response at 5 OSW farms terminal

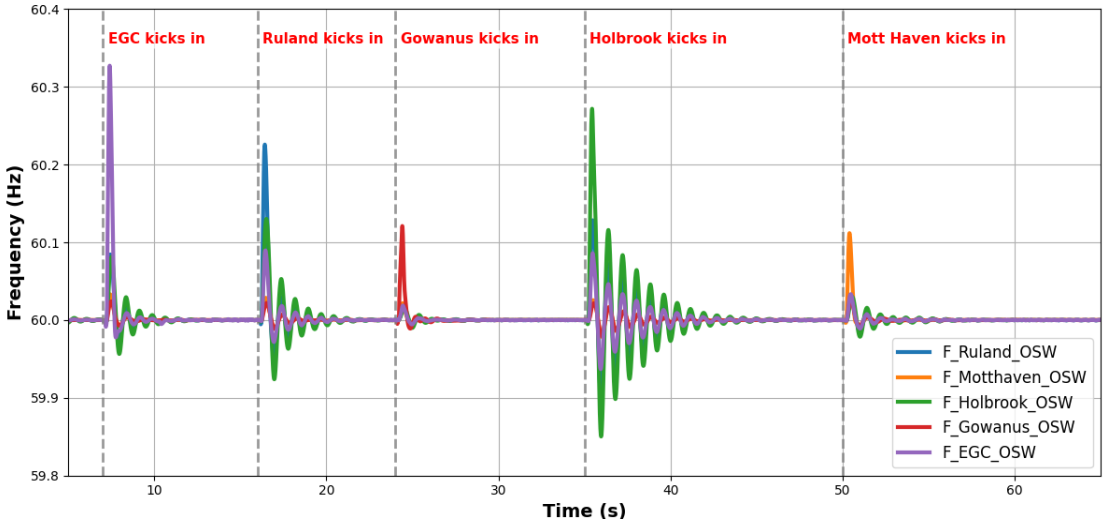

(b) Frequency (Hz) response at 5 OSW farms terminal

Figure 27. Voltage and frequency response at 5 OSW farms terminal

Active power at each offshore wind terminal ramps smoothly to its rated output and remains at that level for the entire simulation. Reactive power adjusts automatically to satisfy voltage-control demands, as shown in Figure 28.

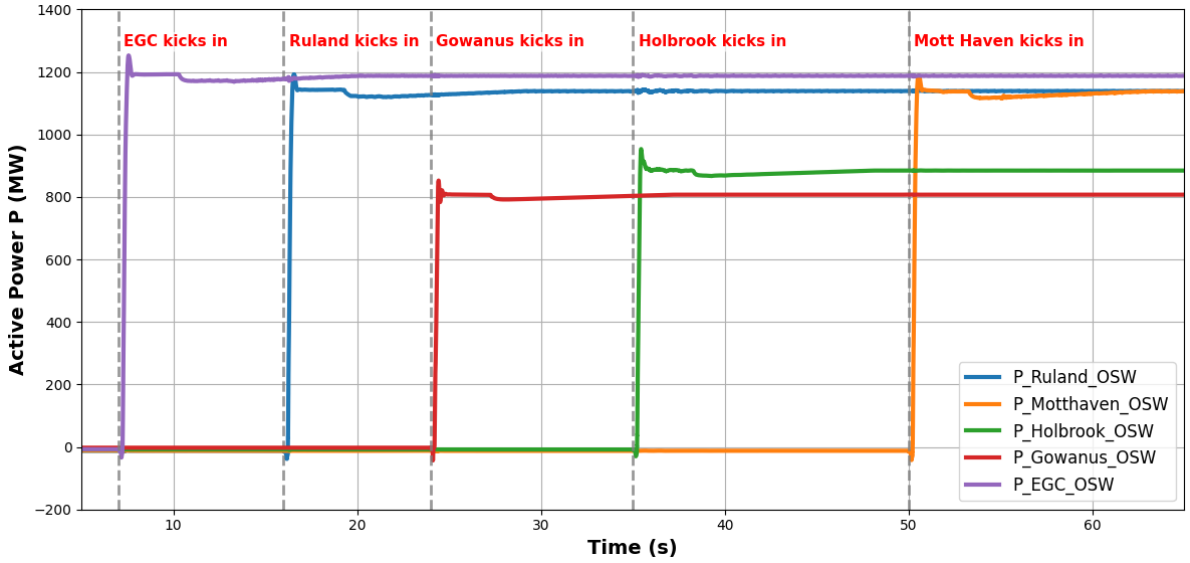

(a) Active power (MW) with 5 OSW farms

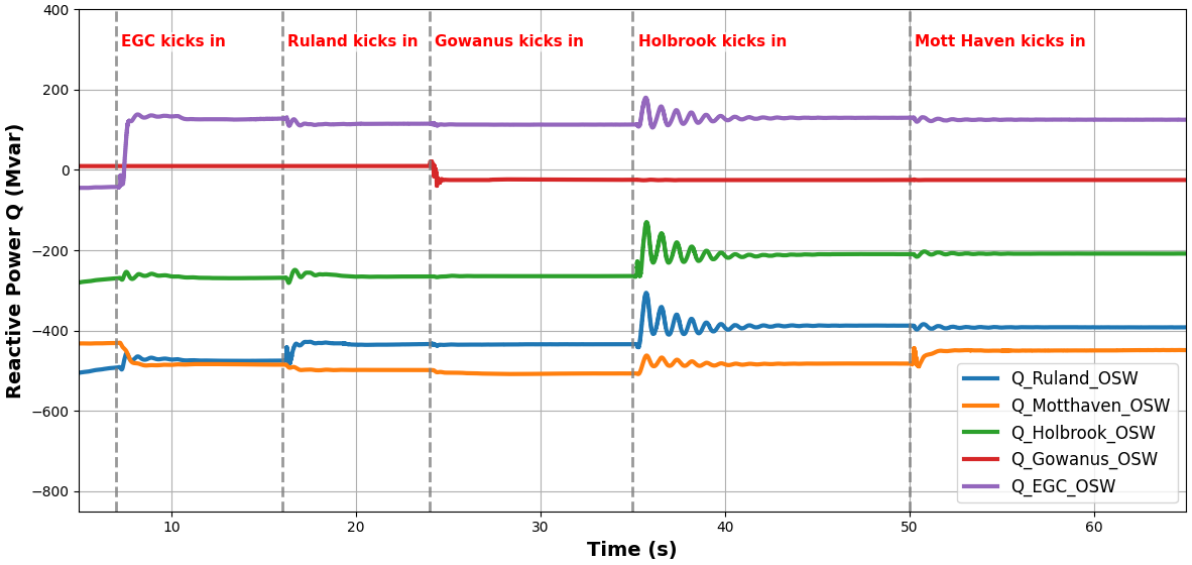

(b) Reactive power (MVAR) with 5 OSW farms

Figure 28. The output power of 5 farms.

Figure 29 shows the per-unit speed and rotor-angle traces for all 31 retained synchronous generators after the five offshore wind farms begin exporting at full power. Generator speeds stay between 0.992 pu and 1.0075 pu (±0.75 % about synchronous). Oscillations are well damped, settling within roughly 10 s, and no machine approaches out-of-step or over-speed protection thresholds. This confirms that the onshore fleet remains in synchronism and the spring light-load grid stays dynamically stable with the 5.5 GW offshore injection.

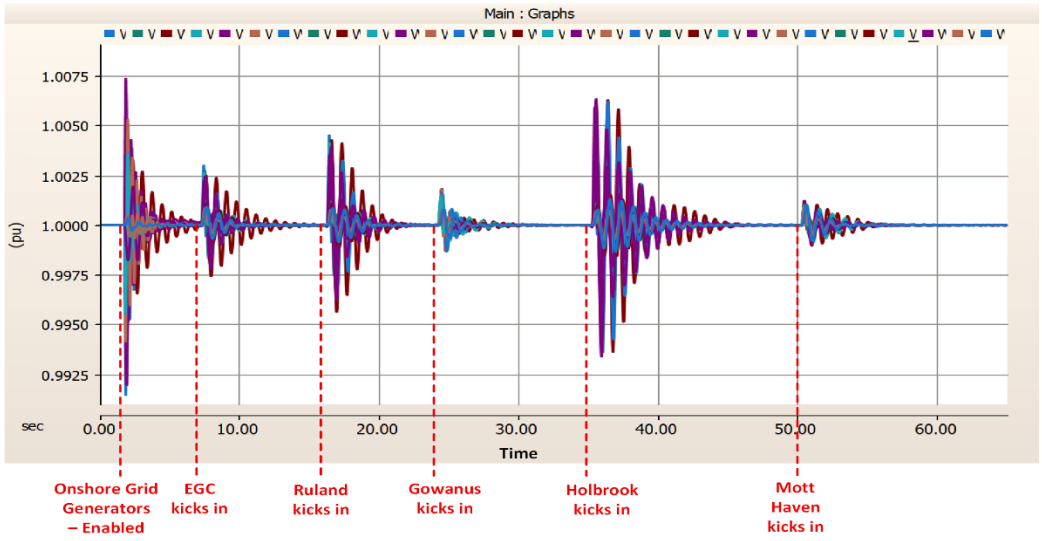

(a) All generator speed profiles (per unit)

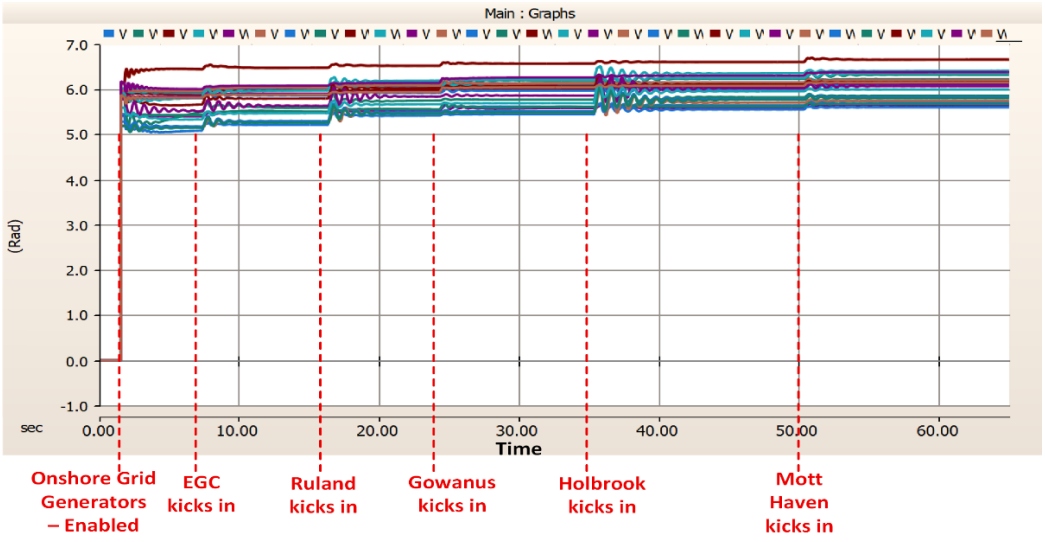

(b) All generator rotor-angle profiles (rad)

Figure 29. Machine speed (per unit) profiles (a) and rotor-angle (rad) profiles (b) of the onshore generator fleet with the 5 farms

Extreme-Weather Mass Trip of Offshore Wind

In this illustrative scenario, the NYISO spring light-load model is subjected to a sustained hurricane wind (> 25 m/s) that triggers the cut-out protection of every offshore wind farm, disconnecting all five installations together exporting 5.5 GW within a few seconds. This full shutdown, selected over the 10 m/s wind-ramp test, imposes a more severe, system-wide disturbance. The study quantifies the ensuing frequency nadir, RoCoF (Rate of Change of Frequency), voltage recovery, and synchronous-reserve deployment following the sudden loss of all offshore generation.

In this scenario, the hurricane level wind sweeps east-to-west across the lease areas:

- t = 0 s: The front first reaches the eastern projects Sunrise Wind (Holbrook LI POI) and Beacon Wind (Mott Haven NYC POI), both sited about 30–60 mi east of Montauk, forcing them to trip simultaneously.
- t = 6 s: The front then hits Juno Power Express (Ruland Road LI POI) and Vineyard Mid-Atlantic (East Garden City LI POI), causing both plants to disconnect.
- t = 11 s: Empire Wind 1 (Gowanus NYC POI) trips, completing the full offshore shutdown.

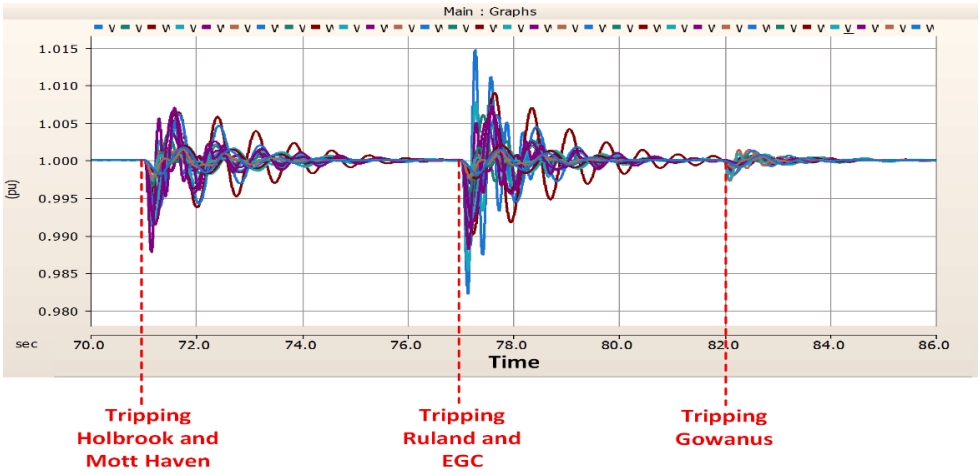

(a) All generator speed profiles (per unit)

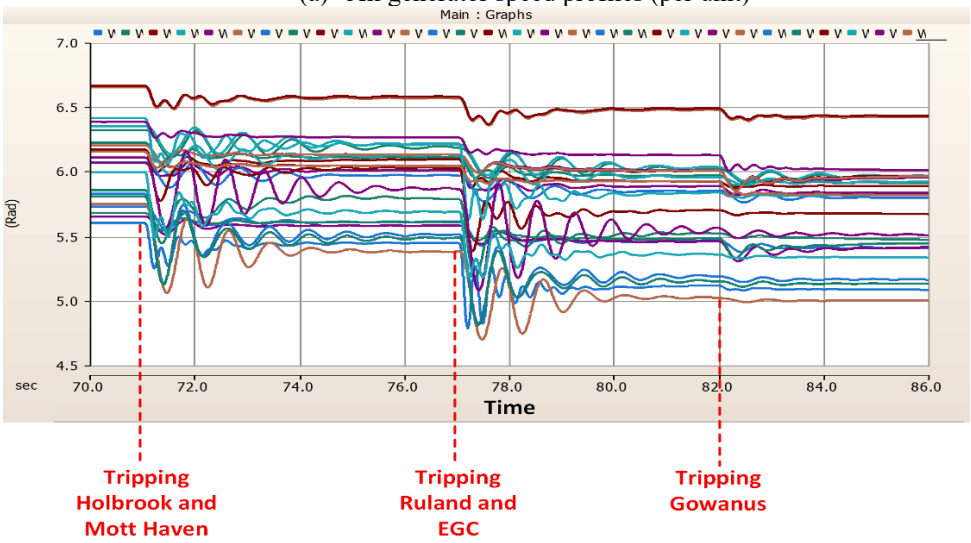

(b) All generator rotor-angle profiles (rad)

Figure 30. Onshore generator speed (per unit) (a) and rotor-angle (rad) (b) responses during the sequential trip of the five offshore wind farms.

Figures 30 (a)–(b) plot the resulting onshore generator speed and rotor-angle trajectories, while Figures 9 (a)–(b) display the frequency and voltage responses at the Gowanus and Holbrook POIs.

Generator rotor speeds remain largely within 0.99–1.005 pu (±1 % of synchronous) throughout the event. The largest excursion occurs in the vicinity of the Ruland Road POI: its speed peaks briefly at 1.015 pu

immediately after the Juno Power Express, and the Vineyard Mid-Atlantic Wind trip. The ringdown is well damped: successive speed maxima drop from 0.015 pu to 0.0075 pu in 0.4 s (half-amplitude time), which corresponds to a decay time constant of ~0.58 s. Rotor-angle swings at Ruland-area machines subside within roughly five seconds, and no unit approaches out-of-step protection thresholds. Overall, oscillations are well controlled, indicating that sequential offshore trips do not endanger transient stability.

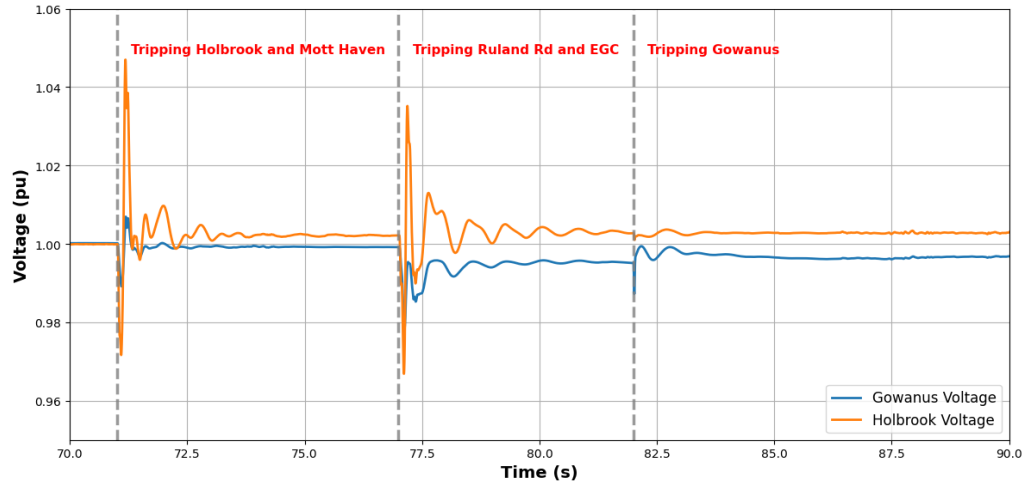

(a) Gowanus, and Holbrook bus voltage (per unit)

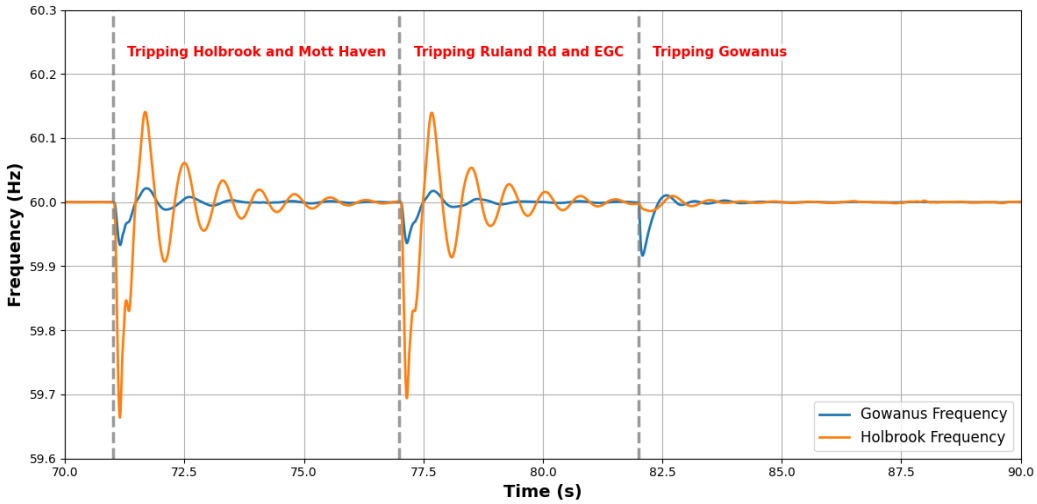

(b) Gowanus, and Holbrook bus frequency (Hz)

Figure 31. Frequency and voltage responses at the Gowanus and Holbrook POIs during the sequential trip of the five offshore wind farms.

Figure 31 highlights the relative stiffness of the two networks. At Holbrook (Long Island), voltage moves between 0.97 pu and 1.045 pu and frequency between 59.65 Hz and 60.15 Hz after the two co-located offshore farms trip. At Gowanus (NYC), the swings are milder, 0.99–1.01 pu for voltage and 59.95–60.02 Hz for frequency because only two farms shut down there and the underlying grid is stronger. All values

stay within the continuous “no-trip” bands of 0.95–1.05 pu and 59.5–60.5 Hz mandated by NERC PRC-024 and IEEE Std 2800-2022, so neither POI violates generator ride-through requirements.

The sequential loss of 5.5 GW of offshore wind remains tolerable for the spring light-load system. Long Island experiences wider excursions, underscoring its weaker short-circuit strength, yet still meets voltage- and frequency-ride-through criteria. No under-frequency load shedding is triggered, and both POIs recover to nominal conditions without additional trips, confirming overall system resilience.

In reality, the high wind cut out function is implemented at the WTG level and the likelihood of all turbines cutting out in a plant exactly at the same time is low. The cut-outs are more likely to be staggered over time. That said, this scenario investigates a worst-case boundary condition that is easier to simulate. Since there were no violations or instabilities under the worst-case illustration when full plants experience simultaneous cut-out, the more realistic scenario of a staggered cut-out poses less risk and also confirms overall system resilience. This simulation may also show, if all 5 wind plants were to trip at nearly the same time due to other reasons, the remaining onshore network maintains stable operation and is able to recover from such an event, albeit unlikely.

4.3. Identify high-risk disturbances

Small Signal Stability Analysis of Large-Scale Grid Model Including Multiple OSWs

This study focuses on evaluating the small-signal stability of the New York State (NYS) onshore power system when integrated with multiple offshore wind farms. A linearized model of the interconnected system spanning NYISO, ISO-NE, and PJM is analyzed using the Small Signal Analysis Tool (SSAT) with the PSS®E format data. Eigenvalue analysis is performed to identify potential oscillatory modes, observe their dominant participating states, and quantify damping levels.

From the data received from NYISO, the team developed Small Signal Models (SSM) indicating a macroscopic view of system stability and oscillatory performance, focusing on long-term planning and overall system health. The MMWG2022Series case data is utilized in this task, with its power flow encompassing approximately 94000 buses and 1100 generators, and there are over 9000 dynamic machine models representing the dynamic behavior of the Eastern power system. The goal is to dynamically reduce the full Eastern Interconnection data case, which is received from NYISO, to a reasonably small size model that can be simulated in SSAT. To this end, the EPRI’s DYNRED application is utilized to implement the reduction process and create the dynamically reduced system. The reduction algorithm of DYNRED is based on identifying coherent generators and aggregating them together into one equivalent machine. After running DYNRED software for Spring Light Load case data, the reduced large-scale model is obtained

with around 14000 buses including three areas (NYISO, ISO-NE, and PJM), particularly focusing on NYISO.

To conduct the small signal analysis of the reduced large-scale model with multiple OSWs, the SSAT from Powertech Labs is applied to compute the eigenvalues of the whole large-scale model and determine different dominant states of the system. Eigenvalue analysis is performed to identify potential oscillatory modes, observe their dominant participating states, and quantify damping levels. The dominant states identify which elements in the reduced large-scale model are driving instability and oscillations. The following table shows various dominant modes of multiple OSWs identified by SSAT.

NYISO

The small signal analysis of the NYS onshore grid system, integrated with multiple offshore wind farms, reveals a spectrum of oscillatory modes associated with different substations SHORE RD, MOTT HAVEN, E.G.C.-1, HOLBROOK, and GOWANUS. These substations correspond to OSW Points of Interconnection (POIs), and each display distinctive dynamic behavior in terms of frequency, damping ratio, and system stability. Two substations exhibited negative damping; Shore Road had -25.3%
damping at 19.8 Hz and E.G.C.-1 had -13.2% damping at 36Hz.

Table 7. Dominant states of OSWs in NYISO

Real	Imaginary	Frequency(Hz)	Damping(%)	Dominant State
32.628	124.7162	19.8492	-25.31	128835 : SHORE RD 345.00
-3.5618	76.3784	12.156	4.66	126641 : MOTT HAVEN 345.00
30.1807	225.944	35.9601	-13.24	128822 : E.G.C.-1 345.00
-15.8354	177.4202	28.2373	8.89	129421 : HOLBROOK 138.00
-4.9268	46.9794	7.477	10.43	126287 : GOWANUS 345.00

ISO-NE

Based on the small signal stability analysis of the offshore wind farms in ISO-NE integrated at WEST BARNSTABLE, BARNSTABLE SWITCHING, BRAYTON POINT, and DAVISVILLE, the results indicate the presence of both unstable and well-damped oscillatory modes, most of which fall within the sub-synchronous frequency range of 16 to 39 Hz commonly associated with converter-driven dynamics in offshore wind integration. Two substations exhibited negative damping; West Barnstable had -30.5%
damping at 21.7 Hz and Brayton Point had -17.4% damping at 24Hz.

Table 8. Dominant states of OSWs in ISO-NE

Real	Imaginary	Frequency(Hz)	Damping(%)	Dominant State
43.6648	136.5393	21.7309	-30.46	111134 : WEST BARNSTABLE 345.00
14.4611	243.0229	38.6783	-5.94	111202 : BARNSTABLE SWITCHING 115.00
26.6871	151.1238	24.0521	-17.39	114734 : BRAYTON POINT 345.00
-20.2446	101.393	16.1372	19.58	117314 : DAVISVILLE 115.00

PJM

The small signal stability analysis of offshore wind farms in PJM interconnected at INDIAN RIVER, BIRDNECK, CARDIFF, LARRABEE, and FENTRESS substations reveals significant oscillatory instability across multiple locations, with dominant states located within the sub-synchronous frequency range (5–35 Hz). Most of these modes exhibit positive real parts and negative damping ratios, indicating growing oscillations that pose a severe threat to system stability and require immediate mitigation. Three substations exhibited negative damping; CARDIFF had -21.8% damping at 9.7 Hz, BIRDNECK had -11.8% at 34.5Hz and Fentress had -40.6% damping at 22.9Hz.

Table 9. Dominant states of OSWs in PJM

Real	Imaginary	Frequency(Hz)	Damping(%)	Dominant State
13.5144	60.6478	9.6524	-21.75	227900 : CARDIFF 230.00
25.7869	217.0061	34.5376	-11.8	314295 : BIRDNECK 230.00
64.0331	144.1759	22.9463	-40.59	314909 : FENTRESS 500.00
-42.2394	111.8828	17.8067	35.32	232006 : INDIAN RIVER 230.00
-4.4985	30.7532	4.8945	14.47	206294 : LARRABEE 230.00

Contingency Scenarios Description

As the objective of this task is to investigate possible high-risk oscillations in the Eastern Interconnection grid model when integrating with multiple Offshore Wind Farms (OSWs), the team proposed dynamic stability assessment contingencies to study our large-scale model based on NERC TPL-001-4 Reliability Standards [8]. There are in total 8 planning events (from P0 – P7) for large-scale grid performance requirements in this standard. However, the team finally decided to study 6 planning events as the received Eastern Interconnection data is not suitable for all planning events. The planning event P0 is the normal system condition and is applicable to steady state only. After the large-scale grid reached a steady state condition, the other 5 planning events are conducted sequentially with the detailed contingency sequence as follows:

- *Planning event P1 (single contingency):* Apply a three-phase fault at the determined bus for a time span, open the outaged element, and clear the fault.
- *Planning event P2 (single contingency):* Open one end of a transmission line section without a fault.
- *Planning event P3 (multiple contingency):* Open the first outaged generator unit and allow steady state system adjustments. Apply a three-phase fault at the determined bus for a time span, open the second outaged element, and clear the fault.
- *Planning event P4 (multiple contingency):* Apply a single-phase fault at the determined bus for a time span, open multiple elements caused by a stuck breaker, and clear the fault.
- *Planning event P6 (multiple contingency):* Open the first outaged element and allow steady state system adjustments. Apply a three-phase fault at the determined bus for a time span, open the second outaged element, and clear the fault.

In addition to these contingencies, the team also investigated the Eastern Interconnection power system model to figure out some specific scenarios to study for NYISO, ISO-NE, and PJM area. All conducted contingency scenarios are listed in detail for each area in the following sections.

NYISO Contingencies and Faults Analysis

A comprehensive fault-and-contingency study has been performed for NYISO, assessing the five offshore wind projects under both spring light-load and summer peak-load conditions. Each fault and contingency scenario were tested with and without offshore wind integration (OSW-HVAC and OSW-HVDC), and faults were applied at critical Points of Interconnection (POIs), such as the Gowanus Substation (NYC) and Ruland Road Substation (Long Island).

<u>NYISO Fault Analysis</u>

This study investigates system stability under fault conditions by analyzing critical contingencies in the New York State power system, both with and without offshore wind (OSW) integration. The objective is to determine the Critical Clearing Time (CCT) for the system under varying levels of OSW deployment, specifically with 1, 2, 3, 4, and all 5 offshore wind projects enabled.

A system-level electromagnetic transient (EMT) fault analysis was performed connecting the whole wind farm and the New York State Power System. The study considered multiple scenarios across different grid conditions, including the Spring Light Load case and Summer Peak Load cases. The summer scenarios incorporated key transmission infrastructure upgrades such as the Champlain Hudson Power Express (CHPE) HVDC line and series-compensated lines, including:

- Marcy South Series Compensation Project (Zone E – Mohawk Valley),
- Knickerbocker Series Compensation Project (Zone 6 – Capital),
- Leeds–Hurley Smart Wires Smart Valve Project (Zone 7 – Hudson)

Scenario 1: 2028 Spring Light–Load (Balanced Fault at Gowanus)

A reduced NYISO spring light-load EMT model was used, retaining Zone J (NYC) buses ≥ 345 kV, Zone K (Long Island) buses ≥ 138 kV, and all internal generators. A three-phase fault was applied at the 345 kV Gowanus substation (POI). Scenario 1 included study of the impact of up to 5 OWS farms on this fault case. The 6 cases study are shown below, with the POI for the connected wind farms given. All wind farms were operating at their rated power.

- 0 OSW: Base model without offshore wind in service.
- 1 OSW: Gowanus (NYC).
- 2 OSW: Gowanus and Mott Haven (NYC).
- 3 OSW: Gowanus, Mott Haven (NYC), and Holbrook (Long Island).
- 4 OSW: Gowanus, Mott Haven (NYC), Holbrook, and Ruland Road (Long Island).
- 5 OSW: Gowanus, Mott Haven (NYC), Holbrook, Ruland Road, and Garden City (Long Island).

For each configuration, the Critical Clearing Time (CCT) was analyzed in the EMT simulations to quantify the impact of incremental offshore wind integration on NYISO transient stability.

Figure 32 compares rotor-speed and rotor-angle responses of the four-OSW models during 15- and 16-cycle, three-phase faults at the 345 kV Gowanus POI. With a 15-cycle fault (the critical clearing time for this configuration) generator speeds experience a damped oscillation of approximately 3 hertz, confirming transient stability. When the fault duration is extended to 16 cycles, a synchronous generating unit near the Gowanus substation loses synchronism, becomes unstable, and will trip once its protection limits are exceeded. Note that the angles shown in these figures are in radians, and it is the relative difference in the angle which is of primary importance.

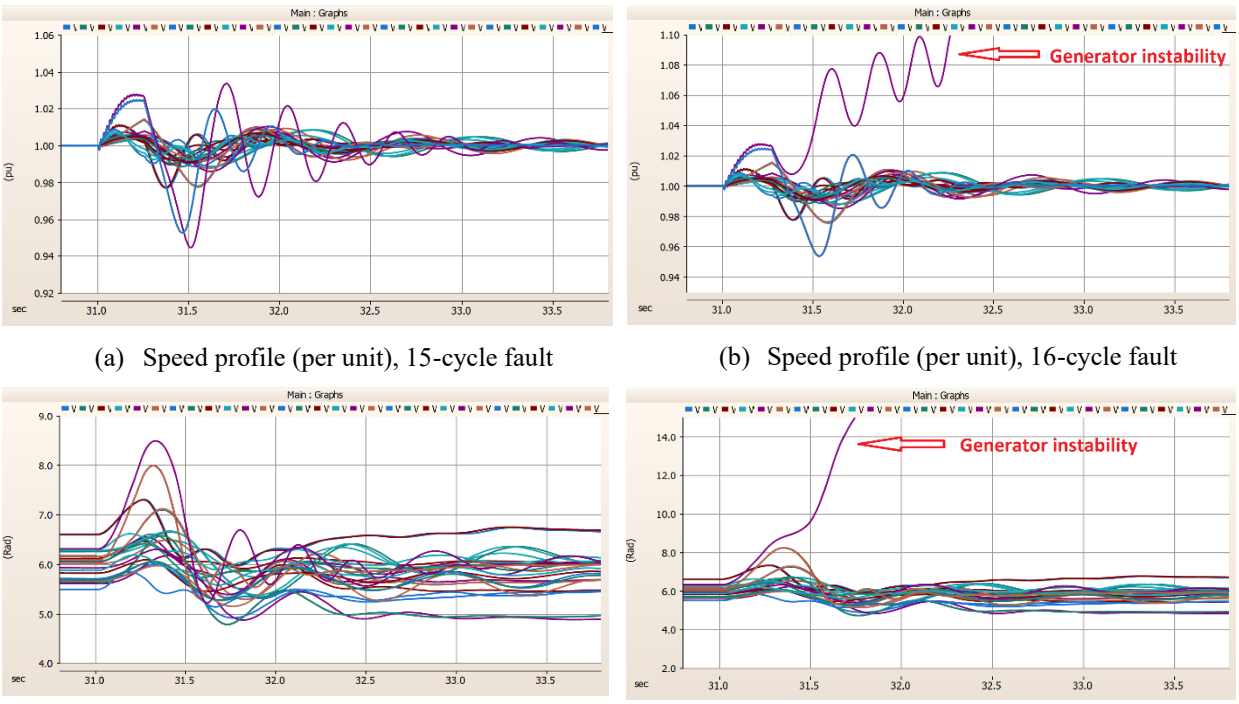

(a) Speed profile (per unit), 15-cycle fault

(b) Speed profile (per unit), 16-cycle fault

(c) Rotor-angle profile (rad), 15-cycle fault

(d) Rotor-angle profile (rad), 16-cycle fault

Figure 32. Comparison of machine speed (a, b) and rotor-angle (c, d) profiles for the 4-wind case at Gowanus under stable (15-cycle clearing) and unstable (16-cycle clearing) conditions.

Table 10 indicates that the critical clearing time (CCT) for a three-phase fault at the 345 kV Gowanus POI stays at 15 cycles for Cases 1 through 5, whether zero or up to four offshore wind farms are in service. In each of those cases, the Fox Hills combustion-turbine unit, located close to the fault, is the first machine to lose synchronism, so local inertia and proximity drive the stability limit rather than offshore generation. When the fifth project is added (Case 6, total offshore injection about 5.5 GW) the CCT falls to 13 cycles and instability shifts to the HVDC-connected plant at East Garden City. That outcome suggests the EGC bus is comparatively weak, with a lower short-circuit ratio, making the converter more sensitive to the voltage dip that follows the fault.

Figure 33 compares onshore generator behavior in the five-OSW model for two fault-clearing times at the Gowanus POI: 13 cycles (stable) and 14 cycles (unstable). With a 13-cycle clearance, all generators show only small speed dips and bounded rotor-angle swings that damp out within about 6 seconds, confirming transient stability. When the clearing time is lengthened to 14 cycles, the Long Island machines, particularly those closest to the East Garden City bus, show reduced damping on their low frequency inertial oscillations. A higher frequency oscillation also appears, and it is also lightly damped.

Table 10. Critical clearing time for a three-phase fault at the Gowanus substation using the spring light load model

Case No	Name	Number of OSW	Description	Critical Clearing Time
1	Zone JK without OSW with 3-phase faults (Gowanus)	0	Zone JK - Spring Light load case with 187 buses, 31 generators with dynamic models, a total generation capacity of 2.5 GW in retained areas. → Synchronous generating unit unstable	15 cycles
2	Zone JK with 1 OSW with 3-phase faults (Gowanus)	1	1 OSW – Gowanus (NYC) → Synchronous generating unit unstable	15 cycles
3	Zone JK with 2 OSW with 3-phase faults (Gowanus)	2	2 OSWs – Gowanus and Mott Haven (NYC). → Synchronous generating unit unstable	15 cycles
4	Zone JK with 3 OSW with 3-phase faults (Gowanus)	3	3 OSWs: Gowanus, Mott Haven (NYC), and Holbrook (Long Island) → Synchronous generating unit unstable	15 cycles
5	Zone JK with 4 OSW with 3-phase faults (Gowanus)	4	4 OSWs: Gowanus, Mott Haven (NYC), Holbrook, and Ruland Road (Long Island) → Synchronous generating unit unstable	15 cycles
6	Zone JK with 5 OSW with 3-phase faults (Gowanus)	5	5 OSWs: Gowanus, Mott Haven (NYC), Holbrook, Ruland Road, and East Garden City (Long Island) → The OSW-HVDC connected to EGC becomes unstable.	13 cycles

Figure 34 shows the voltage and frequency transients at HVDC terminal and the point of grid connection at EGC for this same case. In this scenario, a 13-cycle clearing time allows the EGC HVDC converter to ride through the fault: voltage briefly plunges to 0.10 pu, overshoots to 1.40 pu, and frequency swings between 59.9 Hz and 60.8 Hz, yet both return to nominal within about one second. When clearing is delayed to 14 cycles, post-fault voltage fails to recover to an acceptable voltage, and the POI frequency settles at 61.0–61.25 Hz, distinctly different than the frequency on the grid side of the wind farm's onshore transformer. This violates the continuous ride-through bands in NERC PRC-024 and IEEE 2800 and confirms converter instability.

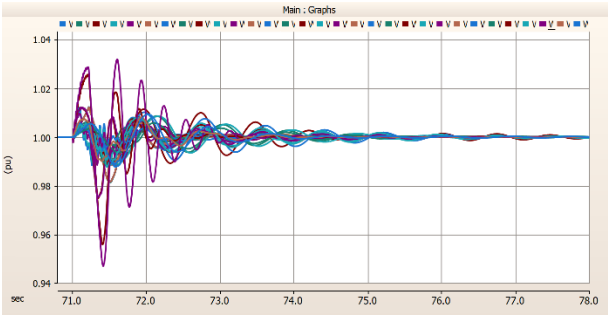

(a) Speed profile (per unit), 13-cycle fault

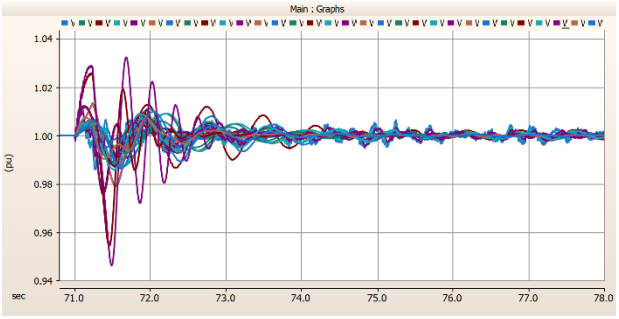

(b) Speed profile (per unit), 14-cycle fault

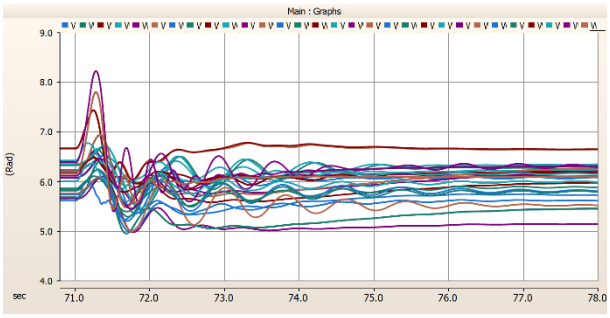

(c) Rotor-angle profile (rad), 13-cycle fault

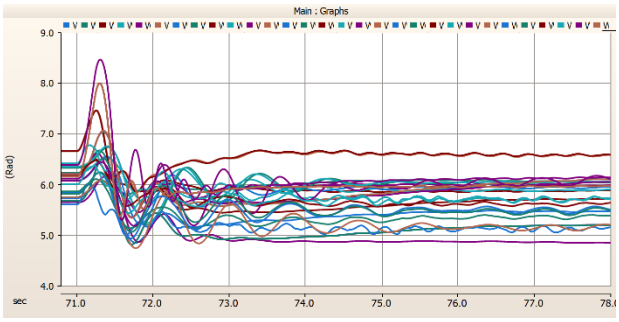

(d) Rotor-angle profile (rad), 14-cycle fault

Figure 33. Comparison of machine speed (a, b) and rotor-angle (c, d) profiles for the 5-wind farm case for a fault at Gowanus under stable (13-cycle clearing) and unstable (14-cycle clearing) conditions.

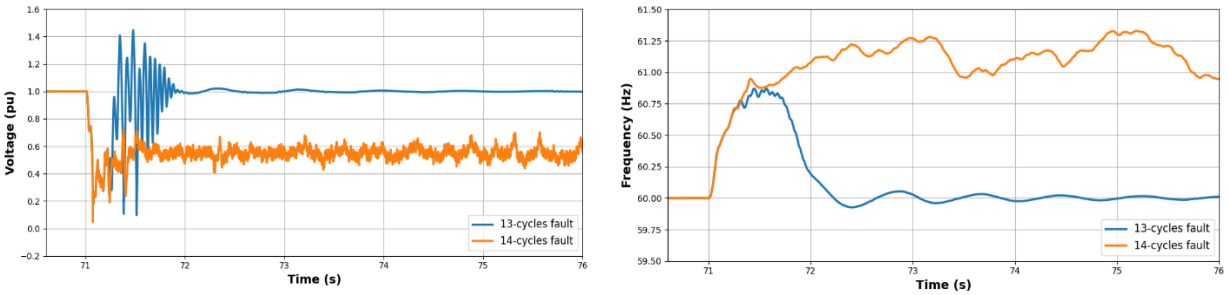

(a) Offshore Substation HVDC-Terminal Voltage, and Frequency Response (13- vs. 14-Cycle Clearing)

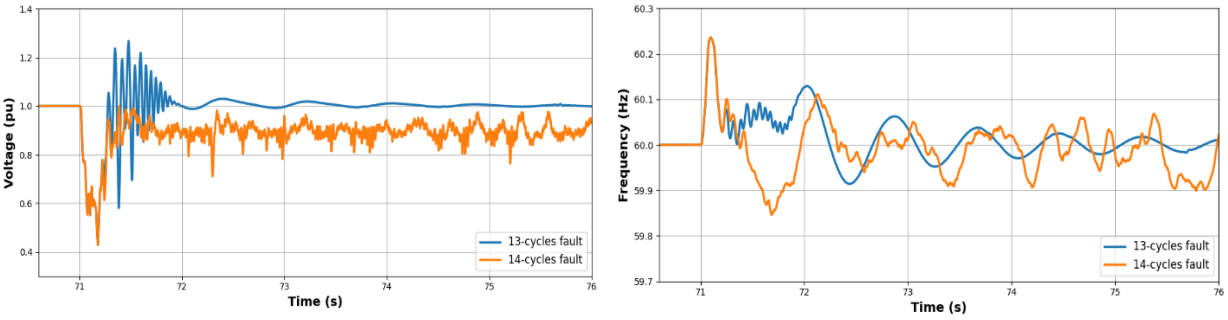

(b) EGC POI Bus Voltage, and Frequency Response (13- vs. 14-Cycle Clearing)

Figure 34. EGC Voltage and Frequency Dynamics of Offshore HVDC Terminal vs. POI Bus for 13- and 14-Cycle Fault Clearing of a fault at Gowanus.

These results establish a critical clearing time of 13 cycles for faults at Gowanus with all five offshore wind farms in service; longer clearing or weaker grid conditions would require added dynamic-VAR support, tuned damping controls, or faster protection to maintain stability.

It is noted that this is a distinctly different instability directly involving the HVDC terminal at EGC. This is as opposed to the case shown in Figure 31, where the HVDC controllers cause a synchronous generator to separate from the system.

Scenario 2: 2028 Spring Light–Load (Balanced/ Unbalanced Fault at Ruland Road)

Scenario 2 employs the same spring light-load EMT model used in Scenario 1, but the disturbance is moved to the 138 kV Ruland Road point of interconnection on Long Island, where three of the offshore projects plan to connect. A balanced three-phase fault is applied at Ruland Road for every offshore-penetration level

Table 11. Critical Clearing Time for a balanced/ unbalanced fault at the Ruland Rd substation using the Spring Light Load model

Case No	Name	Number of OSW	Description	Critical Clearing Time
1	Zone JK without OSW with 3-phase faults (Ruland Rd)	0	Zone JK - Spring Light load case with 187 buses, 31 generators with dynamic models, a total generation capacity of 2.5 GW in retained areas. → Synchronous generating unit unstable	14 cycles
2	Zone JK with 1 OSW with 3-phase faults (Ruland Rd)	1	1 OSW – Ruland (LI) → Synchronous generating unit unstable	17 cycles
3	Zone JK with 2 OSW with 3-phase faults (Ruland Rd)	2	2 OSWs – Ruland and Holbrook (LI) → Synchronous generating unit unstable	18 cycles
4	Zone JK with 3 OSW with 3-phase faults (Ruland Rd)	3	3 OSWs: Mott Haven (NYC), Ruland and Holbrook (Long Island) → Synchronous generating unit unstable	18 cycles
5	Zone JK with 4 OSW with 3-phase faults (Ruland Rd)	4	4 OSWs: Gowanus, Mott Haven (NYC), Holbrook, and Ruland Road (Long Island) Synchronous generating unit unstable	18 cycles
6	Zone JK with 5 OSW with 3-phase faults (Ruland Rd)	5	5 OSWs: Gowanus, Mott Haven (NYC), Holbrook, Ruland Road, and Garden City (Long Island) → The OSW-HVDC connected to EGC becomes unstable.	5 cycles
7	Zone JK with 5 OSW with single- phase faults (Ruland Rd)	5	5 OSWs: Gowanus, Mott Haven (NYC), Holbrook, Ruland Road, and Garden City (Long Island) → The OSW-HVDC connected to EGC becomes unstable.	12 cycles

(0 through 5 OSWs). For the full-penetration case with five offshore wind farms online, an additional single-line-to-ground fault is simulated to compare its critical clearing time with the three-phase result. Table 11 summarizes the findings.

Table 11 shows that, when up to four offshore wind farms are connected, the system's transient-stability margin improves: the critical clearing time (CCT) increases from 14 cycles in the base case to 17–18 cycles. In each case, a synchronous generating unit near Ruland Road is the first unit to lose synchronism.

With the addition of a fifth offshore project, stability deteriorates. For a three-phase fault the CCT drops to 5 cycles, and the element that now becomes unstable is the HVDC-linked offshore plant at East Garden City evidence that converter dynamics and the weak Long Island network have become the limiting factors. A single-line-to-ground fault in the same five-OSW configuration is less severe (CCT = 12 cycles) but still well below the original margin.

Figure 35 contrasts system behavior for a SLG- single-line-to-ground (phase-A-to-ground) fault at Ruland Road when five offshore wind farms are online. With a 12-cycle clearing time the three-phase voltage waveforms eventually stabilize following a period of significant temporary overvoltage. When clearing is delayed to 13 cycles, the line currents and phase voltages both exhibit persistent high-magnitude oscillations. The comparison confirms that 12 cycles is the critical clearing time; any longer delay leads to sustained voltage depression and undamped sub-synchronous current oscillations that threaten protective tripping.

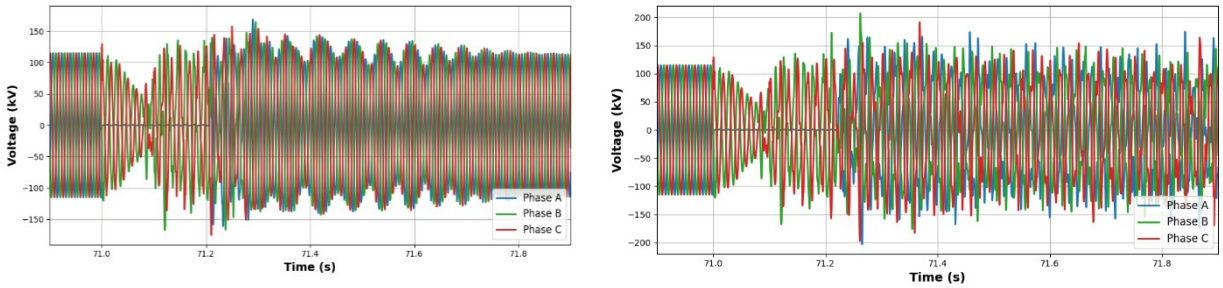

(a) Ruland POI phase-voltage (kV) comparison, 12- vs 13-cycle clearing

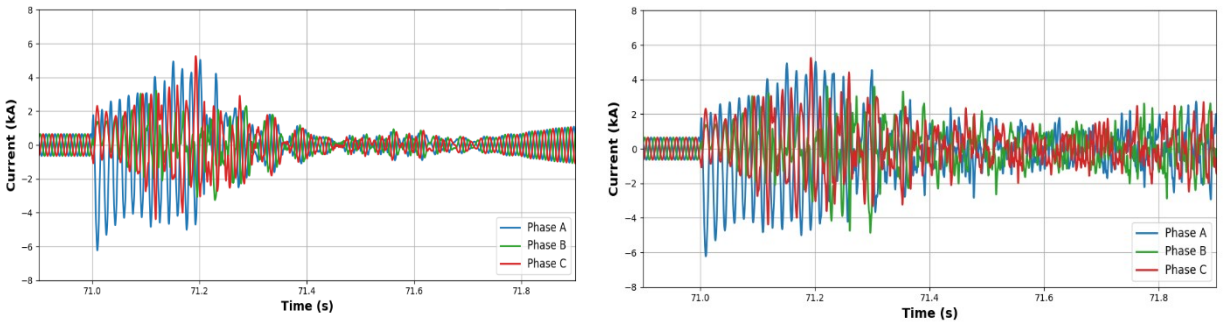

(b) Ruland–Holbrook line-current (kA) comparison, 12- vs 13-cycle clearing

Figure 35. Ruland Road Single-Phase Fault (A-G) with 5 OSWs for 12- and 13-Cycle Fault Clearing

This SLG-fault instability contrasts sharply with the earlier three-phase cases: the sustained low-frequency voltage and current oscillations suggest a converter-driven problem at the EGC HVDC terminal. Here the synchronous fleet remains in step, yet the converter itself becomes the instability source posing a different mitigation challenge.

Scenario 2: 2028 Summer Peak Load (Balanced Fault at Gowanus/ Ruland Rd)

A reduced NYISO Summer peak-load EMT model was used, retaining Zone J (NYC) buses ≥ 345 kV, Zone K (Long Island) buses ≥ 138 kV, and all internal generators. This scenario tests system resilience under the most demanding seasonal condition summer peak when New York City and Long Island load is at or near its annual maximum. Compared with the spring light-load cases, higher demand places greater thermal and voltage stress on the 345 kV backbone and Long Island export corridors, while heavier synchronous-generation scheduling in Zones J and K increases inertia but narrows reactive-power headroom. Simulating balanced three-phase faults at both the Gowanus (NYC) and Ruland Road (Long Island) POIs reveals whether the system can still meet transient stability and voltage-ride-through criteria when transmission corridors are heavily loaded and offshore wind is operating alongside a full conventional-generation fleet.

Table 12. Critical Clearing Time for a three-phase fault at the Gowanus substation using the summer peak load model

Case No	Name	Number of OSW	Description	Critical Clearing Time
1	Zone JK without OSW with 3-phase faults (Gowanus)	0	Zone JK - Summer Load case with 303 buses, 121 generators with dynamic models, and a total generation capacity of 12 GW in retained areas. →Synchronous generating unit unstable	9 cycles
2	Zone JK with 1 OSW with 3-phase faults (Gowanus)	1	1 OSW – Gowanus (NYC) →	8 cycles
3	Zone JK with 2 OSW with 3-phase faults (Gowanus)	2	2 OSWs – Gowanus and Mott Haven (NYC). Synchronous generating unit unstable	8 cycles
4	Zone JK with 3 OSW with 3-phase faults (Gowanus)	3	3 OSWs: Gowanus, Mott Haven (NYC), and Holbrook (Long Island) → Synchronous generating unit unstable	8 cycles
5	Zone JK with 4 OSW with 3-phase faults (Gowanus)	4	4 OSWs: Gowanus, Mott Haven (NYC), Holbrook, and Ruland Road (Long Island) → The Synchronous generating unit unstable	8 cycles
6	Zone JK with 5 OSW with 3-phase faults (Gowanus)	5	5 OSWs: Gowanus, Mott Haven (NYC), Holbrook, Ruland Road, and Garden City (Long Island) →Synchronous generating unit unstable	8 cycles

Table 12 shows that adding offshore wind has only a minor impact on transient stability during the summer-peak case. The base case (no offshore wind) yields a critical clearing time (CCT) of 9 cycles for a three-

phase fault at Gowanus. Once any offshore capacity is added, the CCT drops to 8 cycles and then remains unchanged as additional projects are connected all the way to the five-OSW level. In every study run, the element that first loses synchronism is a synchronous generator, indicating that the offshore wind farms have little impact on the CCT in this case.

Table 13. Critical Clearing Time for a three-phase fault at the Ruland Road substation using the summer peak load model

Case No	Name	Number of OSW	Description	Critical Clearing Time
1	Zone JK without OSW with 3-phase faults (Ruland Road)	0	Zone JK - Zone JK - Summer Load case with 303 buses, 121 generators with dynamic models, and a total generation capacity of 12 GW in retained areas. → Synchronous generating unit unstable	24 cycles
2	Zone JK with 1 OSW with 3-phase faults (Ruland Road)	1	1 OSW – Ruland (LI) → Synchronous generating unit unstable	24 cycles
3	Zone JK with 2 OSW with 3-phase faults (Ruland Road)	2	2 OSWs – Ruland and Holbrook (LI) → Synchronous generating unit unstable	20 cycles
4	Zone JK with 3 OSW with 3-phase faults (Ruland Road)	3	3 OSWs: Mott Haven (NYC), Ruland and Holbrook (Long Island) → Synchronous generating unit unstable	21 cycles
5	Zone JK with 4 OSW with 3-phase faults (Ruland Road)	4	4 OSWs: Gowanus, Mott Haven (NYC), Holbrook, and Ruland Road (Long Island) → Synchronous generating unit unstable	21 cycles
6	Zone JK with 5 OSW with 3-phase faults (Ruland Road)	5	5 OSWs: Gowanus, Mott Haven (NYC), Holbrook, Ruland Road, and Garden City (Long Island) → Synchronous generating unit unstable	20 cycles

The summer-peak results in Table 13 show that offshore additions have a moderate but significant impact on transient stability for a three-phase fault at Gowanus.

In the spring light-load study, connecting all five offshore wind farms cut the critical clearing time for a fault at Ruland Road to just 5 cycles, and the system became unstable when the East Garden City HVDC terminal lost synchronism. Under summer-peak conditions, the same five-OSW configuration still permits 20 cycles at Ruland Road. Peak-season demand keeps many more synchronous generators online, boosting system inertia and reactive support.

Figure 36 shows that, with all five offshore wind farms online, a 21-cycle clearing time at Ruland Road cause one generator to lose synchronism.

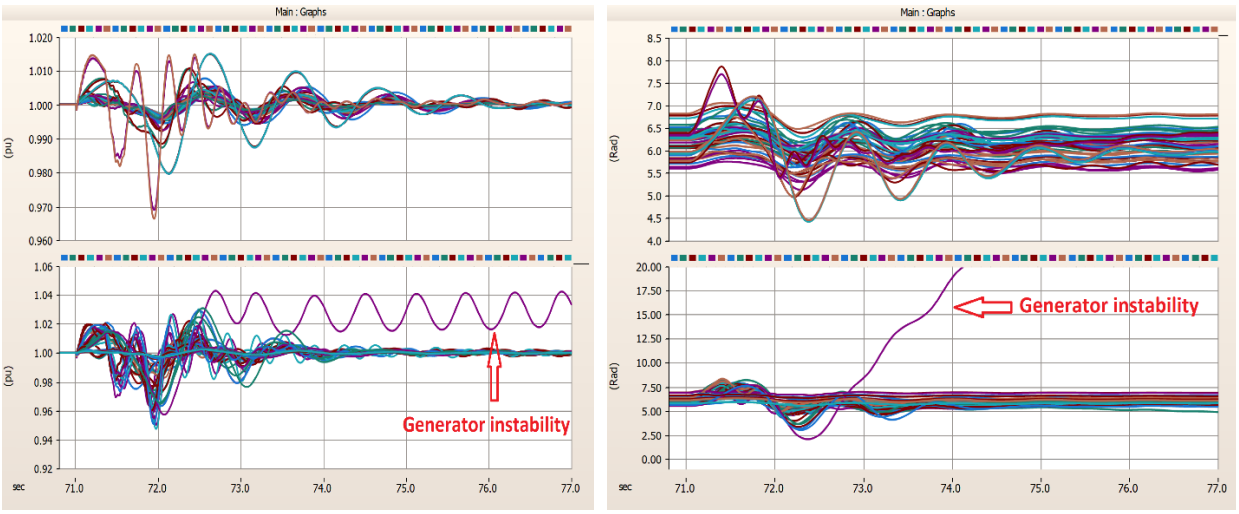

(a) Speed profile (per unit), 21-cycle fault (b) Rotor-angle profile (rad), 21-cycle fault

Figure 36. Comparison of machine speed (a) and rotor-angle (b) profiles for the 5-wind case at Ruland Rd under unstable (21-cycle clearing) conditions. (Note: each plot of speed and angle show half of the synchronous generators in the study).

Figure 37 applies a Fast Fourier Transform (FFT) to the unstable generator rotor-speed waveform and isolates a pronounced spectral peak at 3.125 Hz. This single, well-defined component confirms that the persisting speed oscillation observed in Figure 36 is dominated by a 3.1 Hz electromechanical mode that remains poorly damped after the 21-cycle fault.

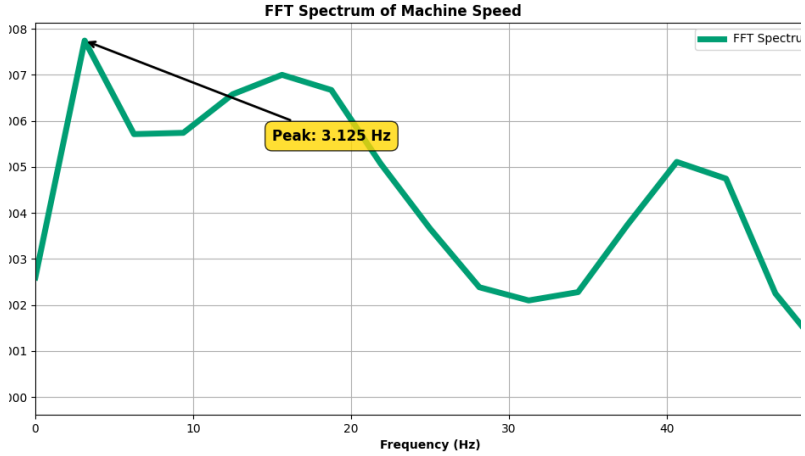

Figure 37. FFT of turbine generator speed following the fault event

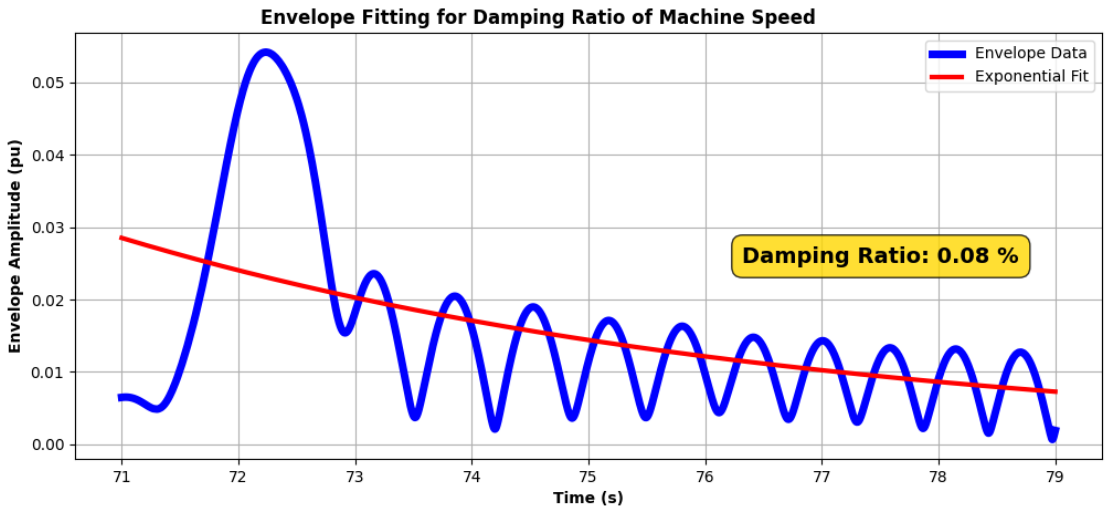

Figure 38. Damping ratio of unstable turbine generator speed following the fault event

To assess how quickly the 3.125 Hz mode decays, a Hilbert-transform envelope was extracted from the rotor-speed signal and fitted with an exponential curve (Figure 38). The fit yields a damping ratio of only 0.08 %, effectively indicating an undamped electromechanical mode: the speed oscillation decays so slowly that it persists after the fault is cleared, confirming the instability observed in the unstable unit shown in Figure 36.

Under 2028 summer-peak conditions, the grid retains solid transient-stability margins despite full offshore penetration: a three-phase fault at Gowanus must still clear in ≤ 8 cycles (one cycle tighter than the no-wind case), while the weaker Long Island pocket at Ruland Road remains stable for clearing times up to 20 cycles.

NYISO Contingency Analysis

In order to determine high-risk oscillations for the NYISO large-scale model, including both onshore and offshore systems, the team implemented multiple practical contingency scenarios to assess the dynamic stability of the NYISO grid under a high level of OSW integration. Table 14 presents the description of the studied contingencies for NYISO and lists some particular example cases for each planning event. The team implemented a total of 60 events for the NYISO large-scale model, with 30 events for the Spring Light-Load (SLL) case and 30 events for the summer peak load case. All contingency scenarios are eventually tested with 5 POIs of OSWs and some critical buses inside the NYISO grid model

Table 14. Studied contingencies for NYISO

Category	No of Events	Initial Condition	Fault Type	Example Scenario
P0	1	Normal	None	None
P1	7	Normal	Three-phase fault	Apply fault at Gowanus POI bus
P2	1	Normal	None	Open a nearby transmission line
P3	7	Trip Large Synchronous Generator	Three-phase fault	Apply fault at Gowanus POI bus
	7	Trip Large Synchronous Generator		Apply fault at Holbrook POI bus
P4	7	Normal	Single-phase fault	Apply fault at Ruland Rd POI
P6	7	Open a nearby transmission line	Three-phase fault	Apply fault at East Garden City POI bus

The NYISO model is tested and found to be stable during normal conditions, satisfying TPL Category P0 requirements. Several of the most significant contingencies studied are discussed below. All other events are found to be stable when testing with the clearing times and their results recover to values consistent with their original steady-state conditions.

Contingency 1: Large Conventional Generator Tripping With 1 OSW

In this study, the large generator tripping scenario is carefully simulated to assess the impact of OSW integration on the stability of the onshore grid system. A large synchronous generator in Zone J is suddenly disconnected from the grid. There are two different configurations for this scenario, which are (i) the NYS grid model and (ii) the NYS grid model with 1 OSW operating at the GOWANUS point of interconnection (POI). At a predefined simulation time instant t = 10 (s), the tripping of the generator is initiated for the configuration (i). For case (ii), the aggregated OSW model begins injecting 100% rated power into the NYS grid system through the GOWANUS POI bus at t = 6 (s) before the synchronous generator trip at t = 10 (s). The responses studied included machine speeds, voltage profiles, power flow redistributions, and frequency dynamic performance.

This case focuses on the transient and steady-state voltage behavior across the OSW POI bus (GOWANUS) following the generator trip contingency. Immediately after the generator outage, the sudden imbalance between generation and load leads to a temporary increase in the POI RMS voltage magnitude, illustrated in Figure 39.

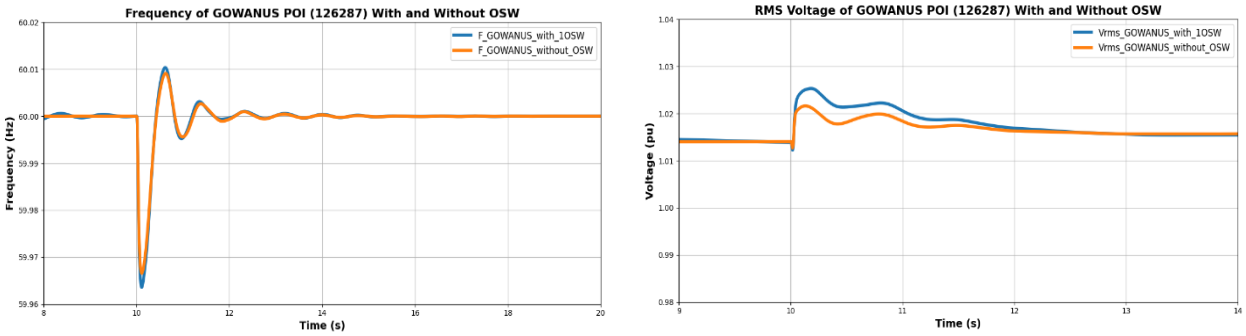

Figure 39. Frequency & voltage of Gowanus POI following the synchronous generator trip event.

The simulation results confirm that, under the studied scenario, the system with and without OSW maintains adequate voltage stability margins without triggering overvoltage load shedding or violating voltage limits. The short-term peak RMS voltage of the system with OSW is slightly higher than the scenario of the system without OSW, which are 1.024 and 1.022 per unit, respectively.

The frequency transient for this case is also shown in Figure 39, for the frequency measured at the POI bus with and without OSW integration. Following the generator trip, both scenarios exhibit similar frequency profiles characterized by a rapid frequency decline as shown in Figure 39. In the scenario without OSW integration, the system experiences a moderate frequency ramp down (RoCoF = 0.71 Hz/s) driven by the available synchronous inertia. The system successfully recovers to the nominal frequency quickly, demonstrating sufficient primary frequency response capability from remaining conventional generators. When a single OSW is integrated into the system at Gowanus POI, a slightly lower frequency nadir is observed at t = 10.11 (s). However, the RoCoF increases to 0.79 (Hz/s), suggesting that the additional offshore wind capacity contributes lower effective inertia compared to synchronous machines, resulting in a steeper initial frequency drop. To sum up, the recovery time remains nearly identical and the frequency stability is preserved under the studied condition, with the frequency nadir remaining above critical underfrequency thresholds and recovery occurring within acceptable time frames. These results highlight that while OSW integration may slightly reduce system inertia, its impact on frequency minimum and recovery remains acceptable for the studied case.

Contingency 2: Large Conventional Generator Tripping followed by three phase fault with 5 OSWs

In Contingency 2, the performance of the NYISO grid model with a high level of OSWs penetration (all 5 farms). In this case, the NYISO grid model is initialized through a flat-start power flow, and each OSW is sequentially integrated into the grid in order to ensure all operating conditions are in steady-state equilibrium prior to the disturbances. In this study case, the large synchronous generator tripped at t = 61(s) and then a three-phase fault is applied at Gowanus POI bus at t = 65 (s). Figure 40 shows that the remaining synchronous generators in Zones J and K remain in synchronism for both 10 and 11 cycle faults.

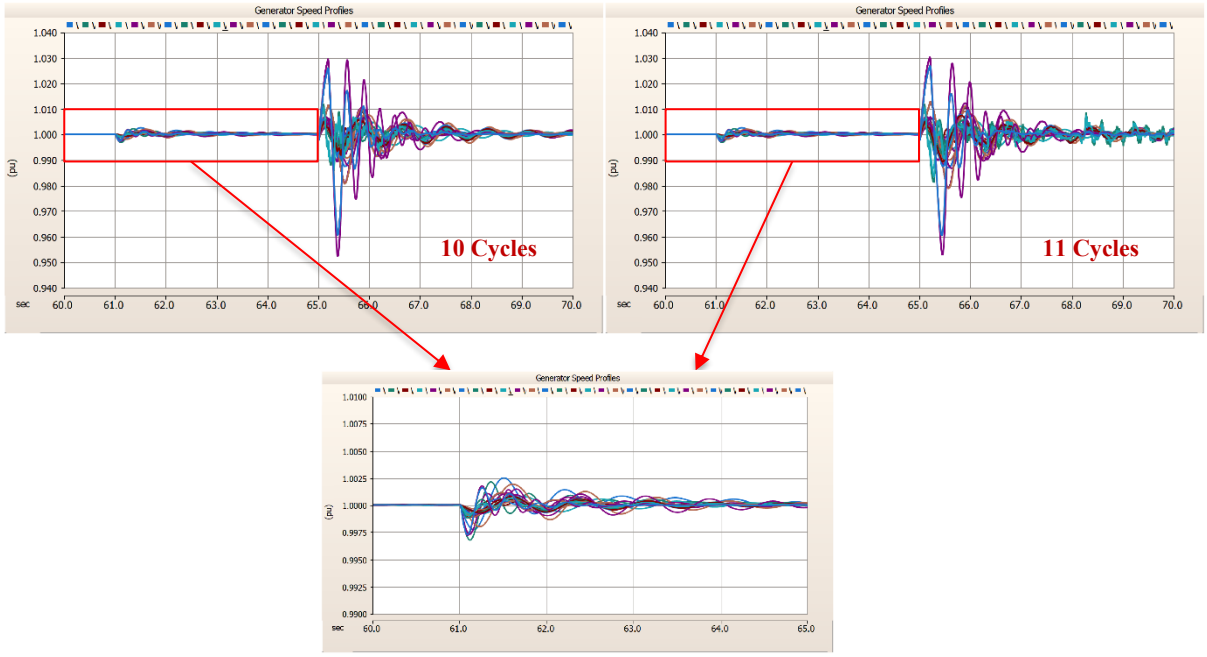

Figure 40. Generator speed profiles on-line units after generator trip

Figure 41 shows the performance of the OSW landing at East Garden City. While the East Garden City OSW is able to recover to the steady state conditions with the fault in 10 cycles, unstable voltage and frequency is observed at the East Garden City OSW terminal with the fault in 11 cycles. This result is further analyzed with the oscillation frequency and damping ratio estimation. For the stable case, the voltage response of the system has the averaged sub-synchronous oscillation frequency of 22.40 Hz and damping ratio of 1.38%. On the other hand, the voltage signal in case of 11-cycle fault is undamped with 35.14 Hz oscillation frequency.

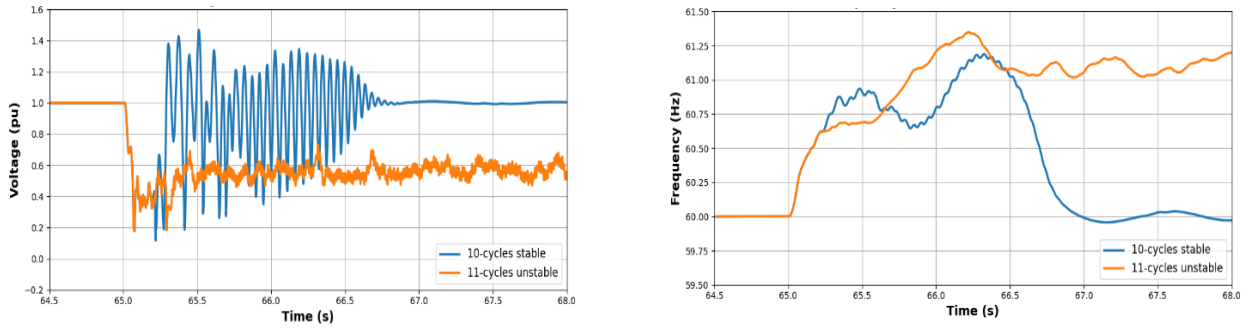

Figure 41. Voltage and frequency of East Garden City POI after generator trip

In summary, when the large synchronous generator was tripped, simulating a Category P6 contingency involving sequential outages, the system's stability was adversely affected. The CCT at the Gowanus POI decreased by 3 cycles, dropping to 10 cycles. This reduction underscores the sensitivity of the system to combined events involving loss of conventional inertia-rich generation and subsequent fault-induced

disturbances. The trip of this generator not only altered the pre-fault steady-state equilibrium but also removed critical inertia and voltage support, thereby lowering the fault ride-through capability of the grid at key POI locations.

Contingency 3: Stuck Breaker Study

This part investigates a Category P4 stuck breaker contingency as defined by NERC TPL-001-4, specifically focusing on the Long Island area of the NYS transmission network. The selected scenario involves a single-phase fault initiated on a transmission line near the Ruland RD bus. The Ruland RD bus is the POI for Juno Power Express wind farm, and this bus is a critical node within the Long Island transmission corridor. This bus is electrically proximate to several major transmission interfaces. The fault scenario assumes that, following the fault application, the line circuit breaker at Ruland Road fails to operate. Consequently, fault current continues to flow.,

To mitigate the breaker failure, a backup protection scheme is activated. This initiates the tripping of circuit breakers electrically adjacent to the failed breaker. The tripping of these elements introduces significant changes in network topology than under normal fault-clearing scenarios, impacting power flow distribution, system inertia, and voltage stability margins.

The EMT model of the NYS grid was initialized under flat-start steady-state conditions, with all relevant loads, generators, and 5 OSWs active. A single-line-to-ground fault on the transmission line TLINE NY at t = 60.1 (s). A line breaker failed to clear, backup protection was then triggered, and the fault was cleared through breaker action on a breaker and half bus scheme within 12 cycles. These actions led to the isolation of the faulted transmission line. Figure 42 shows the Ruland RD bus voltage for this contingency. The voltage profile at Ruland RD substation shows the unfaulted phase has a slow decay during the fault, followed by a sustained period of non-sinusoidal overvoltage following fault recovery. Figure 43 shows significant distortion in the TLINE NY line current during the fault, particularly in the unfaulted phases. Similarly, the undamped frequency oscillations in Figure 44 are triggered at both the terminal of Ruland RD OSW as well as Ruland RD substation. Thus, this stuck breaker contingency demonstrated the possible instability of the Ruland Road OSW in this case. In this event, it is clear that the Juno Power Express Wind Farm would trip off line to avoid damage to the converters.

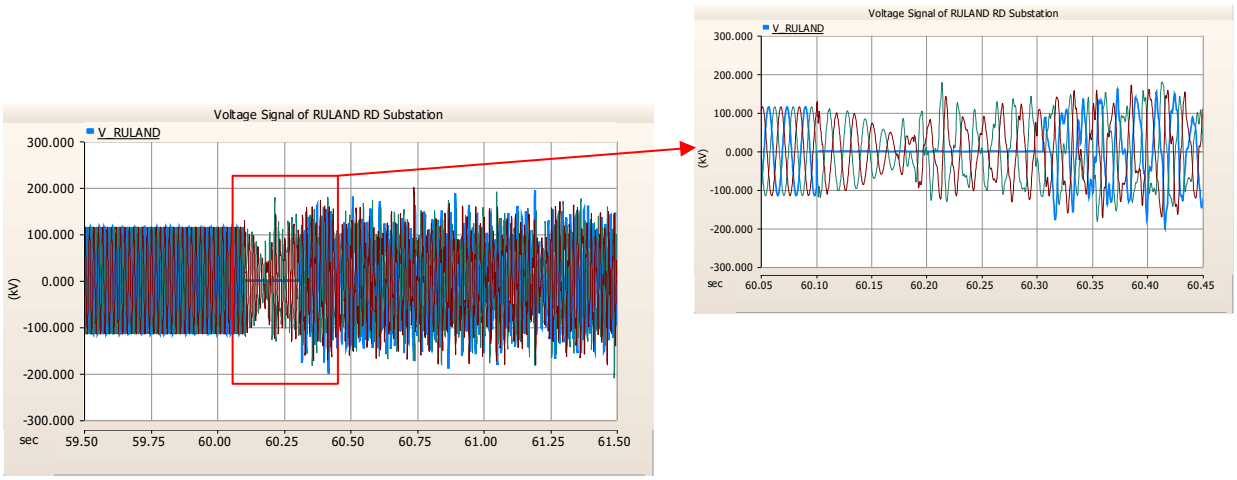

Figure 42. Voltage (kV) profile at Ruland RD substation

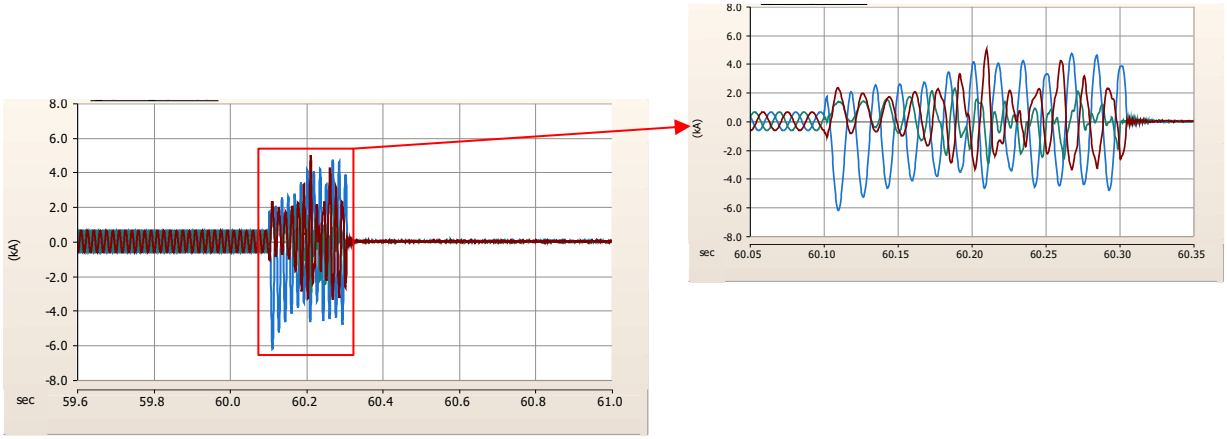

Figure 43. Current flow (kA) on the faulted transmission line

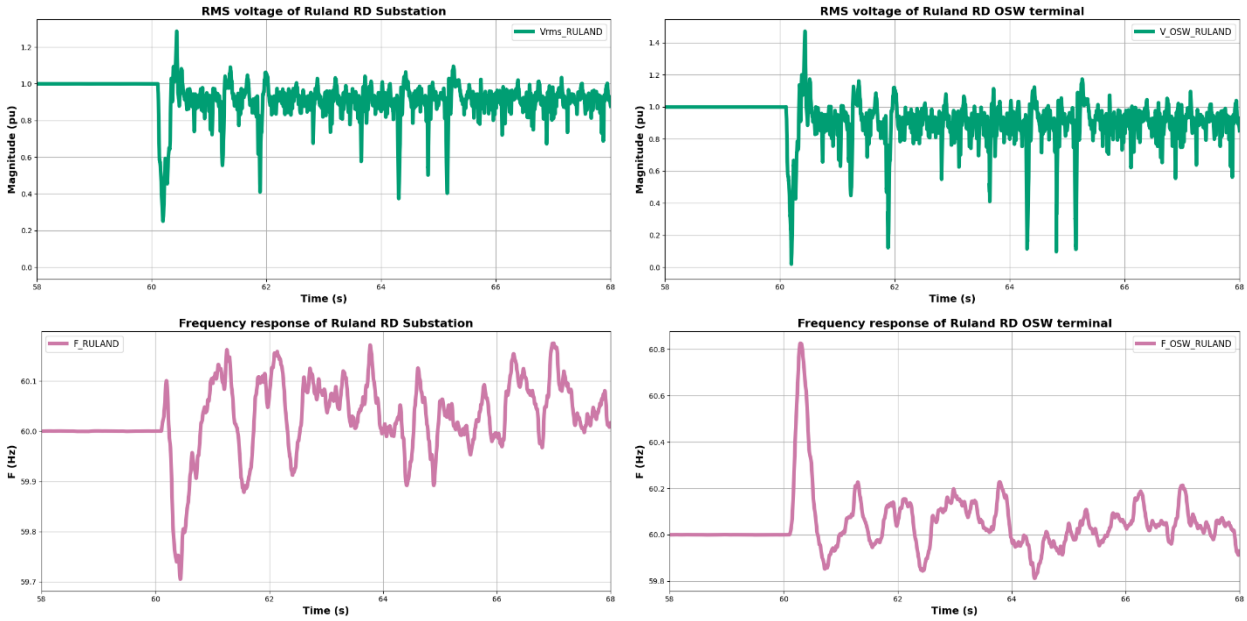

Figure 44. Voltage and frequency responses at Ruland RD Substation and OSW terminal

4.3.ISO-NE Contingencies and Faults Analysis

A comprehensive fault and contingency study for ISO-NE has been performed on the four offshore wind projects. Table 15 summarizes these projects, detailing their capacities, proposed POIs, voltage levels, designated onshore substations, and export technologies.

Table 15. Configuration of ISO-NE Proposed Offshore Wind Farms

Name	Capacity	Transmission	POI Substation	Voltage
South Coast Wind	1204 MW	HVDC	Brayton Points - Massachusetts	345 kV
New England Wind 1	804 MW	HVAC	West Barnstable -Massachusetts	345 kV
Vineyard Wind 1	800 MW	HVAC	Barnstable -Massachusetts	115 kV
Revolution Wind	704 MW	HVAC	Davisville Substation – Rhode Island	115 kV

These 4 OSWs with a total rating of 3.5GW are proposed to connect to three points of interconnection (POIs) in Massachusetts (MA) and one POI in Rhode Island (RI). It is noted that there recently have been significant changes to these proposed wind farms, including several cancellations.

A reduced ISO-NE EMT model for spring light-load and summer-peak conditions was used, retaining all internal generators and all Massachusetts (MA) and Rhode Island (RI) buses at 220 kV or above.

ISO-NE Fault Analysis

A balanced three-phase fault was applied at the 345 kV West Barnstable (MA) POI. Four offshore-wind penetration levels were evaluated:

- 0 OSW: Base model without offshore wind in service.
- 1 OSW: West Barnstable (MA).
- 2 OSW: West Barnstable (MA), and Davisville (RI).
- 3 OSW: West Barnstable, Brayton Points, and Davisville (RI)
- 4 OSW: West Barnstable, Brayton Points, Barnstable (MA), and Davisville (RI)

For each penetration level, an EMT-based fault study was carried out under both spring light-load and summer peak-load conditions to determine the system's critical clearing time (CCT). The analysis compares stability margins with and without offshore-wind integration, identifying how the progressive addition of one, two, three, and all four projects affects transient stability across the ISO-NE network.

A system-level electromagnetic-transient (EMT) fault analysis was carried out on the fully integrated offshore wind farms and the ISO-NE power system. The study examined multiple scenarios under different grid conditions, including spring light-load and summer peak-load cases.

Scenario 1: 2028 Spring Light–Load (Balanced Fault at West Barnstable)

Table 16 summarizes the critical clearing times (CCTs) obtained as up to four offshore projects are added to the ISO-NE spring light-load model for the Massachusetts (MA) and Rhode Island (RI) retained areas. In the base case with no offshore wind, the system is stable for a 21-cycle fault three phase fault. Adding the first offshore plant at West Barnstable reduces the CCT to 19 cycles, and adding a second plant at Davisville lowers it further to the study minimum of 17 cycles. After the third and fourth projects are connected, the margin improves slightly to 20 and 19 cycles, respectively showing that the impact depends on system topology and conditions, and not merely on the total offshore capacity. Figure 45 shows the stability boundary for the 4 OSW case.

The minimum critical clearing time of 17 cycles remains above typical 345 kV breaker-clearing targets of 8–10 cycles, so transient-stability headroom is still ample.

Scenario 2: 2028 Summer Peak Load (Balanced Fault at West Barnstable)

Table 17 shows that under summer-peak conditions, with about 11.5 GW of synchronous generation online, the base case (no offshore wind) withstands a three-phase fault at the 345 kV West Barnstable POI for 13 cycles. Adding the first and second offshore projects reduces the critical clearing time (CCT) to 12 cycles. Introducing a third project raises the CCT back to 13 cycles, while connecting all four projects lowers it

again to 12 cycles. This ±1-cycle swing indicates that offshore wind has only a minor influence on transient stability at peak load.

Table 16. Critical Clearing Time for a three-phase fault at the West Barnstable substation using the spring light load model

Case No	Name	Number of OSW	Description	Critical Clearing Time
1	Zone MA-RI without OSW with 3-phase faults (West Barnstable)	0	Massachusetts (MA) and Rhode Island (RI) - Spring Light load case with 169 buses, 38 generators with dynamic models, and a total generation capacity of 1.86 GW in retained areas. → Synchronous generating unit unstable	21 cycles
2	Zone MA-RI with 1 OSW with 3-phase faults (West Barnstable)	1	1 OSW – West Barnstable (MA) → Synchronous generating unit unstable	19 cycles
3	Zone MA-RI with 2 OSW with 3-phase faults (West Barnstable)	2	2 OSWs – West Barnstable (MA), and Davisville (RI). → Synchronous generating unit unstable	17 cycles
4	Zone MA-RI with 3 OSW with 3-phase faults (West Barnstable)	3	3 OSWs: West Barnstable, Brayton Points, and Davisville (RI) → Synchronous generating unit unstable	20 cycles
5	Zone MA-RI with 4 OSW with 3-phase faults (West Barnstable)	4	4 OSWs: West Barnstable, Brayton Points, Barnstable (MA), and Davisville (RI) → Synchronous generating unit unstable	19 cycles

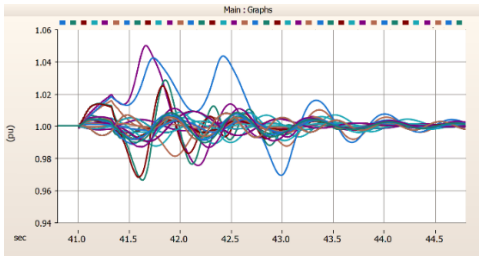

(a) Speed profile (per unit), 19-cycle fault

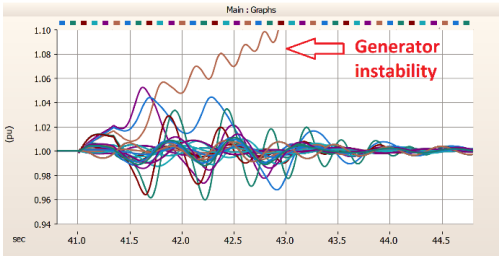

(b) Speed profile (per unit), 20-cycle fault

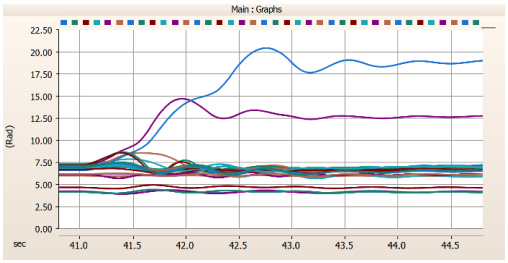

(c) Rotor-angle profile (rad), 19-cycle fault

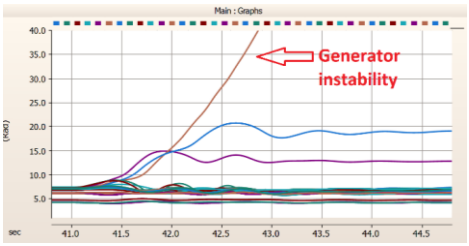

(d) Rotor-angle profile (rad), 20-cycle fault

Figure 45. Comparison of machine speed (a, b) and rotor-angle (c, d) profiles for the 4-wind case at West Barnstable under stable (19-cycle clearing) and unstable (20-cycle clearing) conditions. Spring Light Load Case

Table 17. Critical Clearing Time for a three-phase fault at the West Barnstable substation using the summer peak load model

Case No	Name	Number of OSW	Description	Critical Clearing Time
1	Zone MA-RI without OSW with 3-phase faults (West Barnstable)	0	Massachusetts (MA) and Rhode Island (RI) - Summer load case with 218 buses, 70 generators with dynamic models, and a total generation capacity of 11.5 GW in retained areas. → Synchronous generating unit unstable	13 cycles
2	Zone MA-RI with 1 OSW with 3-phase faults (West Barnstable)	1	1 OSW – West Barnstable (MA) → Synchronous generating unit unstable	12 cycles
3	Zone MA-RI with 2 OSW with 3-phase faults (West Barnstable)	2	2 OSWs – West Barnstable (MA), and Davisville (RI). → Synchronous generating unit unstable	12 cycles
4	Zone MA-RI with 3 OSW with 3-phase faults (West Barnstable)	3	3 OSWs: West Barnstable, Brayton Points, and Davisville (RI) → Synchronous generating unit unstable	13 cycles
5	Zone MA-RI with 4 OSW with 3-phase faults (West Barnstable)	4	4 OSWs: West Barnstable, Brayton Points, Barnstable (MA), and Davisville (RI) → Synchronous generating unit unstable	12 cycles

ISO-NE Contingency Analysis

In order to determine high-risk oscillations for the ISO-NE large-scale model, including both onshore and offshore systems, the team implemented multiple practical contingency scenarios to assess the dynamic stability of the ISO-NE grid under a high level of OSW integration. Table 18 presents the description of the studied contingencies for ISO-NE and lists some particular example cases for each planning event. The team implemented a total of 54 events for the ISO-NE large-scale model, with 27 events for the Spring Light-Load (SLL) case and 27 events for the Summer Peak Load case. All contingency scenarios are eventually tested with 4 POIs of OSWs and some critical buses inside the ISO-NE grid model, as shown in Table 19.

Table 18. Studied contingencies for ISO-NE

Category	No of Events	Initial Condition	Fault Type	Example Scenario
P0	1	Normal	None	None
P1	6	Normal	Three-phase fault	Apply fault at Barnstable POI bus
P2	2	Normal	None	Open a transmission line 1
				Open a transmission line 2
P3	6	Trip Synchronous Generator 1	Three-phase fault	Apply fault at West Barnstable POI bus
	6	Trip Synchronous Generator 2		Apply fault at Brayton Point POI bus
P4	6	Normal	Single-phase fault	Apply fault at Davisville POI bus
P6	6	Open a transmission line 2	Three-phase fault	Apply fault at Bus 2

The ISO-NE model is tested and found to be stable during normal conditions, satisfying TPL Category P0 requirements. In order to study the impact of the high-level IBR penetration, the team focused on one particular contingency for the ISO-NE grid model. All other events are found to be stable when testing with the clearing times and their results recover to values consistent with their original steady-state conditions.

Table 19. Critical buses to study for ISO-NE

Name	Comment
Bus 3	Bus located adjacent to nearby generator
Bus 4	Bus located at nearby generator

Contingency 1: Loss of a transmission line between West Barnstable POI and Substation 1

This section presents a two-element contingency event applied to the ISO-NE power system model with high offshore wind penetration. The EMT model of the ISO-NE grid was initialized under flat-start steady-state conditions, verifying pre-contingency power flow convergence across all network nodes. All significant system components, including conventional generators, loads, and 4 OSWs located at West Barnstable, Barnstable, Brayton Point, and Davisville were modeled as active and synchronized with the onshore grid.

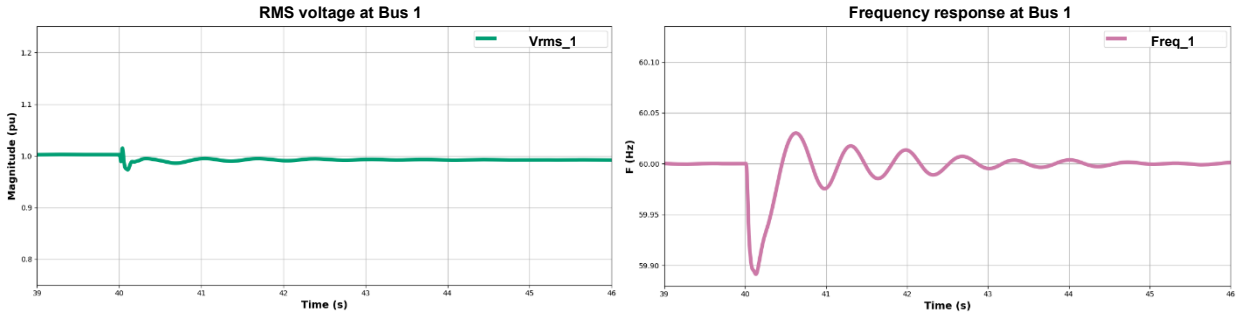

Figure 46. Bus 1 RMS voltage and frequency responses following the transmission line trip event

The contingency sequence involves the tripping of a line in the transmission corridor between West Barnstable POI and Bus 1 substation. The transmission line tripping is initiated at time t = 40 (s) through the opening of the circuit breaker on the line connecting the West Barnstable POI to Bus 1. Figure 46 shows the voltage and frequency response to this event. This event leads to a sudden redistribution of power flow and alters the local impedance seen by the offshore wind farm at West Barnstable. Following the tripping event, a significant voltage rise in Figure 47 is observed at the OSW terminal connected to the West Barnstable substation. The voltage magnitude rises above 1.2 p.u, surpassing the upper threshold defined in the OSW's protection relay settings. As a result, the OSW at West Barnstable is automatically disconnected by its local circuit breaker protection system within 21 ms in order to prevent overvoltage-induced equipment damage.

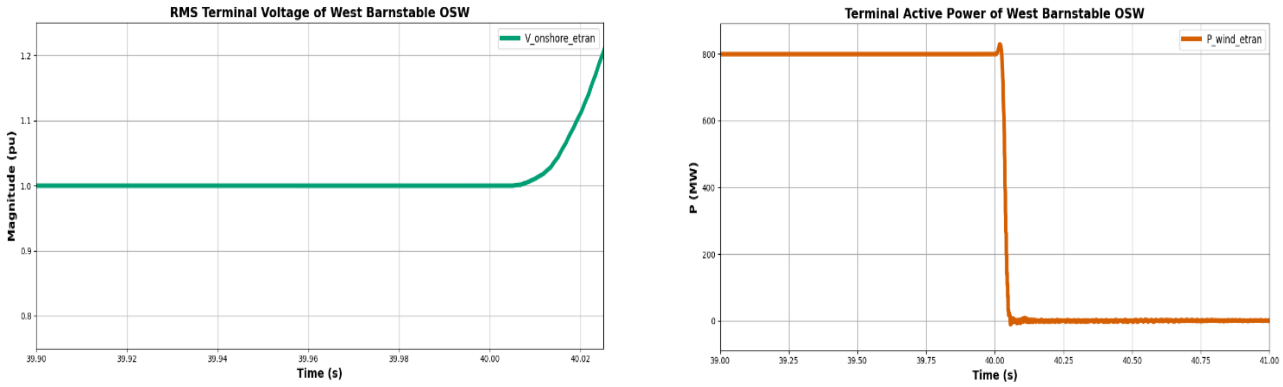

Figure 47. Overvoltage Event leading to shutdown of West Barnstable OSW

This disconnection removes a major wind generation source (800 MW) from the area, further intensifying the local voltage and reactive power imbalance. The event triggers the oscillatory behavior in Figure 46, and the reduction in generation support at the POI also introduces temporary voltage and frequency sag. Moreover, the sudden removal of OSW output causes a localized inertial frequency transient for conventional generators, illustrated in Figure 48. This figure shows that the system stabilizes with a damped 15-hertz inertial oscillation.

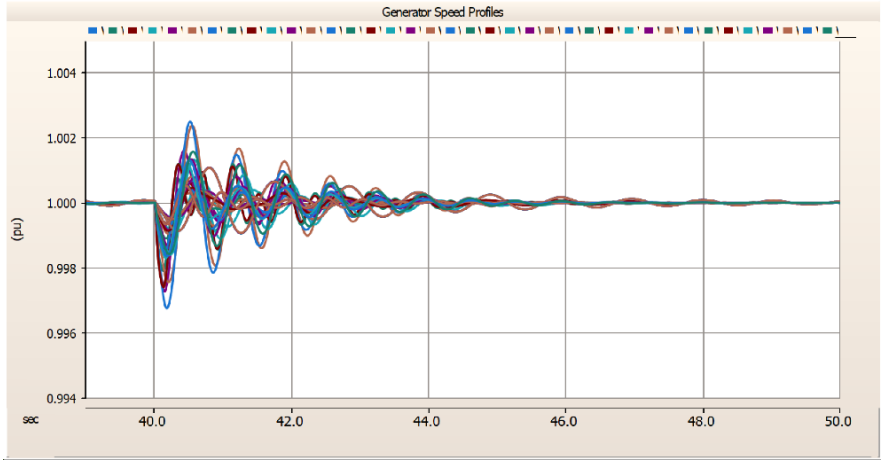

Figure 48. Generator speed profiles following transmission line tripping

The results of this study indicate that while the ISO-NE grid can withstand two-element contingency under high OSW integration, line outage events (Category P6) can precipitate the tripping of vital renewable generation resources due to transient overvoltage conditions.

II. PJM Contingency and Fault Analysis

A fault and contingency analysis has been completed for PJM's seven offshore wind projects. Table 20 outlines each project's capacity, point of interconnection (POI), voltage level, onshore substation, and export technology.

Table 20. Configuration of PJM Proposed Offshore Wind Farms

Name	Capacity	Transmission	POI Substation	Voltage
Atlantic Shores South Wind Project, Phase 1	1510 MW	HVAC	Cardiff Substation (New Jersey)	230 kV
Atlantic Shores South Wind Project, Phase 2	1327 MW	HVAC	Larrabee Substation (New Jersey)	230 kV
Momentum Wind, Phases 1 and 2	1109 MW	HVAC	Indian River Substation (Delaware)	230 kV
Coastal Virginia Offshore Wind (CVOW) Commercial Project	2640 MW	HVAC	Fentress substation (Virginia)	500 kV
Kitty Hawk South Wind	2465 MW	HVAC	Birdneck Substation (Virginia)	230 kV
Kitty Hawk North Wind	1035 MW	HVAC	Birdneck Substation (Virginia)	230 kV

These seven offshore wind projects totaling ≈ 10 GW are slated to connect to the PJM grid at points of interconnection in New Jersey (Atlantic City Electric, AE), Delaware (Delmarva Power & Light, DP&L), and Virginia (Virginia Beach/VABEACH, Dominion). The study uses a reduced PJM EMT model for both spring light-load and summer peak-load conditions

1. PJM backbone: all buses ≥ 500 kV
2. Dominion (DVP) area: buses ≥ 500 kV
3. Atlantic City Electric (AE) area: buses ≥ 230 kV
4. Delmarva Power & Light (DP&L) area: buses ≥ 230 kV
5. Virginia Beach (VABEACH) area: buses ≥ 230 kV

All generating units within the AE, DP&L, and VABEACH areas are explicitly included in the simulations.

4.4. PJM Fault Analysis

This section evaluates the transient stability of PJM with the proposed seven-project, 10 GW offshore portfolio. Two seasonal cases are studied:

- Scenario 1: 2028 Spring Light–Load (Balanced Fault at different POIs)
- Scenario 2: 2028 Summer Peak Load (Balanced Fault at different POIs)

For each scenario, a reduced EMT model retains the 500 kV backbone, all internal generators, and the AE, DP&L, JCPL, and VABEACH areas down to 230 kV. Balanced three-phase faults, cleared in 25 cycles, are applied at six representative points of interconnection: Bird Neck, Landstown, Cardiff, Larrabee, Fentress, and Indian River. Results for the base system (no offshore wind) are compared with the full seven-OSW build-out to determine whether the added offshore generation affects stability margins under spring light-load and summer peak load conditions.

Scenario 1: 2028 Spring Light–Load (Balanced Fault at different POIs)

Table 21 summarizes the spring light-load screening of balanced three-phase faults at six key PJM points of interconnection. In this case, 1.6GW of synchronous generators are online.

Table 21. Summary of three-phase fault at PJM POIs using the SLL model.

Case No	Name	Number of OSW	Description
1	Base Case: No OSWs	0	Conducted 6 scenarios with three-phase faults at the following POIs: Three-phase faults at the following POIs: • Bird Neck • Landstown • Cardiff • Larrabee • Fentress • Indian River → The system remained stable for a 25-cycle clearing time.
2	Full wind case: All wind farms operating at rated output	7	Conducted 6 scenarios with three-phase faults at the following POIs: • Bird Neck • Land Stone • Cardiff • Larrabee • Fentress • Indian River →The system remained stable for a 25-cycle clearing time.

Scenario 2: 2028 Summer Peak Load (Balanced Fault at different POIs)

PJM's robust 500 kV grid keeps the system stable for a 25-cycle clearing time in every scenario. This allows sufficient for time backup fault clearing. The base case without offshore wind and the full build-out with seven offshore projects (≈ 10 GW) both retain stability through these faults at Bird Neck, Landstown, Cardiff, Larrabee, Fentress, and Indian River. The unchanged outcome shows that the network's strength and high inertia, rather than offshore-wind injection, set the transient-stability limit under spring light-load conditions.

Table 22 summarizes the summer-peak screening for balanced three-phase faults at six PJM points of interconnection.

In this case, 5.3 GW of synchronous capacity is on line in the study area. The grid stays stable when a 25-cycle fault is applied at Bird Neck, Landstown, Cardiff, Larrabee, Fentress, or Indian River. This unchanged

outcome, like the spring light-load result, shows that the robust 500 kV backbone and high summer inertia dominate transient behavior; offshore additions do not erode stability within the tested clearing window.

Table 22. Summary of three-phase fault at PJM POIs using the summer peak load model for 25 cycles

Case No	Name	Number of OSW	Description
1	Base case: No wind	0	Conducted 6 scenarios with three-phase faults at the following POIs: Three-phase faults at the following POIs: • Bird Neck • Landstown • Cardiff • Larrabee • Fentress • Indian River → The system remained stable for a 25-cycle clearing time.
2	Zone AE, DP&L, and VA with 7 OSWs with three-phase faults at different POIs	7	Conducted 6 scenarios with three-phase faults at the following POIs: • Bird Neck • Land Stone • Cardiff • Larrabee • Fentress • Indian River →The system is stable with 25 cycles faults

PJM Contingency Analysis

In order to determine high-risk oscillations for the PJM large-scale model including both onshore and offshore system, the team implemented multiple practical contingency scenarios to assess the dynamic stability of PJM grid under the high level of OSW integration. Table 23 presents the description of the studied contingencies for PJM and lists particular example case for each planning event. The team implemented a total of 54 events for PJM large-scale model with 27 events for Spring Light-Load (SLL) case and 27 events for summer case. All contingency scenarios are eventually tested with 5 POIs of OSWs and 1 critical bus inside PJM grid model.

Table 23. Studied contingencies for PJM

Category	No of Events	Initial Condition	Fault Type	Example Scenario
P0	1	Normal	None	None
P1	6	Normal	Three-phase fault	Apply fault at Birdneck POI bus
P2	2	Normal	None	Open a transmission line between in the study area
P3	6	Trip Gas & Steam generator	Three-phase fault	Apply fault in the study area
P4	6	Normal	Single-phase fault	Apply fault at Fentress POI bus
P6	6	Open a transmission line between Cardiff and Orchard substation	Three-phase fault	Apply fault at Cardiff POI bus

The PJM model is tested and found to be stable during normal conditions, satisfying TPL Category P0 requirements. In order to study the impact of the high-level IBR penetration, the team conducted 54 contingency studies for PJM grid model. Several of these studies are discussed below. All other events for PJM grid are found to be stable when testing with the clearing times and their results recover to values consistent with their original steady-state conditions.

Contingency 1: Loss of 3 Gas & Steam Turbine Units + Three-Phase Bus Fault

Category P3, as defined by NERC TPL-001-4 standards, addresses disturbances involving a generator tripping event followed by a three-phase fault on the critical bus. The purpose of this study is to assess the system's dynamic performance under this sequence of disturbances and evaluate the response of both synchronous and inverter-based resources under such conditions. This P3 contingency was notably implemented in two sequential events:

- Event 1 – Generator Tripping: 3 synchronous generators, were tripped simultaneously at t = 40 (s).
- Event 2 – Three-Phase Fault Study: Once the system recovered from the initial generator trip, a three-phase fault was applied at a critical bus at t = 45 (s). The fault persisted for 24 cycles (0.4 (s)) before being cleared.

The first event causes a small localized temporary oscillation for other conventional generators, as shown in Figure 49. Moreover, the generator tripping event resulted in an insignificant frequency dip at nearby Atlantic Shores South Wind 1 terminal as shown in Figure 50.

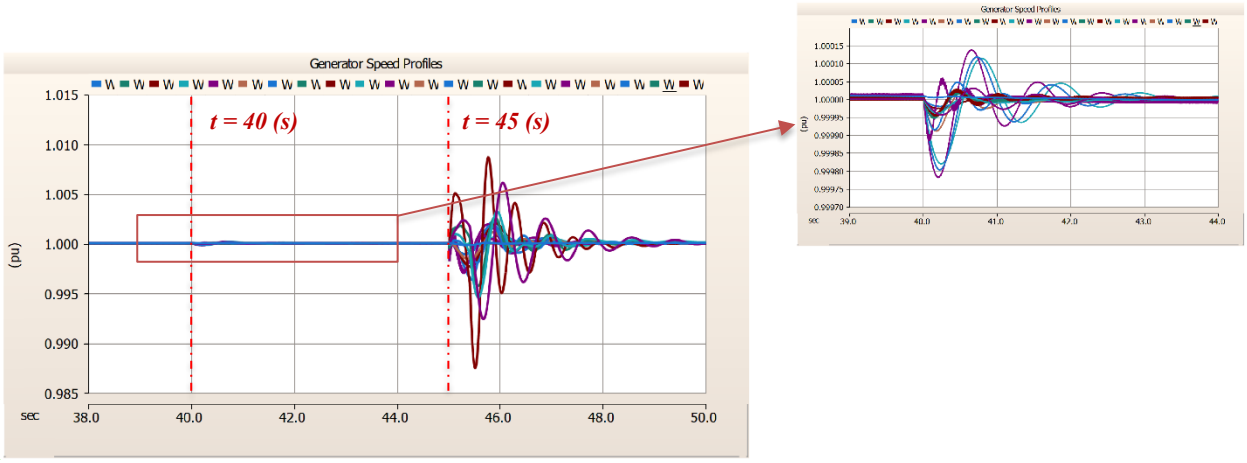

Figure 49. Generator speed profiles following the contingency

For Event 2, the three-phase fault in 24 cycles at the critical substation led to a sharp voltage drop at the faulted to 0 pu. At the faulted bus, the rms voltage varied during the fault, between 0.3 and 0.55 pu, as shown in Figure 50. No undervoltage protection was triggered, as appropriate. During Event 2, fault-ride through feature of Atlantic Shores South Wind 1 assisted in supporting voltage and frequency responses. This study confirms that the PJM large-scale grid can tolerate sequential high-impact events, provided appropriate control responses are embedded within OSW systems.

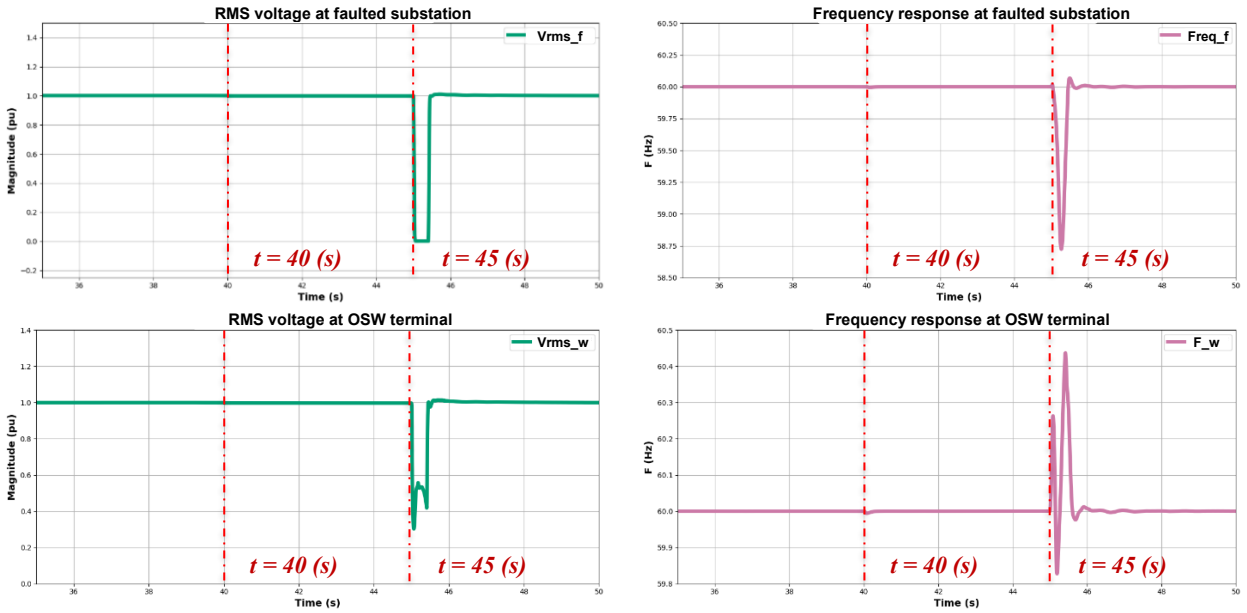

Figure 50. Voltage and frequency response at faulted substation and Atlantic Shores South Wind 1 terminal (Frequency measured by the GFM HVDC controller).

4.5. Task 2.1 Summary

In Task 2.1, the team has successfully laid the foundational framework for evaluating control instability risks associated with large-scale OSWs integration into the Atlantic grid. A comprehensive methodology has been developed to identify high-risk system conditions and disturbances, grounded in industry standards such as NERC PRC-006, PRC-024, IEEE P2800, and regional utility requirements.

Key risk metrics include:

- Negative damping and low-damping ratio scenarios identified in small-signal studies
- Rotor angle transient instabilities of synchronous generators that can be negatively impacted by OSW installations
- Misoperation of HVDC line converters during transient stability studies
- Sustained overvoltage conditions during fault recovery

Key risk factors for grid characteristics and operating scenarios identified in Task 2.1 include:

- Weak grid operating conditions,
- High wind ramp rates
- Low-inertia systems
- Extreme weather-related contingencies

Task 2.1 also investigated the consequences of high-impact events, including:

- Stuck breaker contingency events
- Loss of large synchronous generator
- Loss of major transmission line
- Both balanced and unbalanced faults
- Offshore substation faults

These risks identified in Task 2.1 will be the primary focus of study in Task 2.2.In Task 2.2, the focus was shifted toward root cause analysis of control instability phenomena and the development of targeted mitigation strategies. This includes evaluating the origin of sub-synchronous and harmonic oscillations arising from interactions among wind turbines, HVDC systems, series-compensated lines, and weak-grid conditions. Through EMT-based simulation, small signal analysis, and control tuning, the team will jointly assess the effectiveness of proposed countermeasures such as additional damping devices, controller retuning, and operational isolation of critical components.

5. Task 2.2. Risk Analysis and Mitigation

In Task 2.2, the risk-origination analysis was conducted and risk mitigation measures were evaluated, building on the risk conditions and disturbances identified in Task 2.1. This includes designing and executing simulation cases and reporting results on the onshore-equivalent PSCAD models of the East Coast regional transmission grids (NYISO, ISO-NE, and PJM) and their associated wind farms.

This task comprised two distinct steps, which are documented in Sections 5.1 and 5.2 of this section.

5.1. Identify the potential original sources of risk

The potential sources of control instability risks in the integrated Atlantic OSW grid include both electrical and mechanical interactions between renewable generation, transmission infrastructure, and system controls. The identification of potential original sources of oscillatory risk was conducted using small-signal eigenvalue analysis with the Small Signal Analysis Tool (SSAT) from DSATools. This methodology provides a system-wide modal analysis, allowing the team to identify lightly damped or unstable modes under a variety of operating conditions. By combining eigenvalue analysis with damping ratio evaluation and participation factor assessment, the project team was able to systematically identify the origin of risks and prioritize those modes with the greatest potential impact on system stability.

As the objective of this task is to identify possible high-risk oscillations in the Eastern Interconnection grid model when integrating with multiple Offshore Wind Farms (OSWs), the team proposed small-signal stability assessment contingencies to study our large-scale model. There are a total four cases (from S0 – S3): a baseline (no contingency) and three N-1 contingencies (bus, line, generator outage) as shown in Table 24. For each case, SSAT computes system eigenvalues $s = \sigma \pm j\omega$ of the linearized state matrix around the operating point. Derived stability metrics include oscillation frequency and damping ratio.

In consultation with the project's Industry Advisory Board, the team identified critical contingencies for each of the NYSIO, ISO-NE and PJM areas. These contingencies were then used to conduct small-signal stability analysis for the NYISO, ISONE, and PJM areas. The nature of these contingencies are listed in Tables 25-27. Specifics are not given due to security constraints.

Table 24. Small-Signal Analysis Description

Scenario	Type	Description
S0	Baseline (No Contingency)	All generators/loads/OSWs in service.
S1	Bus Outage (N-1)	Specified buses were removed.
S2	Line Outage (N-1)	Specified transmission line opened.
S3	Generator Outage (N-1)	Specified unit tripped.

Table 25. Contingencies of the NYISO area

Contingency Name	Contingency	Comment
GEN LI	Generator Outage trip on Long Island)	System response to Outage of conventional generator.
GEN NYC	Generator Outage in NYC	System response to Outage of the conventional generator.
TLINE NY	Transmission Intertie Outage	System response to line Outage (N-1).
BUS NY	New York Bus Outage	System response to bus Outage (N-1).

Table 26. Specific contingencies of the ISONE area

PSSE Bus #	Name	Comment
GEN NE1	Generator Outage in New England)	System response to conventional generator Outage.
GEN NE 2	Generator Outage in New England	System response to conventional generator Outage trip.
TLINE NE	Transmission Lines Outage in New England	System response to line Outage (N-1).
BUS NE	New England Bus Outage	System response to bus Outage (N-1).

Table 27. Specific contingencies of the PJM area

PSSE Bus #	Name	Comment
GEN PJM	PJM Generator Outage	System response to conventional generator Outage.
BUS PJM	PJM Bus Outage	System response to bus Outage (N-1).
TLINE PJM	PJM Line Outage	System response to line Outage (N-1).

NYISO Small-Signal Stability Analysis

The team implemented a total of 12 contingencies for the NYISO large-scale model using SSAT eigenvalue analysis, with 6 cases for the Spring Light-Load (SLL) case and 6 cases for the summer peak load case. All contingency scenarios are eventually tested with 5 OSWs online. For the SLL dataset, there are a total of three cases showing negative damping ($\zeta < 0\%$) for at least one electromechanical mode. Two of them are generator-outage contingencies, and one is a line-outage contingency. Negative damping ratios correspond to modes with positive real eigenvalues ($\sigma > 0$), signifying unstable modes where oscillations grow unbounded. All other cases were observed with positive damping ratios ($\zeta > 0\%$); and no mitigations are required beyond baseline monitoring.

Contingency 1: Line Outage (TLINE NY)

In this case, the line-outage scenario is simulated to assess the impact of OSWs integration on the stability of the onshore grid system. This contingency involves a transmission line between a LI POI and an adjacent substation. SSAT will automatically recompute the post-outage linearized system model and run eigenvalue analysis on the post-contingency state matrix.

Under the studied line-outage contingency, all five offshore wind projects exhibit sub-synchronous, control-driven modes in the 6–13 Hz range. One project, Vineyard Mid Atlantic Wind, participates in a 13.3 Hz mode with a negative damping ratio ($\zeta = -10.4$ %). Moreover, Juno Express Wind is involved in a mode with marginal damping ($\zeta = 1.7$ %) at 6.6 Hz. The remaining modes, Empire Wind 1 ($\zeta = 3.5$ % at 8.0 Hz), Sunrise Wind ($\zeta = 4.5$ % at 6.1 Hz), and Beacon Wind ($\zeta = 5.6$ % at 7.3 Hz) meet the common 3–5 % planning guideline for damping ratios. Following the line trip, the effective short-circuit strength at the relevant POIs decreases and the network impedance profile shifts. This altered environment increases the sensitivity of outer-loop voltage/reactive controls in IBRs, producing lightly damped or unstable modes. The 13.2 Hz unstable mode at Vineyard Mid Atlantic Wind is consistent with a converter–grid interaction

rather than a classic electromechanical swing mode. The 6.6 Hz marginal mode at Juno Express Wind likely shares the same mechanism (weaker POI). By contrast, Empire, Sunrise, and Beacon retain adequate damping (3.5–5.6 %) in the same band, which suggests that controller parameterizations are less interactive with the post-contingency network.

Table 28. SSAT results of 5 OSWs in NYISO for the TLINE NY contingency.

OSW participation	Frequency (Hz)	Damping Ratio (%)	Risk Flag
Empire Wind 1	8.0	3.5	OK
Sunrise Wind	6.1	4.5	OK
Beacon Wind	7.3	5.6	OK
Juno Express Wind	6.6	1.7	Low ζ
Vineyard Mid Atlantic Wind	13.2	-10.4	Unstable

Contingency 2: Generator Outage GEN NYC

In this case, a generator outage in New York City is simulated to assess the impact of OSWs integration on the stability of the onshore grid system. SSAT will automatically recompute the post-outage linearized system model and run eigenvalue analysis on the post-contingency state matrix. This tripping not only reduced active power supply but also decreased system inertia and reactive support, thereby weakening the short-circuit strength in the surrounding network. The SSAT eigenvalue analysis revealed significant changes in system oscillatory behavior, particularly 5 OSWs.

Table 29. SSAT results of 5 OSWs in NYISO for GEN NYC

OSW	Frequency (Hz)	Damping Ratio (%)	Risk Flag
Empire Wind 1	1.6	8.1	OK
Sunrise Wind	3.2	-6.0	Unstable
Beacon Wind	10.1	3.8	OK
Juno Express Wind	11.9	0.9	Low ζ
Vineyard Mid Atlantic Wind	2.6	-5.3	Unstable

The generator-outage contingency exposes two unstable and one marginal modes among the five OSWs, with two additional plants remaining acceptable. As shown in Table 28, Empire Wind 1 exhibits a local plant electromechanical mode at 1.6 Hz with $\zeta = 8.1$ %, indicating an adequate damping margin. Beacon Wind presents an electrical mode at 10.1 Hz with $\zeta = 3.8$ %; within the common 3–5 % planning guideline. Juno Express Wind is involved in a mode at 11.9 Hz with $\zeta = 0.9$ %, which is marginal and requires attention due to the low damping margin and proximity to converter control bandwidths. Most critically, Sunrise Wind and Vineyard Mid Atlantic Wind both present unstable modes (negative damping ratios): Sunrise Wind at 3.2 Hz with $\zeta = -6.0$ % and Vineyard Mid Atlantic Wind at 2.6 Hz with $\zeta = -5.3$ %. The generator outage reduces system strength and reactive margin in the vicinity of the affected corridors and POIs, shifting the relative dynamic dominance toward inverter-based resources (IBRs). In this condition, PLL dynamics of HVDC grid-side inverter become more exposed to the network's frequency-dependent impedance (aggressive outer-loop/PLL bandwidth). Given these findings, the risk ranking for this contingency is unambiguous. Sunrise Wind (3.2 Hz, $\zeta = -6.0$ %) and Vineyard Mid Atlantic Wind (2.6 Hz, $\zeta = -5.3$ %) are critical (unstable) and require immediate corrective actions. Juno Express Wind (11.9 Hz, $\zeta = 0.9$ %) is marginal and should be treated as a near-term mitigation candidate to avoid slipping into instability under alternative dispatches or additional outages. Beacon Wind (10.1 Hz, $\zeta = 3.8$ %) is adequate but should be monitored, especially for operating points with lower SCR. Empire Wind 1 (1.6 Hz, $\zeta = 8.1$ %) is adequate with a comfortable margin. These results confirm that the loss of a major generator reduces system damping margins and highlights the importance of supplemental damping support from IBRs.

5.2. ISO-NE Small-Signal Stability Analysis

The team implemented a total of 8 contingencies for the ISO-NE model using SSAT eigenvalue analysis, with 4 cases for the Spring Light-Load (SLL) case and 4 cases for the summer peak load case. All contingency scenarios are eventually tested with 4 OSWs online. All cases were observed with positive damping ratios ($\zeta > 0\%$); and no immediate mitigations are required beyond baseline monitoring. The generator contingency results are presented below.

Contingency: Generator Outage GEN NE1

In this case, the generator tripping scenario is simulated to assess the impact of OSWs integration on the stability of the onshore grid system. The contingency GEN NE1 SSAT eigenvalue analysis indicates that all observed oscillatory modes remain adequately damped and comfortably within accepted planning criteria. Specifically, the mode most related to Park City Wind exhibits a local oscillatory mode at 1.6 Hz with a damping ratio of 4.7%, while Vineyard Wind demonstrates a mode at 1.7 Hz with a damping ratio of 8.9%, representing the strongest damping margin among the group. Bay State Offshore Wind shows a mode at 2.2 Hz with a damping ratio of 4.1%, and Revolution Wind presents a mode at 1.8 Hz with a damping ratio of 3.9%. All damping ratios exceed the critical 3% threshold commonly applied in small-signal stability assessments, and no negative damping was observed. These results confirm that the integration of these four offshore wind farms under generator-outage conditions does not introduce any unstable or poorly damped modes into the system. Because all modes are stable and adequately damped, no further mitigation measures are required for these four offshore wind farms under this generator-outage scenario.

Table 30. SSAT results of 4 OSWs in ISO-NE for contingency GEN NE1.

OSW	Frequency (Hz)	Damping Ratio (%)	Risk Flag
Park City Wind	1.6	4.7	OK
Vineyard Wind	1.7	8.9	OK
Bay State Offshore Wind	2.2	4.1	OK
Revolution Wind	1.8	3.9	OK

5.3. PJM Small-Signal Stability Analysis

The team implemented a total of 6 contingencies for the PJM large-scale model using SSAT eigenvalue analysis, with 3 cases for the Spring Light-Load (SLL) case and 3 cases for the summer peak load case. All contingency scenarios are eventually tested with 5 OSWs online. All cases were observed with positive damping ratios ($\zeta > 0\%$); and no immediate mitigations are required beyond baseline monitoring. The GEN PJM contingency results are presented below.

Contingency: GEN PJM

For the generator-outage contingency case with seven offshore wind farms integrated into the PJM grid, the SSAT eigenvalue analysis demonstrates that all modes remain stable and adequately damped, with no negative damping observed. The oscillatory spectrum is dominated by inertial modes in the 0.9–1.6 Hz range, all exceeding the critical 3% damping guideline commonly adopted in small-signal stability assessments. The most robust performance is observed at Momentum Wind, which exhibits an oscillation at 0.9 Hz with a damping ratio of 9.4%, indicating strong inherent damping of inter-area-like dynamics. Similarly, Atlantic Shores South Wind 2 and Atlantic Shores South Wind 1 show well-damped modes at 1.2 Hz ($\zeta = 8.9\%$) and 1.3 Hz ($\zeta = 8.7\%$), respectively, reinforcing the stability of their control systems under this contingency. Kitty Hawk South Wind presents a mode at 1.4 Hz with a damping ratio of 6.5%, and Coastal Virginia Offshore Wind demonstrates a mode at 1.6 Hz with $\zeta = 5.9\%$. Both values remain

Table 31. Key SSAT results of 7 OSWs in PJM under generator tripping

OSW	Frequency (Hz)	Damping Ratio (%)	Risk Flag
Atlantic Shores South Wind 1	1.3	8.7	OK
Momentum Wind	0.9	9.4	OK
Kitty Hawk Wind	1.4	6.5	OK
Coastal Virginia Offshore Wind	1.6	5.9	OK
Atlantic Shores South Wind 2	1.2	8.9	OK

comfortably above the 3% threshold and provide sufficient stability margins consistent with accepted planning standards. In summary, these results confirm that the integration of the six offshore wind farms under a generator-outage contingency does not pose any oscillatory stability risk. Similar results were found for the transmission line and bus contingencies.

Evaluate potential risk mitigation techniques

This section evaluates three mitigation pathways: (i) temporarily isolating or bypassing series-compensated devices under stressed operating conditions to suppress sub-synchronous interactions and limit fault severity; (ii) deploying damping equipment synchronous condensers (SCs) and static synchronous compensators (STATCOMs) to raise short-circuit strength, improve voltage recovery, and increase modal damping; and (iii) retuning wind-turbine and plant-level controllers (phase-locked loop (PLL), active/reactive loops) to enhance ride-through and avoid adverse control interactions. Effectiveness is quantified by changes in critical clearing time, modal damping ratios, sub-synchronous interaction indices, and post-fault voltage recovery in EMT and small-signal studies.

5.4. Deploying Damping Equipment

This section evaluates damping-oriented devices SCs and STATCOMs deployed at candidate buses, including points of interconnection (POIs), converter terminals, and generator high-side buses. SCs add rotational inertia and short-circuit strength, which improves voltage support and rotor-angle stability. STATCOMs deliver fast dynamic MVAr and, when equipped with a power-oscillation-damping controller, increase inter- and intra-area mode damping and accelerate post-fault voltage recovery.

Synchronous condensers (SCs)

To strengthen the system, install one or more synchronous condensers (SCs) at major 345-kV substations near OSW points of interconnection in Zones J and K. The objectives are to increase short-circuit strength at weak buses, provide dynamic reactive support for faster voltage recovery, and add rotational inertia to slow frequency and angle excursions.

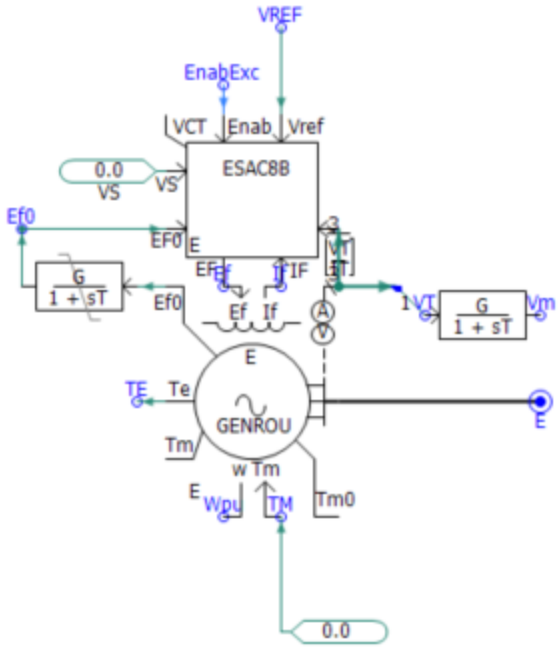

Figure 51. Model synchronous condenser in PSCAD

Each SC is modeled as a synchronous machine without a prime mover. The electrical model includes subtransient dynamics (Xd″, Xq″) and damper windings to capture the high initial fault current. The voltage control model uses an ESAC8B automatic voltage regulator (AVR) implemented as a Basler DECS-type digital regulator that drives a brushless rotating exciter rather than a static exciter. The AVR provides high-gain voltage control with lead–lag compensation and includes VRMAX and VRMIN ceiling limits, and field-current limiting. The regulator can measure local bus voltage or a remote POI setpoint with line-drop compensation to hold the desired POI voltage with a small Q–V droop. A power-system stabilizer input can be enabled and tuned to add small-signal damping. Figure 51 shows the PSCAD synchronous-condenser model used in this study, and Figure 52 shows the ESAC8B exciter block diagram.

Synchronous condensers stabilize the system over three-time scales. In the first few cycles of a fault, they supply large sub-transient current that props up the POI voltage, reducing the dip and helping converter PLLs stay locked. In the next few hundred milliseconds, the AVR injects reactive power, which speeds voltage recovery and increases synchronizing torque. Over the following seconds, the stored kinetic energy adds inertia, slowing frequency and rotor-angle drift, extending the critical clearing time and damping post-fault oscillations.

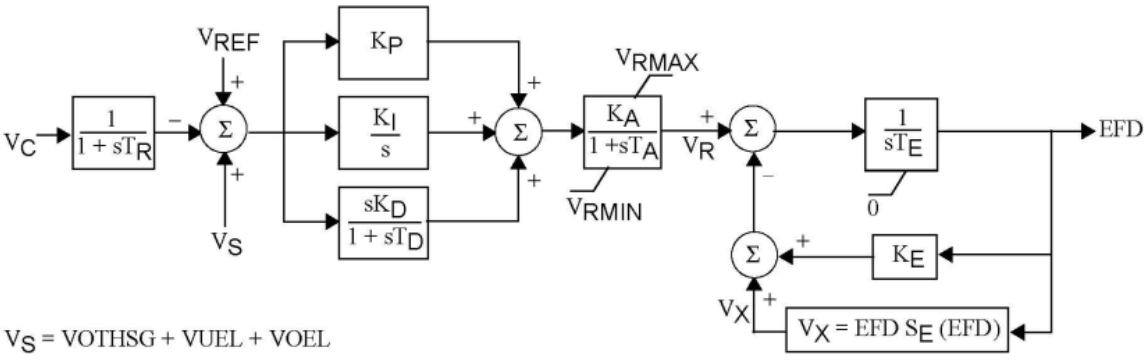

Figure 52. ESAC8B - Basler DECS-type exciter/AVR [9]

Static Synchronous Compensators (STATCOMs)

A STATCOM uses a voltage-sourced converter built from high-power switches such as IGBTs. It can regulate voltage more quickly than a synchronous condenser, but does not provide inertia. By adjusting its internal AC voltage relative to the grid voltage at the connection bus, it can either supply or absorb reactive power: raising the internal voltage above the grid voltage generally produces reactive volt-amps (VARs); while lowering it consumes VARs. The DC-link capacitor sets the voltage headroom and influences the device's reactive capability and speed. Figure 53 shows the 6 Pulse STATCOM used in this study.

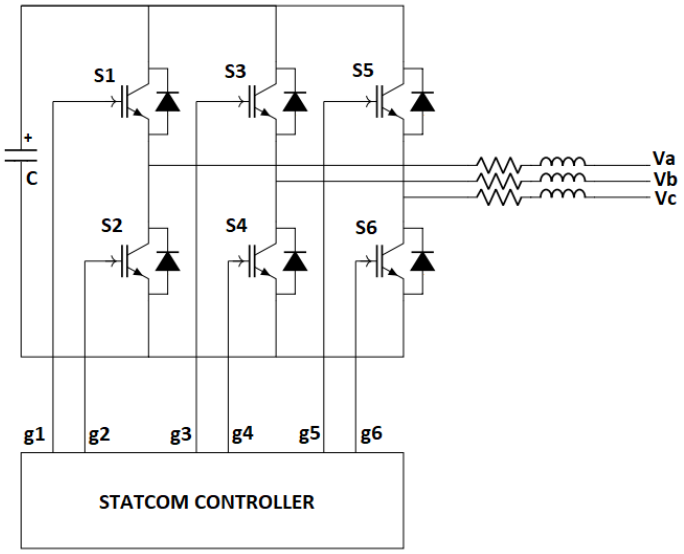

Figure 53. 6 Pulse STATCOM

A six-pulse PWM STATCOM is modeled with a bus-voltage regulator based on a PI controller. The voltage-control loop compares the measured bus voltage with its reference and generates a field voltage for the synchronous condenser.

Damping-Equipment Mitigation: Regional Case Studies

This section evaluates damping-based mitigations using synchronous condensers and STATCOMs to strengthen weak points of interconnection and improve dynamic performance across NYISO and ISO-NE.

NYISO

Scenario 1: 2028 Spring Light–Load (Balanced Fault at Gowanus)

A reduced NYISO spring light-load EMT model was used, retaining Zone J (NYC) buses ≥ 345 kV, Zone K (Long Island) buses ≥ 138 kV, and all internal generators. A three-phase fault was applied at the 345 kV Gowanus substation (POI) with no damping equipment.

Pre-mitigation (no SC/STATCOM): With zero to four offshore-wind projects online, the critical clearing time (CCT) remained 15 cycles, and a gas unit in the vicinity of the fault was the first to lose synchronism when that limit was exceeded. Adding a fifth project (about 5.5 GW total) reduced the CCT to 13 cycles and shifted the instability to the HVDC terminal at East Garden City, indicating a comparatively weak bus.

Mitigation with a synchronous condenser: In the five-OSW case, installing a 250-MVAr synchronous condenser at the East Garden City POI in the 2028 spring light-load scenario restored the CCT to 15 cycles and stabilized the HVDC terminal. Figure 54 compares the EGC onshore HVDC terminal voltage with and without the condenser. When the fault duration was extended to 16 cycles, the first unit to lose synchronism is a synchronous generator near the fault, consistent with the zero-to-four-OSW cases (Figure 55).

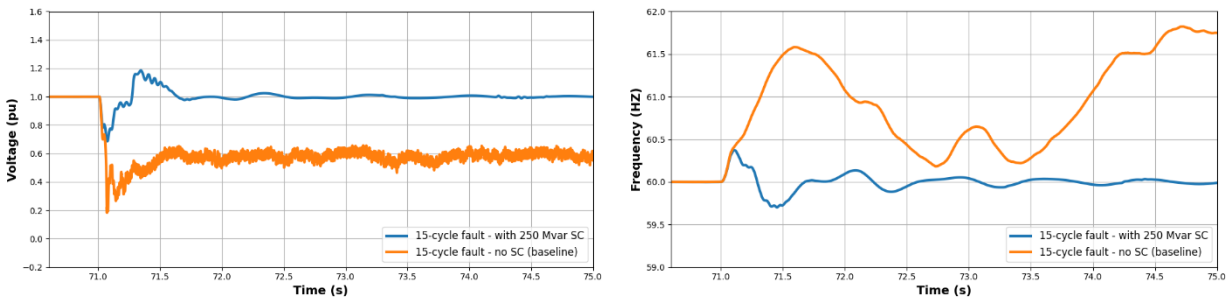

Figure 54. EGC onshore HVDC terminal voltage and frequency dynamics for 15-cycle fault clearing (five-OSW case, with and without 250 MVAr SC)

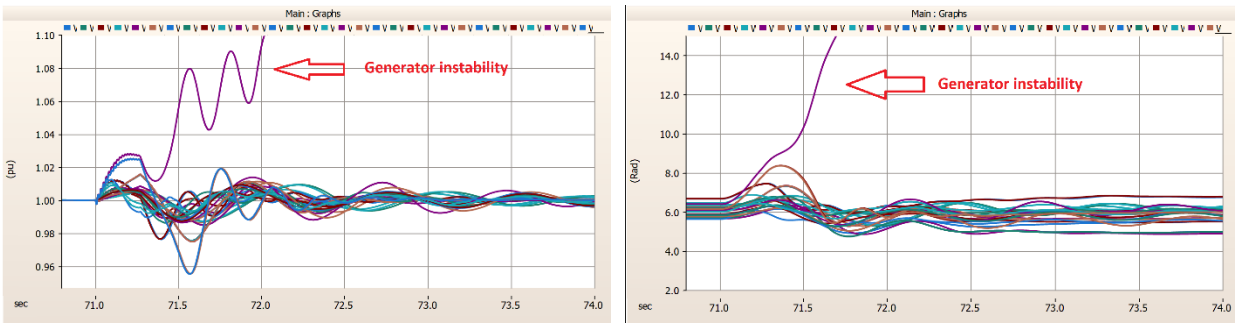

(a) Speed profile (per unit), 16-cycle fault (b) Rotor-angle profile (rad), 16-cycle fault

Figure 55. Generator speed and rotor-angle profiles for the five-OSW case at Gowanus under unstable (16-cycle clearing) conditions with a 250-MVAr synchronous condenser

Scenario 2: 2028 Spring Light–Load (Balanced Fault at Ruland Road)

Scenario 2 employs the same spring light-load EMT model used in Scenario 1, but the disturbance is moved to the 138 kV Ruland Road point of interconnection on Long Island; Long Island hosts three of the offshore-wind interconnections.

Pre-mitigation (no SC/STATCOM): In the five-OSW case, a three-phase fault produced a CCT of 5 cycles and the East Garden City (EGC) HVDC terminal became unstable for a 6-cycle fault (Figure 56). For a single-line-to-ground (SLG) fault, the CCT was 12 cycles.

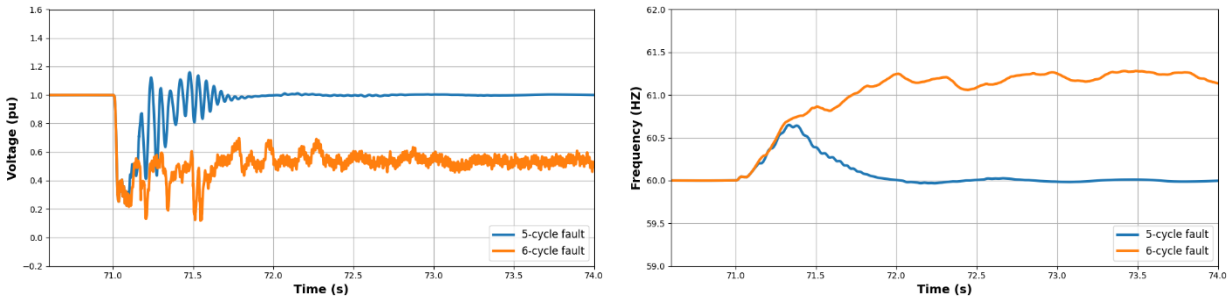

Figure 56. EGC onshore HVDC terminal voltage and frequency dynamics for 5- and 6- cycle fault clearing (five-OSW case, without adding damping equipment)

Mitigation with a synchronous condenser: Installing a 250-MVAr synchronous condenser at the EGC POI increased the three-phase CCT to 17 cycles and stabilized the HVDC terminal (Figure 57). Instability reappeared when clearing was delayed to 18 cycles. For the single-line-to-ground (SLG) case, stability held at 30 cycles, implying a lower bound on CCT above 30 cycles.

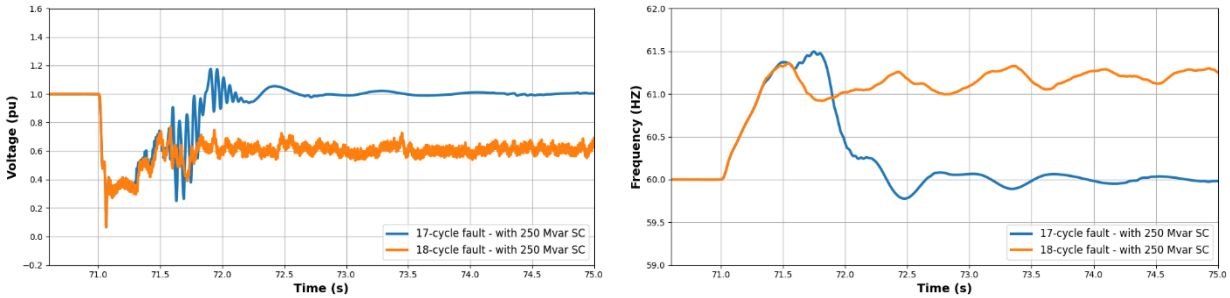

Figure 57. EGC onshore HVDC terminal voltage and frequency dynamics for 17- and 18- cycle fault clearing (five-OSW case, with 250 MVAr SC)

Mitigation with a STATCOM: Adding a ±250-MVAr STATCOM at the same POI raised the three-phase CCT to 18 cycles and stabilized the HVDC terminal (Figure 58). When the clearing time was extended to 19 cycles, the first unit to lose synchronism shifted back to the generator near the fault, consistent with the zero-to-four-OSW cases (Figure 59). For SLG faults, stability also held through 30 cycles in the STATCOM case, indicating CCT ≥ 30 cycles (Figure 60).

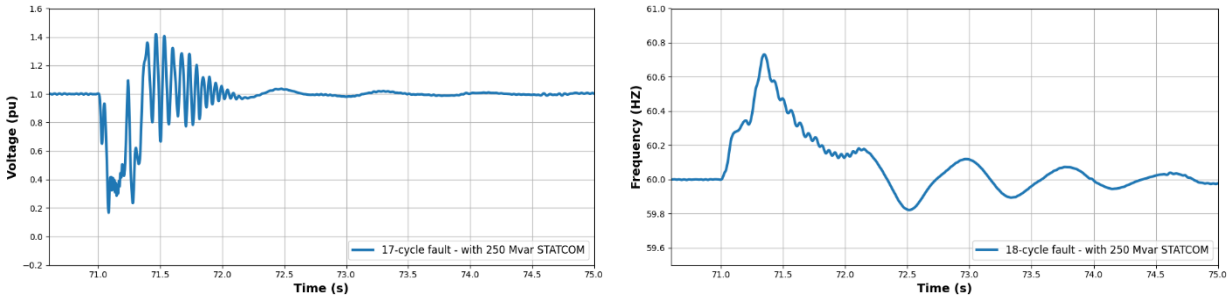

Figure 58. EGC onshore HVDC terminal voltage and frequency dynamics for 18- cycle fault clearing (five-OSW case, with 250 MVAr STATCOM)

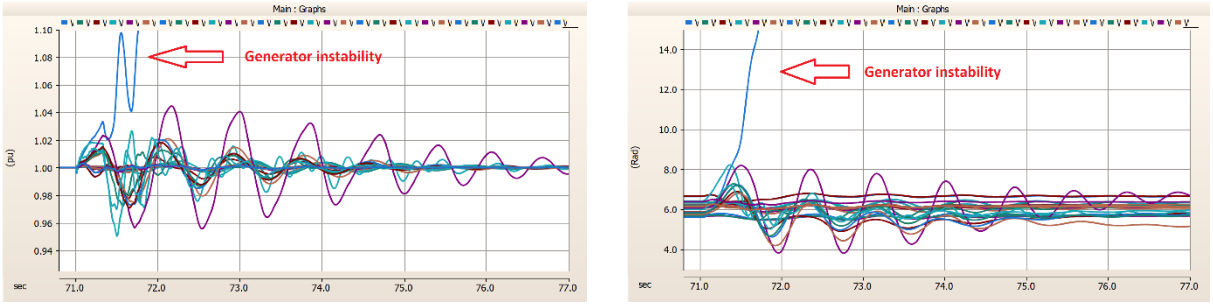

(a) Speed profile (per unit), 19-cycle fault (b) Rotor-angle profile (rad), 19-cycle fault

Figure 59. Generator speed and rotor-angle profiles for the five-OSW case at Ruland under unstable (19-cycle clearing) conditions (with 250 MVAr STATCOM)

Figure 60 shows representative SLG fault waveforms at Ruland Road bus voltages and currents in a nearby transmission line with five OSW projects online. With a 30-cycle clearing time, the bus phase voltages recover quickly: phase A rises from near zero to ~0.99 pu, while phases B and C remain within 0.98–1.02 pu. The line currents return to pre-fault values within about four seconds, demonstrating stable ride-through.

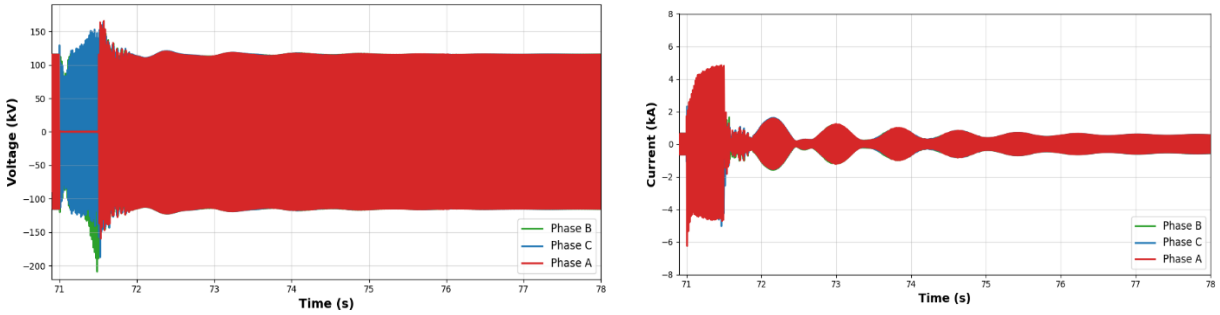

(a) Ruland POI phase-voltage (kV) (b) Transmission line-current (kA)

Figure 60. Ruland Rd Single-Phase Fault (A-G) with 5 OSWs for 30-Cycle Fault Clearing (stable)

Scenario 3: 2028 Summer Peak–Load (Balanced Fault at Gowanus)

Using the reduced NYISO EMT model (Zone J ≥ 345 kV, Zone K ≥ 138 kV, all internal generators), we tested three-phase faults at the Gowanus and Ruland Road POIs under summer-peak conditions. Offshore wind had only a modest effect on transient stability: the base case produced a CCT of 9 cycles at Gowanus (Figure 61), and once any offshore capacity was added the CCT dropped to 8 cycles and stayed there up to five projects. In every run, the synchronous generators near the fault lost synchronism first, indicating that local inertia and electrical proximity set the stability limit rather than offshore injection.

Mitigation tests controller retuning: The team retuned exciters and governors (higher PI gains and widened regulator/output limits). This raised the CCT from 8 to 9 cycles, but the improvement was marginal, motivating a device-based mitigation.

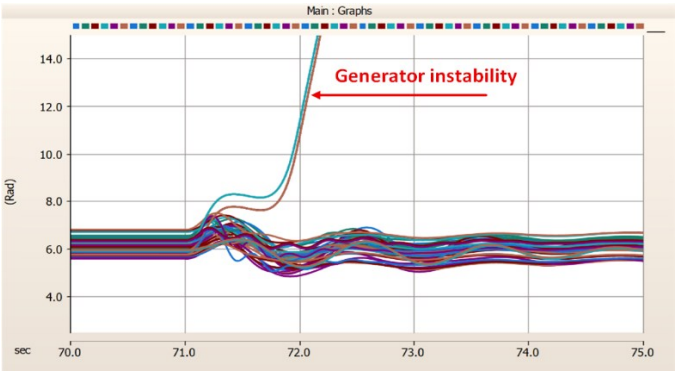

Figure 61. Rotor-angle profiles for the five-OSW configuration at Gowanus during summer-peak load with 9-cycle clearing

Mitigation synchronous condenser at the generator high-side bus: Installing one 250-MVAr synchronous condenser at the affected generator's high-side bus increased the three-phase POI-fault CCT from 8 to 11 cycles. At 12 cycles, the nearby gas units exhibited sustained rotor-angle divergence and tripped (Figure 62).

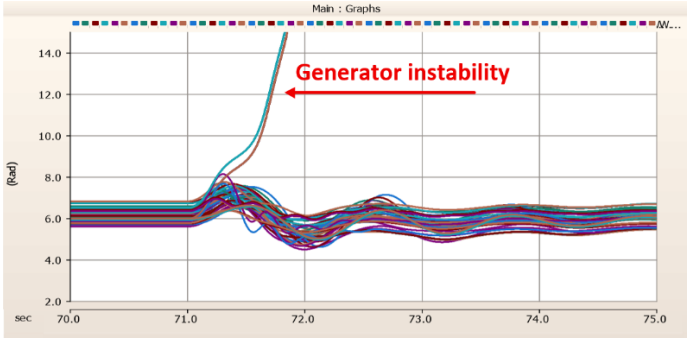

Figure 62. Rotor-angle profiles for the five-OSW configuration at Gowanus during summer-peak load with 12-cycle clearing (with one 250 MVAr SC)

With two 250-MVAr units at the same bus (500 MVAr total), the CCT extended to 13 cycles, with instability reappearing at 14 cycles (Figure 63). These gains are consistent with added fault current at the generator bus (effective SCR uplift and higher voltage nadir), AVR-driven reactive support that speeds post-fault voltage recovery, and additional inertia that slows rotor-angle acceleration.

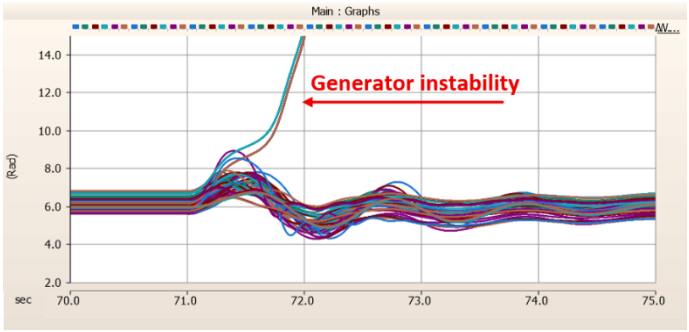

Figure 63. Rotor-angle profiles for the five-OSW configuration at Gowanus during summer-peak load with 14-cycle clearing (with two 250 MVAr SC)

The synchronous condenser contributes fault current that boosts the effective short-circuit ratio and lifts the voltage nadir. The AVR can drive the field to deliver short-term reactive power, speeding post-fault voltage recovery. Added inertia slows rotor-angle acceleration and helps converter PLLs maintain lock. When the binding limit is synchronous-angle stability close to the fault, placing the device at the generator high-side bus is most effective. Sizing shows diminishing returns. The first 250 MVAr delivers the largest step in margin, while increasing to 500 MVAr adds a smaller but still meaningful improvement and raises the short-circuit duty that protection must accommodate.

ISO-NE

Scenario 1: 2028 Summer Peak Load (Balanced Fault at West Barnstable)

Using the reduced ISO-NE EMT model for summer-peak conditions (MA/RI ≥ 220 kV retained, all internal generators online, ~11.5 GW synchronous), the baseline (no OSW) rides through a three-phase fault at the West Barnstable POI for 13 cycles. With four OSW projects (~3.5 GW) online, the CCT is 12 cycles, as shown in Figure 64. In both cases, a synchronous generator near the fault is the first to lose synchronism, indicating that local inertia and strong coupling to the fault set the stability limit.

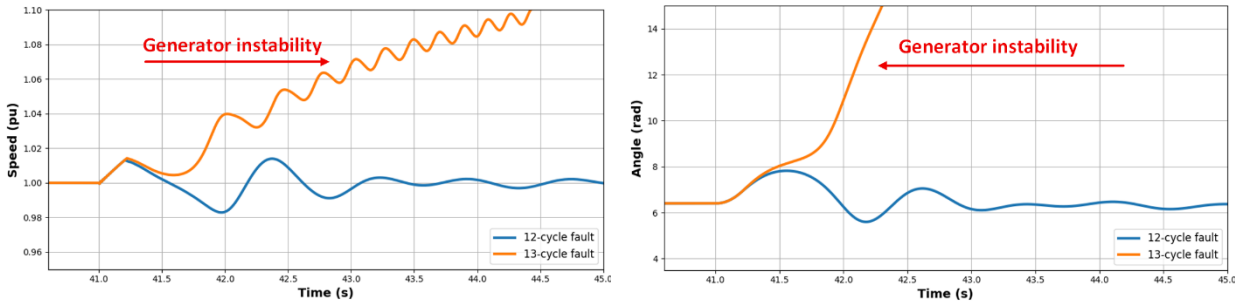

(a) Speed profile (per unit) (b) Rotor-angle profile (rad)

Figure 64. West Barnstable fault: critical generator speed and rotor angle for 12-cycle (stable) vs 13-cycle (unstable) clearing (4-OSW case, no mitigation)

Mitigation synchronous condenser at the generator high-side bus: Installing a 250-MVAr synchronous condenser at the affected generator's high-side bus raises the three-phase POI-fault CCT from 12 to 13 cycles, matching the no-OSW baseline. With a 14-cycle clearing time, the nearby generators exhibit sustained rotor-angle divergence and go out of step, as illustrated in Figure 65. The improvement is consistent with added fault current (effective SCR uplift and a higher voltage nadir), AVR field forcing that supplies short-term reactive power, and added inertia that slows rotor-angle acceleration.

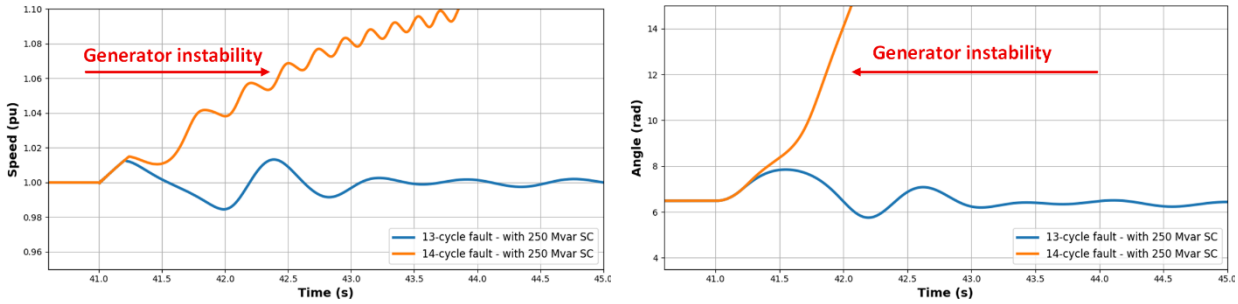

(a) Speed profile (per unit) (b) Rotor-angle profile (rad)

Figure 65. West Barnstable fault: critical generator speed and rotor angle for 13-cycle (stable) vs 14-cycle (unstable) clearing (4-OSW case, with 250 MVAr SC)

5.5. Tuning Controllers

Tuning PLL and Adding Anti-Windup Mechanism

One of the most effective approaches to mitigate control-driven interactions in offshore wind plants is the targeted adjustment of wind turbine and plant-level controllers, particularly the Phase-Locked Loop (PLL). The PLL model used in this study is shown in Figure 66. The PLL serves as the primary synchronization

mechanism between inverter-based resources and the host grid, estimating the phase angle and frequency of the voltage at the Point of Interconnection (POI). Under weak-grid conditions (e.g., when the short-circuit ratio is low or following a major contingency), the PLL becomes highly sensitive to voltage sags, harmonics, and oscillatory disturbances, which can introduce poorly damped or unstable modes in the sub-synchronous range.

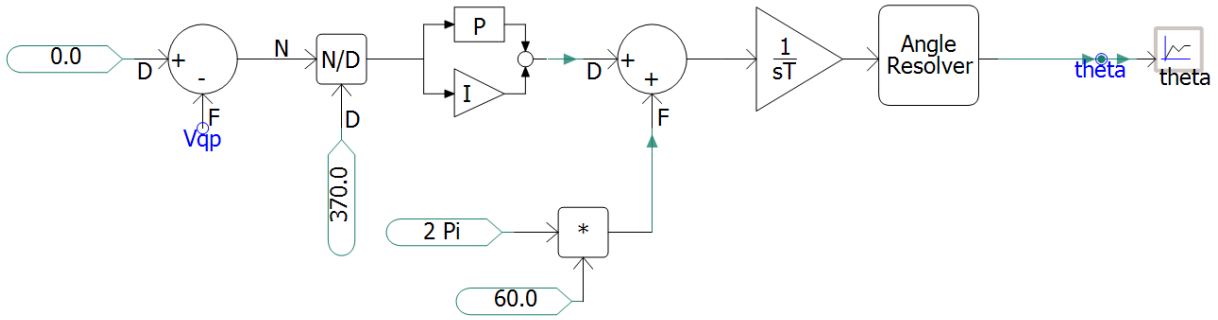

Figure 66. PLL control diagram

PLL Tuning involves reducing the PLL bandwidth and carefully coordinating the proportional–integral (PI) gains within the PLL controller. By lowering the PLL bandwidth, the synchronization dynamics are slowed down, reducing the likelihood of chasing fast transients or amplifying noise from the grid impedance. At the same time, tuning the PLL PI controller must balance stability and responsiveness: overly aggressive tuning may destabilize the system, while overly conservative tuning may impair frequency tracking.

In addition to bandwidth tuning, the introduction of anti-windup mechanisms in the PLL controller further enhances robustness. During large disturbances, such as voltage dips or prolonged unbalanced faults, the integrator in the PLL PI controller may saturate, leading to delayed recovery and sustained oscillations once normal conditions return. Anti-windup logic prevents this by limiting the accumulation of the integrator state when the PLL output reaches predefined saturation limits. This ensures that, when the disturbance clears, the PLL resumes operation smoothly without overshoot or prolonged oscillatory recovery. By combining bandwidth reduction with anti-windup protections, the PLL is less prone to destabilize under weak-grid or faulted conditions, thereby significantly improving overall plant stability.

NYISO Contingency: Generator Outage (GEEN NYC) + Three-Phase Fault at Gowanus POI

In this case, the NYISO grid model is initialized through a flat-start power flow, and each OSW is sequentially integrated into the grid in order to ensure all operating conditions are in steady-state equilibrium prior to the disturbance. At a predefined simulation time instant t = 61 (s), the tripping of GEN NYC is initiated for the configuration by sending an opening signal to the corresponding circuit breaker,

and then a three-phase fault is applied at Gowanus POI bus in a time span of 12 cycles at t = 68 (s) after the system returned to normal condition. The generator-outage contingency in Section 5.1 exposes two unstable and one marginal modes among the five OSWs, with two additional plants remaining acceptable. Most critically, the EMT simulation in PSCAD shows that Sunrise Wind and Vineyard Mid Atlantic Wind both present unstable modes (negative damping ratios) for terminal voltage in Figure 67. These results match correctly with SSAT eigenvalue analysis results.

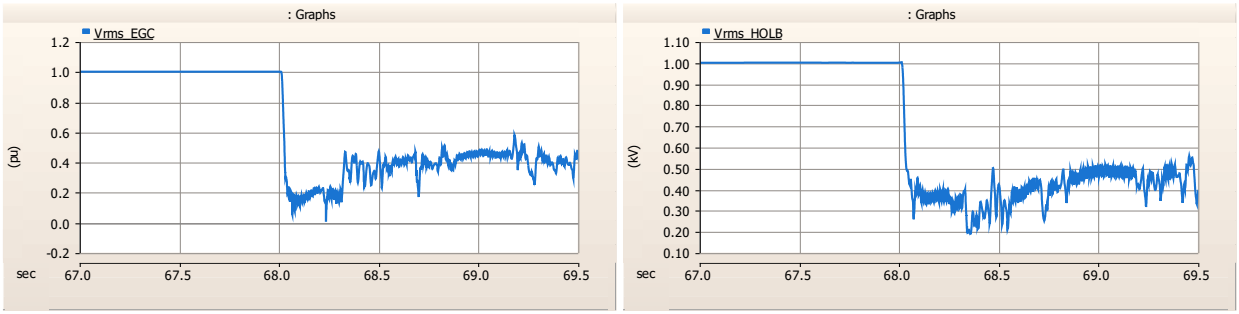

Figure 67. RMS POI terminal voltage of Vineyard Mid Atlantic Wind (Left) and Sunrise Wind (Right)

The PLL controller tuning strategy is shown in Figure 68. After retuning and adding the anti-windup mechanisms, the terminal voltage of both OSWs can recover to the normal steady-state conditions, as shown in Figure 69.

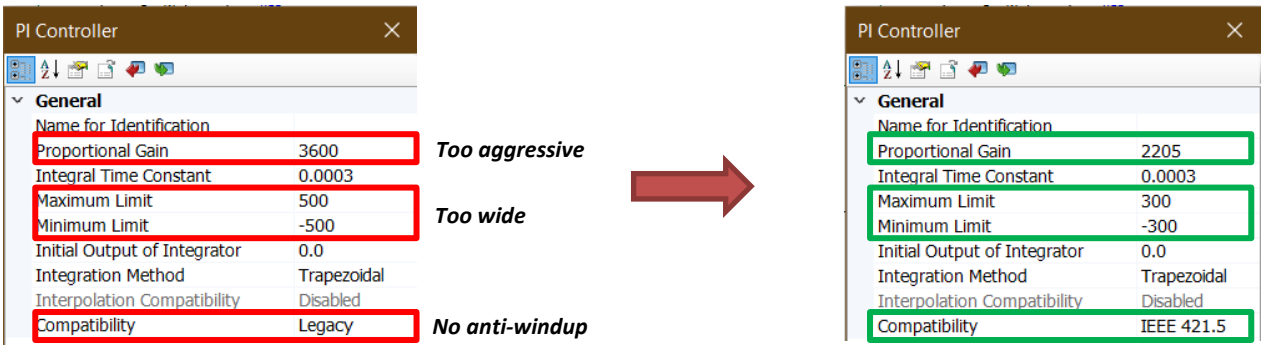

Figure 68. PLL Controller Tuning

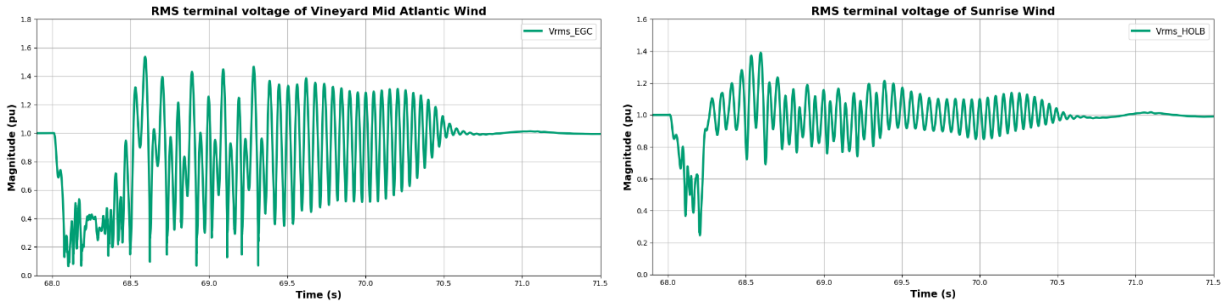

Figure 69. RMS voltage of Vineyard Mid Atlantic Wind (Left) and Sunrise Wind (Right) after tuning

Tuning HVDC Grid-Side Inverter Controller

NYISO Contingency: Line Outage (TLINE NY) + Three-Phase Fault at EGC POI

This case presents a two-element contingency event applied to the NYISO power system model with high offshore wind penetration. The EMT model of the NYISO grid was initialized under flat-start steady-state conditions, ensuring accurate power flow convergence across all network nodes. All significant system components, including conventional generators, loads, and 5 OSWs were modeled as active and synchronized with the onshore grid. The contingency sequence involves the tripping of the TLINE NY. The transmission line tripping causes the loss of active and reactive power flow on this transmission line. This event leads to a sudden redistribution of power flow and alters the short circuit ratio at EGC 345kV POI. Once the system recovered from the initial line trip, a three-phase fault was applied at EGC, at 60.1 seconds. The fault persisted for 6 cycles before being cleared.

Under the line-outage contingency in Section A, only one HVDC-connected OSW exhibited electrical unstable modes in the mid sub-synchronous band. This result is confirmed with EMT cross-validation, showing that Vineyard Mid Atlantic Wind failed to recover to steady-state condition under three-phase fault study, as shown in Figure 70. Post-trip, the POI strength falls and the network's frequency-dependent impedance shifts, increasing the sensitivity of the grid-side converter loops. In the baseline implementation in Figure 71, the d-axis current is regulated by a DC-link voltage controller and the q-axis current by an AC-terminal voltage controller. Notably, the DC-voltage loop becomes overly stiff against the weakened grid, driving a negative-damped mode.

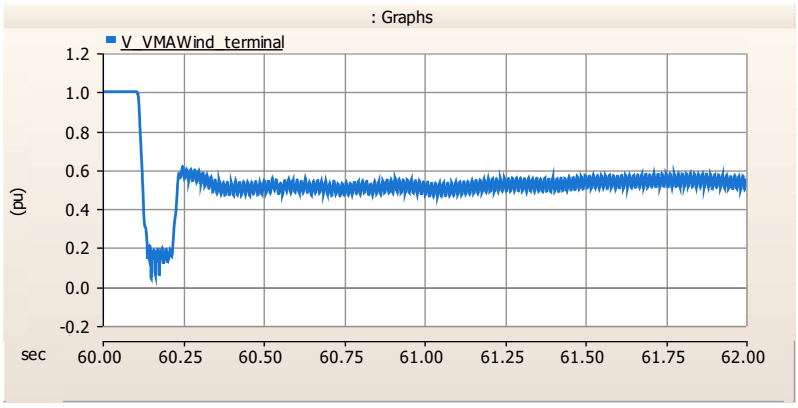

Figure 70. RMS terminal voltage of Vineyard Mid Atlantic Wind

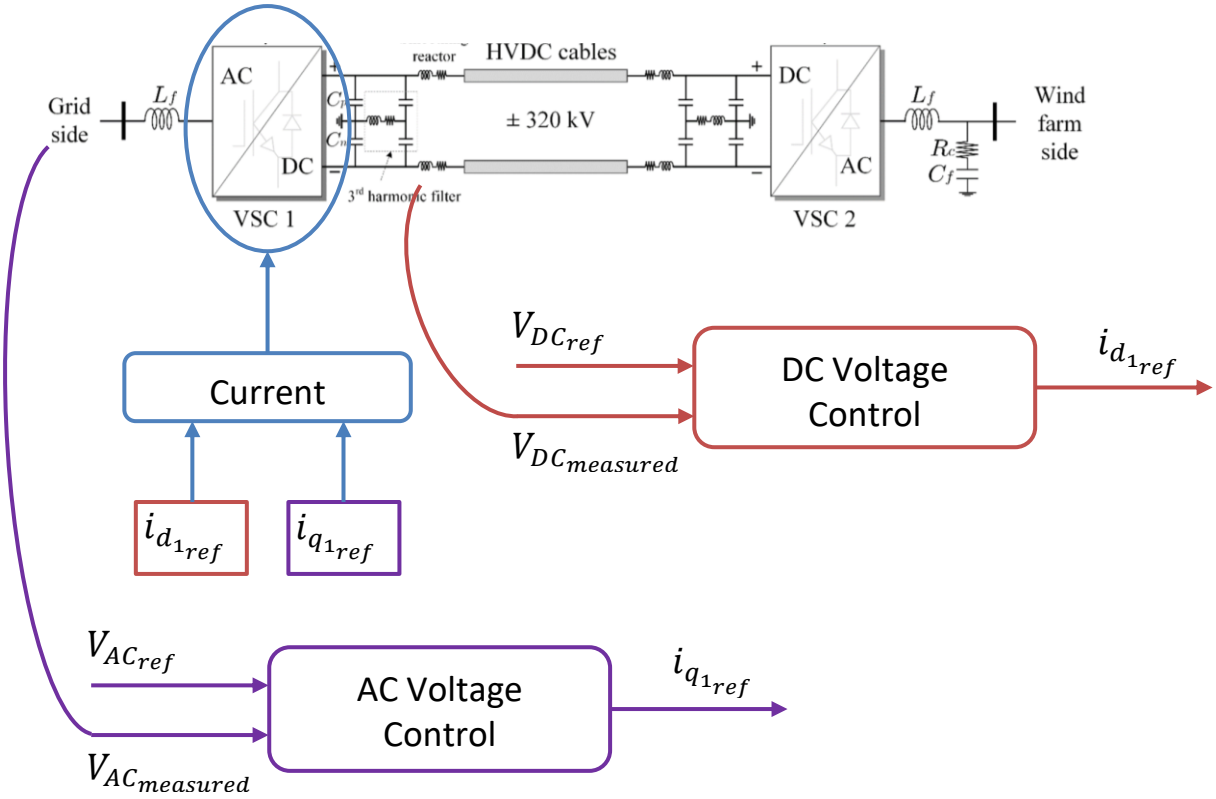

Figure 71. HVDC grid-side inverter control topology

In order to mitigate this unstable case, a blended active-power control channel in parallel with the DC-voltage regulator on the d-axis is proposed in Figure 72. Intuitively, instead of forcing the DC-link capacitor to absorb fast power mismatches (which can create effective negative damping when the grid is weak, as illustrated in Figure 73), the converter is encouraged to modulate active power to rebalance energy. This reduces the stiffness of the DC-voltage regulation, adds positive damping to the power/voltage dynamics, and breaks the adverse loop coupling that produced the unstable eigenvalue.

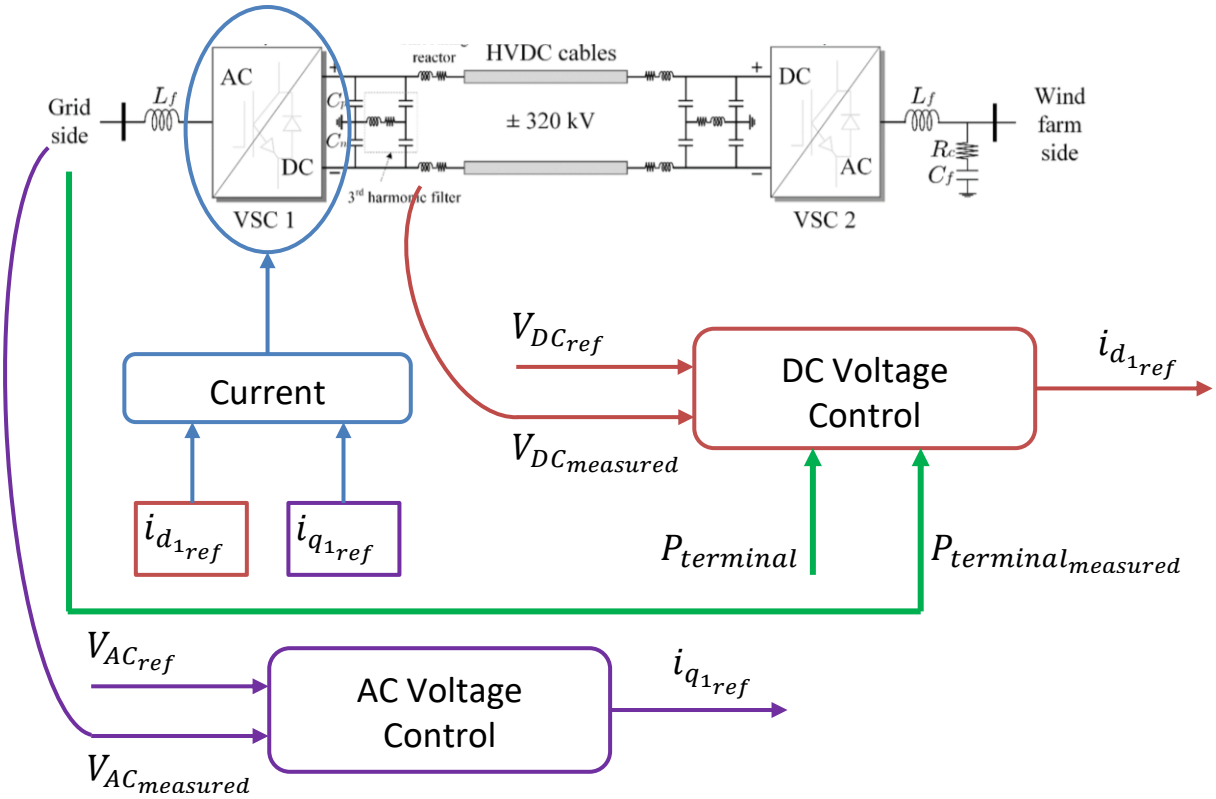

Figure 72. HVDC grid-side inverter controller tuning

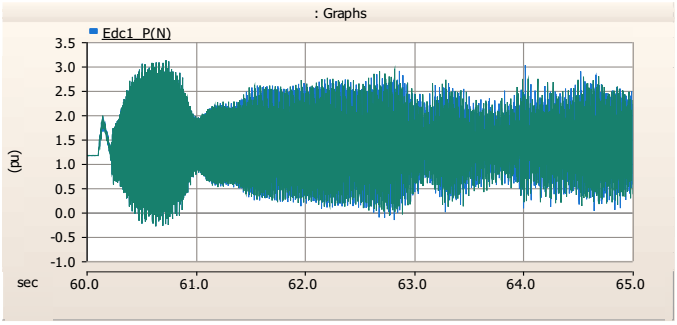

Figure 73. DC voltage before tuning the controller

As a result, Vineyard Mid Atlantic Wind can recover to the flat start conditions under the three-phase fault study after tuning the HVDC grid-side inverter controller, ensuring the stability for the large-scale NYISO model. Figure 74 shows this stable case.

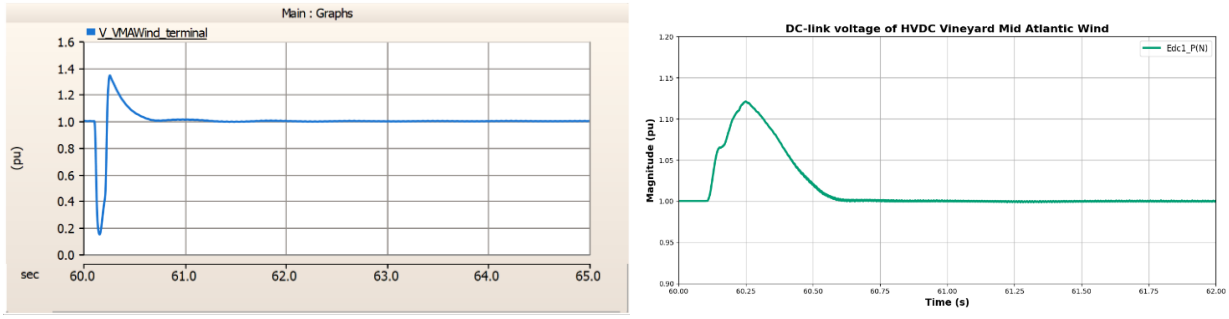

Figure 74. RMS terminal voltage and DC-link voltage of Vineyard Mid Atlantic Wind after tuning

5.6. Impact of Series Compensation Project

This subsection evaluates the impact of a New York Clearing Area series compensated transmission line with all five NY OSW projects (~5.5 GW) in service under two operating conditions 2028 Summer Peak and 2028 Spring Light Load using reduced NYISO EMT models (Zone J ≥ 345 kV, Zone K ≥ 138 kV, all internal generators retained).

Summer Peak Load (2028): A 12-cycle three-phase fault is applied at the Beacon Wind POI (NYC). Figure 75 compares the onshore HVDC terminal voltages at Beacon Wind and Sunrise Wind with MSSCP in and out of service. The voltage recovery is essentially unchanged by MSSCP.

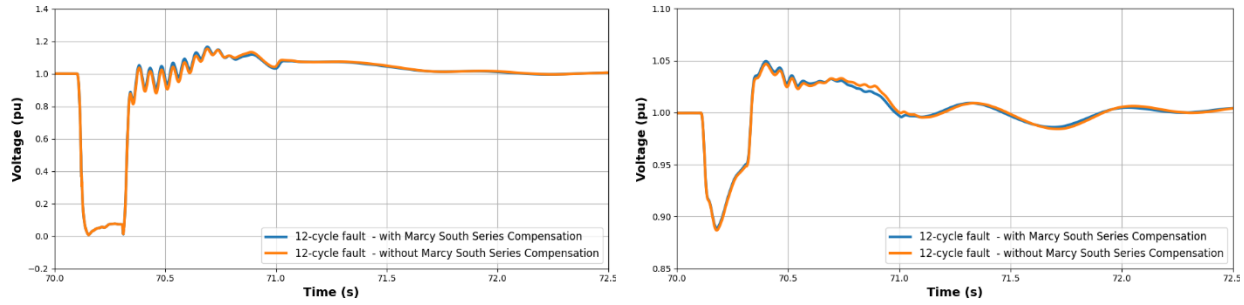

(a) Beacon Wind onshore HVDC terminal voltage (b) Sunrise Wind onshore HVDC terminal voltage

Figure 75. Onshore HVDC terminal voltages at (a) Beacon Wind and (b) Sunrise Wind for a 12-cycle clearing time (five-OSW case), with and without the series compensation in service.

Spring Light Load (2028): A 17-cycle three-phase fault is applied at the Juno Express Wind POI (Long Island). Figure 76 compares the onshore HVDC terminal voltages at Beacon Wind and Juno Express Wind with and without MSSCP. Again, little to no difference is observed in voltage recovery.

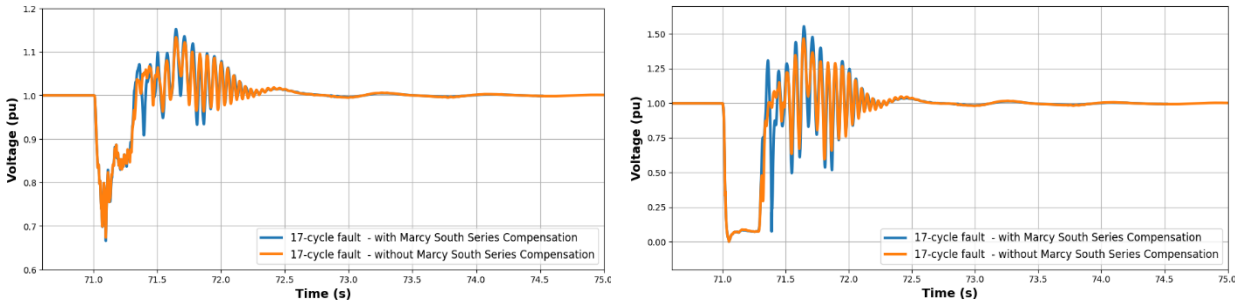

(a) Beacon Wind onshore HVDC terminal voltage (b) Juno Express onshore HVDC terminal voltage

Figure 76. Onshore HVDC terminal voltages at (a) Beacon Wind and (b) Juno Express Wind for a 17-cycle clearing time (five-OSW case), with and without the series compensation in service.

Interpretation: For the tested NYC/Long Island faults, local network conditions dominate the terminal-voltage response; the remote series-compensated corridor yields minimal influence on immediate post-fault recovery.

5.7. Evaluate the effectiveness of wind speed forecasting in the mitigation

To understand how wind speed variations influence the interaction between OSWs and the onshore grid, a simplified study was conducted using the NYISO grid model with a single OSW – Juno Express (Ruland RD POI). In this case, the wind speed at the offshore farm was reduced from 10.0 m/s to 7.5 m/s, resulting in a corresponding decrease in the farm's active power output from 100% of rated capacity (1200 MW) to 50% of rated capacity (600 MW). All other system conditions, including onshore generation dispatch, transmission topology, and load levels were held constant in order to isolate the effect of reduced offshore generation. A three-phase fault study was conducted at the Holbrook substation at t = 16 (s), and the fault persisted for long duration of 18 cycles (0.3 (s)) before being cleared.

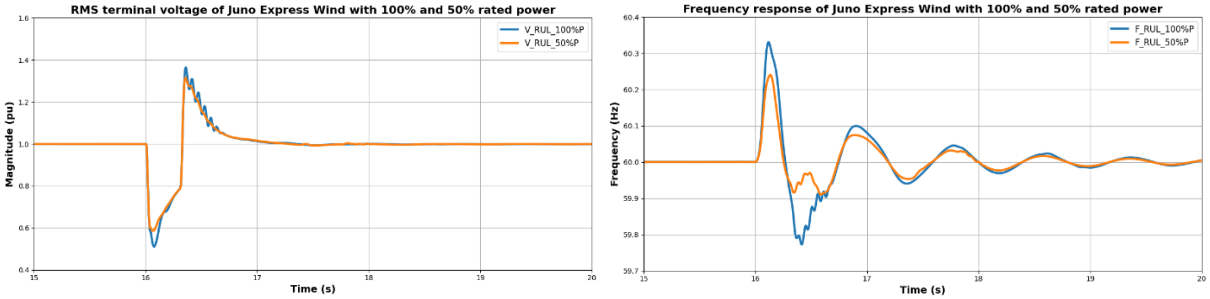

Figure 77. RMS terminal voltage and frequency of Juno Express Wind with 100% and 50% rated power

At both 100% and 50% pre-fault active power levels, the terminal OSW's voltage will collapse sharply during the fault as shown in Figure 77. The depth of the voltage dip is not significantly different between

the two power levels since it is dictated by fault impedance and system strength. However, the voltage recovery profile of two power levels differs slightly. With full-rated power, the offshore wind farm injects a larger pre-fault current. After fault clearing, the controller must ramp back to rated conditions, and the POI voltage may overshoot more before stabilizing. In addition, the mismatch between generation and grid conditions is larger in this case, so the frequency excursions at the POI would be slightly greater than half-rated power case. On the other hand, the injection current is lower with 50% output case and the active power control loop has less stress recovering to its setpoint, so post-fault voltage, frequency overshoot and oscillations are typically smaller, and the recovery appears smoother.

Notably, no unstable or poorly damped oscillatory modes were observed in either case. The similarity of responses at full and half-rated power implies that the contingency risks identified in earlier studies are driven more by network topology, system strength, and controller interactions than by instantaneous wind power level.

5.8. Summary

In Task 2.2, the team completed a root-cause analysis of control-instability risks associated with large-scale OSW integration and assessed targeted mitigations across representative NYISO, ISO-NE, and PJM cases. An EMT- and small-signal–based workflow (with sensitivity studies and controller tuning) was used to quantify impacts and verify fixes.

Key sources of risk identified include:

- Weak-grid points of interconnection with low effective SCR that stress converter PLLs.
- Interactions among wind-turbine/plant controllers, HVDC terminals, and the AC network under faults.
- Series-compensated corridors that can couple with converter controls and excite sub-/inter-harmonic oscillations (little impact was seen in the NYISO case study).
- Wind-speed examine: examine the impact of leveraging wind-speed on system stability

Mitigation techniques evaluated include:

- Additional damping equipment: synchronous condensers and STATCOMs to raise effective SCR, supply fast dynamic MVAr, improve voltage recovery, and increase modal damping.
- Controller retuning/enhancing: wind-turbine and plant controllers (PLL bandwidth, Q–V droop, reactive/active current limits) to enhance ride-through and avoid adverse control interactions.

Representative findings:

- Damping equipment materially improves stability in weak areas raising the voltage nadir, increasing modal damping, and extending CCT. Effective placement depends on the limiting mechanism (e.g., generator high-side bus vs. POI).
- Controller retuning and enhancement provide incremental gains and are most effective when coordinated with device-based support.

6. Task 3. Dissemination and Technology Transfer

6.1. Dissemination

The Industry Advisory Board (IAB) for this project includes:

- Saad Syed, Ocean Winds
- Robert Eisenhuth, PSEG
- Matthew Koenig, Consolidated Edison
- Rachel MacDonald, California Energy Commission
- Jian Fu, DOE
- Scott Egbert, NYSERDA

Our research team and project manager have met with our IAB quarterly throughout this project. The IAB has been actively engaged in this project. In particular, IAB members have provided significant useful input on the characteristics of the NYISO, ISO-NE and PJM grid, which provided focus for the research team's efforts in Task 2 of the project. These inputs provided invaluable insight around system characteristics that ultimately were used to shape and improve the grid modeling efforts for this project. The team investigated various aspects of grid and control stability upon recovery of disturbances and during normal operation. Modeling results identified a set of unstable conditions for both small and large signal phenomena. Mitigations for these instabilities were also investigated and recommended. These phenomena and mitigations were presented and discussed with the IAB, disseminating the learnings and outcomes of this effort to key stakeholders.

The research team presented project updates at the NOWRDC Symposia in 2022, 2023 and 2024, and received useful comments at these events.

The modeling and analysis performed throughout this project is further disseminated through professional publications. We currently have two research papers in preparation, leveraging the work done to identify and mitigate stability risks in the New York State and surrounding power systems in the Northeast US. We currently have two research papers in preparation. The paper "Small Signal Stability Analysis of New York State Power Grid with Large-Scale Offshore Wind Integration" is in near-final draft stage, and only needs to be approved by our subcontractors before being submitted to the journal "Energies". Our second paper is entitled "Enhancing Transient Stability with Synchronous Condensers under High OSW Penetration in NYS," and will be submitted to the 2026 General Power Meeting of the IEEE Power and Energy Society (PES). The full draft of this paper is being reviewed by our subcontractors, and will be submitted by the November deadline for this meeting. Once published and presented, these publications may further enlighten key stakeholders including system operators, utilities, generation plant owners & developers, and policymakers to understand key constraints and enablers to building out offshore wind in New York State and Northeastern US.

We have been invited to participate in the panel session "Leveraging IBRs for Power System Stability" for the PES GM 2026, which has been proposed to the Power System Stability Controls (PSSC) Subcommittee of the IEEE PES. We also will present results from this study in a seminar at the Capital District Engineer's Week Event sponsored by the New York State Society of Professional Engineers. These presentations and panel sessions will be an enabling vehicle for further dissemination of this work where power system experts and decision makers attend and can learn about important enablers to deploying offshore wind technology in New York and Northeastern US.

From these project meetings, publications, and industry presentations, key findings from this work may be leveraged by various relevant parties with responsibility to maintain a reliable, affordable and clean energy supply. Through these various channels, further work may be identified to support the implementation of recommendations from this work. This will continue to be a critical enabler to achieving New York's evolving CLCPA energy and climate goals by addressing stability and grid integration constraints to deploying 9GW of offshore wind technology.

6.2. Technology Transfer

The Clarkson, NYPA and GE Vernova participants in this project have discussed Technology Transfer. In particular:

- The Risk Evaluation methodology developed by GE Vernova and implemented by the full team is presented in the Task 2.1 section of this report. Similarly, the mitigation methods developed in this project were the result of the regular bi-weekly full team meetings plus the two dedicated in person sessions that were conducted during this project. Knowledge and expertise around technology capability, offshore wind electrical equipment and power system modeling, detailed knowledge of New York, New England, New Jersey, Pennsylvania and Maryland power grids as well as deep domain knowledge of renewable inverter-based resource integration have been transferred across the project team and external stakeholders in the IAB. This technology transfer will further support commercialization of a service that intends to accelerate the buildout of offshore wind integration, as described in detail in the next section.
- The first set of intellectual property developed in this project involve the evaluation methods that are required to develop practical PSCAD and SSAT models from a full CEII database used by utilities and system operators for grid planning and operation. The knowledge of modeling tools, methodologies and IBR equipment developed in this project uniquely positions the project team to address the needs of New York's power system and the various parties responsible for reliable, affordable and clean energy supply. These evaluation methods are specific to power system topology and critical operational and stability constraints, protected under the CEII umbrella. Access to CEII databases is strictly controlled, and use is restricted to specific projects, rather than specific users. Additionally, the CEII data will be regularly updated so that a specific project may well require the use of a different CEII data set than was used in this project. Transfer of this intellectual property will be done between qualified CEII entities, strictly following CEII procedures.
- The second set of intellectual property developed in this project involves the risk evaluation and the risk mitigation methods developed in Task 2 of this project. This intellectual property, to the degree it may be disclosed, is being reported in the research papers and presentations that are coming out of this project. The deep domain expertise across GE Vernova, NYPA and Clarkson University in renewable IBR integration, power system analysis and offshore wind technology uniquely positions the project team to further address the needs of New York's power system and the various parties responsible for reliable, affordable and clean energy supply. This is an extremely active area of investigation worldwide. The methodology to identify stability risks and constraints, quantify their impact and recommend technological and procedural mitigations is a key part of the intellectual property that will be transferred to relevant stakeholders for action. The team has discussed this issue, and determined that disseminating this intellectual property through the open literature is the appropriate avenue for this work. Follow on efforts to collaborate between the project team and industry partners and carry out evaluations and technology deployment may then be done, as outlined in the commercialization strategy below. The team has discussed this issue, and determined that disseminating this intellectual property through the open literature is the appropriate avenue for this work.
- The research team has discussed the potential for commercialization of the results of the service that has been developed in this project. While the recommendations and methods that will be commercialized following this work have substantial potential to address deployment of offshore wind in New York, we do not see potential for patent protection for this service. We have discussed the potential for licensing the data reduction techniques developed in this project, and have discussed these with Jamey Hoose, Director of the Shipley Center and Associate Director of

Research and Technology at Clarkson University. There is agreement that Clarkson University is not interested in developing a licensing product based on these data reduction methods.

Project partners New York Power Authority and their AGILe Lab, GE Vernova Consulting Services are involved in the interconnection studies and system studies that are the subject of this project. The results of this project will used by these three entities in their ongoing efforts to integrate the full range of carbon free generation onto the electric power grid, further enabling the evolving goals of New York State's CLCPA, further enabling the evolving goals of New York State's CLCPA.

6.3. Commercialization

Clarkson will create the process for future service commercialization. The service process from developed models and methods will be documented and discussed with Clarkson's Sponsored Research Services office for the next phase of commercialization. Our approach is to provide modeling and advisory for OSW customers with the developed software & dataset package and evaluation methods.

Commercialization plan

1) Model components to be commercialized

In previous tasks of this project, the focus was on developing an interregional EMT model for the offshore wind fleet with the eventual intent of then creating a new commercial service based on these models.

The AGILe, a division of the New York Power Authority, currently maintains a system-wide stability model of the New York State power grid. As shown in Figure 78, this AGILe model formed the base for the New York system part of the interregional model developed under this project. Under this project, Clarkson University and GE Vernova's Consulting Services developed an additional PSCAD model for analyzing integration of offshore wind that represents the following components:

1) PSCAD model of the Atlantic offshore fleet
2) PSCAD system models for neighboring systems of PJM and New England
3) PSCAD model of the New York power system

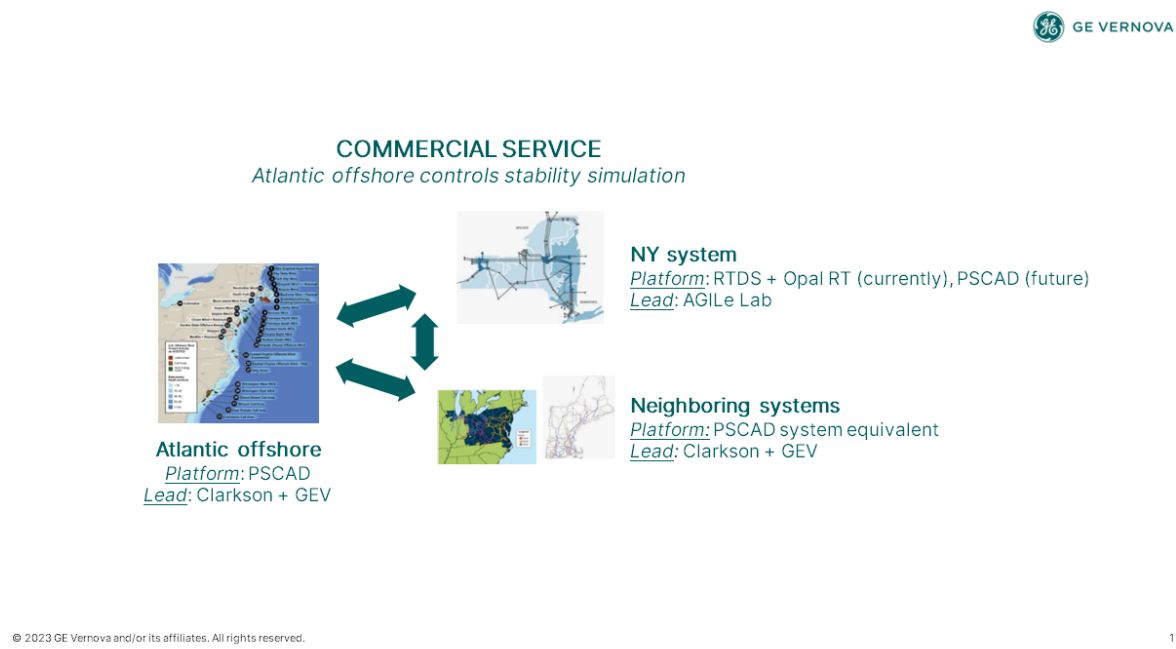

Figure 78. Diagram illustrating the model components that make up the service to be commercialized based on this project.

In order for the model to be offered as a commercial service, a user would need to be able to access and run simulations across all three model components together. Given that the AGILe is already set up to offer OEM-agnostic model usage services to the public with appropriate confidentiality firewalls, we recommend that the model developed under this project be commercialized as a partnership between Clarkson and the AGILe with GE Vernova Consulting Services continuing to serve as technical advisors.

AGILe is in the process of developing a comprehensive digital twin of New York State's electric grid, which will include a repository of models of transmission, distribution, market and communication network of past, current and future years. The developed models in this project are potentially integrated into AGILe's digital twin platform, enabling detailed offshore wind studies, improved grid planning and operation, and comprehensive scenario analysis.

2) Partnership elements

The next step in the commercialization process involves negotiating the terms of the partnership. Key elements to consider include licensing the interregional model, contracting consulting services for client advisory support, establishing internship programs for talent development in EMT modeling and simulation, and future collaborative efforts to update and refine the models. This partnership can leverage the strengths of all three parties involved, fostering innovation, knowledge transfer, and the development of a skilled workforce ready to tackle future challenges in the energy sector.

3) Commercial service definition

The commercial service would utilize the models described above to enable an assessment of system-wide controls stability risks for a client project (e.g. developer or system operator clients) or technology (e.g. OEM client). This modeling capability would be used in conjunction with other established modeling capabilities (e.g. power flow, dynamics, production cost, adequacy) to holistically assess overall reliability and resilience risks. This service wouldn't replace those other modeling capabilities but would be used in a collaborative fashion.

Potential clients may utilize the models by procuring advisory services via the AGILe. Depending on resource availability, the AGILe could perform such advisory services themselves, or they could contract with GE Vernova Consulting Services and/or Clarkson to run the models and advise clients regarding the results.

4) Model validation

In order to gain credibility with potential customers, the model will need a validation effort to confirm that the baseline model reflects expected system performance. The appropriate validation tests would need to be defined and simulated. Another possible step could be factory acceptance tests for renewables equipment to ensure that renewables models reflect OEM performance.

5) Ongoing model maintenance

After the model has been commercialized, ongoing maintenance will be required in order to ensure that the system-wide model reflects the up-to-date views both of the current and future system. It is expected that such maintenance efforts would be funded by the revenue of the commercial service. Personnel for maintenance efforts could be a partnership opportunity between AGILe, Clarkson and GE Vernova.

6) Target customers and revenue estimation

Potential customers for this service could be utilities, offshore wind developers, transmission developers, TOs, RTOs. We estimate that our proposed study service would cost $200,000-$500,000 per study. There are about 33 offshore wind projects potentially being developed across the Atlantic Seaboard for completion by 2035. We assume that each developer client performs one EMT study per OSW project while transmission operators and system operators may perform EMT studies in clusters.

Table 32 projects the potentials for the Offshore Wind Industry alone with the assumption that each study costs $250,000 on average. Based on this assumption, we estimate that the service will have an approximated revenue of $13 million by 2035. At the same time, contraction of the offshore market could be a risk to potential revenue streams.

Another market opportunity beyond offshore development would be onshore resource evaluations. Given the expected high penetrations of IBRs in the onshore system due to onshore wind and solar development, having an EMT model that includes the offshore system would be beneficial for evaluating potential interactions between onshore and offshore resources. Using this model for such evaluations would increase the market opportunity for this service beyond the $13M estimate.

Table 32: Potential market opportunity & revenue estimate. Note that cost units are in thousands.

Prospective Client	Estimated number of EMT studies	Cost per study ($k)	Total cost ($k)
Offshore Wind Developers	33	$250	$8,250
System Operator	10	$250	$2,500
Transmission Developer	10	$250	$2,500
Total market opportunity by 2035			**$13,250**

7) Marketing strategy

Our marketing strategy to reach, engage, and promote this new service could include the following:

- **Conferences & Exhibition:** The following venues could be appropriate for presenting the new service offering to potential customers: IEEE T&D Conference & Exposition, American Clean Power's (ACP's) Offshore WINDPOWER Conference & Exhibition, Energy Systems Integration Group (ESIG) and the National Offshore Wind R&D Symposium.
- **Webinar:** The team could host a webinar to describe the service and take audience questions in a virtual format.
- **References:** Our next channels would be our existing industry collaborations from our Advisory Boards including utilities, developers, and vendors. GE Vernova Consulting Services would be able to introduce this service to their existing connections who will need the service in the near future.
- **White papers and magazines:** We could develop a white paper describing this new service and publish in industry magazines such as T&D World Magazine, IEEE Power & Energy Magazine, etc.

7. Conclusions

This final report is for the NOWRDC project "Atlantic seaboard offshore stability risk evaluation & service." This project was led by Clarkson University, with subcontractors GE Vernova and New York Power Authority.

This project consisted of 3 technical tracks:

- Task 1: Develop a System-Wide Model
- Task 2: Controls Instability Risks Evaluation and Service Development
- Task 3: Dissemination and Technology Transfer

In Chapter 2, Subtask 1.1 presents the development of offshore wind farm (OSW) models suitable for grid level studies. This subtask also included the development of both AC and DC transmission models for linking the OSW to the point of interconnection (POI) with the onshore bulk electric power grid.

In Chapter 3, Subtask 1.2, it was found to be necessary to develop multiple models of the Eastern Seaboard electric power grid. This modeling effort began with a 94,000 bus CEII dataset. Substantial model reduction efforts were conducted to reduce this to an equivalent model of the study system. From this reduced model, a 1400 bus model was developed and validated for the small signal study of this project. For the transient stability study of the project, three distinct PSCAD models were required in order to complete the required simulations for the NYISO,
ISO-NE and PJM study areas.

Chapter 4 of this report contains the small signal and transient stability studies that identified the control and stability risks of the proposed OSW installations. The documented risks included transient stability limits in the 1-3 hertz inertial grid frequencies as well as control instabilities and damping issues in the 3-50 frequency band. The controller interaction studies were conducted with the small signal model, and the stability issue identified were verified with the time domain PSCAD models.

Task 2.2 involved the analysis and mitigation of the risks identified in Task 2.1. These efforts are documented in Chapter 6. Three risk mitigation technologies were included in the study:

- Application of synchronous condensers (SC) at OSW POI or synchronous generator buses
- Application of static VAR sources (STATCOM) at OSW POI or synchronous generator buses
- Inverter Based Resource (OBR) controller tuning.

The SC and STATCOM options were found to be useful in addressing inertial instabilities and increasing the critical clearing times for grid faults. The controller tuning approach was successfully applied to IBR control interactions as well as in instances where onshore HVDC inverters were implicated in transient stability issues.

Chapter 7 presents the team's Dissemination and Technology Transfer efforts. It is concluded that there is the opportunity for commercialization of project results with a collaboration of project partners NYPA, GE Vernova, and Clarkson University.

References

[1] "Annual Transmission Planning and Evaluation Report." New York ISO, March, 2024.

[2]"Eastern Interconnection Reliability Assessment Working Group (ERG) Strategic Plan." Eastern Interconnection Reliability Assessment Group. Nov. 2023.

[3] "DYNRED Dynamic Reduction." Powertech, https://dsatools.com/dynred/

[4] "E-Tran Translator for Power System Simulation. User's Manual Version 3.0." Electranix.

[5] *2800-2022 - IEEE Standard for Interconnection and Interoperability of Inverter-Based Resources (IBRs) Interconnecting with Associated Transmission Electric Power Systems*. IEEE, 2022.

[6] "Standard PRC-006-2: Automatic Underfrequency Load Shedding." National Electric Reliability Council (NERC).

[7] "Standard PRC-024-2: Generator Frequency and Voltage Protective Relay Settings". National Electric Reliability Council (NERC).

[8] "Standard TPL-001-4 — Transmission System Planning Performance Requirements." National Electric Reliability Council (NERC).

[9] "Exciter ESAC8B_PTI." https://www.powerworld.com/WebHelp/Content/TransientModels_HTML/Exciter%20AC8B.htm.